Spectrum coexistence in the 6 GHz and 13 GHz bands

by

Nadia Patricia Yoza Mitsuishi

B.S., Pontifical Catholic University of Peru, 2007

M.S., University of Colorado Boulder, 2015

A thesis submitted to the

Faculty of the Graduate School of the

University of Colorado in partial fulfillment

of the requirements for the degree of

Doctor of Philosophy

College of Engineering and Applied Science

2021

Committee Members:

Dr. Peter Mathys, Chair

Dr. David Reed

Dr. Sangtae Ha

Dr. Dirk Grunwald

Dr. Christopher Anderson

Yoza Mitsuishi, Nadia Patricia (Ph.D., Telecommunications)

Spectrum coexistence in the 6 GHz and 13 GHz bands

Thesis directed by Prof. Dr. Peter Mathys

There is an increasing demand for spectrum due to the expanding use of wireless technologies. In April of 2020, the Federal Communications Commission (FCC) opened the 6 GHz band (5925-7125 MHz) for unlicensed use, such as Radio Local Area Networks (RLANs), while sharing the spectrum with current terrestrial and satellite incumbents. Since the demand for spectrum will continue to grow in the next years, another candidate for unlicensed use is the 13 GHz band (12700-13250 MHz), allocated to the same types of incumbents. In this work, we will determine the feasibility of spectrum sharing in the 6 GHz and 13 GHz bands. These bands are used for fixed and mobile Broadcast Auxiliary Service (BAS) and Cable Television Relay Service (CARS), fixed microwave links and Fixed Satellite Service (FSS) links. This work investigates, through measurements and simulations, the implications of coexistence in these bands. First, due to the lack of propagation studies, we conduct path loss measurements at 7 GHz and 13 GHz in an urban environment to determine the best propagation model to use in the simulations. A path loss model is calculated and compared with site-specific and empirical propagation models. Second, using a case study approach, we simulate the aggregate interference from Wi-Fi access points (APs) to terrestrial incumbents and vice versa, considering terrain and clutter information and real data of the incumbents. Incumbent emissions are also measured in this area to determine the spectrum use. Finally, aggregate interference models are proposed to calculate the interference to terrestrial and satellite incumbents using space, time, and frequency-domain considerations and real data. Additionally, the Risk-Informed Interference Assessment approach is used to provide quantitative analysis to characterize the likelihood and impact of interference on the incumbent links. According to the results, spectrum sharing with RLANs is possible in these bands and the models and methodology developed here can be replicated in coexistence studies in other bands.

Dedication

To my beloved parents, Teodoro and Elena

Acknowledgements

First and foremost, I would like to express my deepest gratitude to my advisor, Professor Peter Mathys, for his continuous support in the development of this dissertation. I enjoyed learning about communications and signal processing in his class and through his insightful suggestions and our inspiring discussions. I would also like to thank Dr. Kenneth Baker for being my advisor during the first two years and a half, for his great support, guidance and lessons about wireless communications. I am also grateful to Professor David Reed for his inputs and advice on this dissertation, Dr. Christopher Anderson for sharing his knowledge on radio propagation and measurements, and the rest of the committee members, Professor Dirk Grunwald and Professor Sangtae Ha, for their time and comments.

I am deeply grateful to CableLabs for funding my research and providing me with continuous assistance during these years. My special thanks to Dr. Belal Hamzeh for trusting in me to work on this project and for his thoughtful inputs and invaluable support. I am also extremely grateful to Dr. Ruoyu Sun, for his inspiring guidance on radio propagation and wireless communications, his help with the path loss measurements and his constant support and generous advice during the past years. I would also like to thank Mark Poletti and Bao Phommatha for their useful suggestions and support, Anthony Untalan for his help with the field measurements in the Denver area, and the rest of the team. I would like to extend my appreciation to EDX Wireless for providing me access to their SignalPro software, terrain and clutter databases; NTIA/ITS and CableLabs for facilitating the equipment used in the field measurements; and the department of Computer Science and the University Memorial Center at the University of Colorado Boulder for allowing access to

the transmit locations used in the path loss measurements.

I am extremely grateful to my parents for their endless love and support, for inspiring me throughout my life and being an example of courage in hard times. I would also like to thank my sisters, Natalia and Katia, and the rest of my family and friends for their permanent support. I would like to give my special thanks to Dr. William Krantz and June Krantz, who became my Boulder family, and to Dr. Mario Vidalon and Dr. David Espinoza, for their guidance and advice since I arrived in Boulder. I would also like to thank my fellow TCP classmates: André Rosete, Irena Stevens, Ibrahim Ayad, Evariste Some, Waleed Almarshedi, Zhang Liu and Xinyang Zhou.

Finally, I would like to express my deepest gratitude to my wonderful Boulder friends, who encouraged me and made this journey better: Qing Chao, Stephanie Swartz, Sepideh Kianbakht, Jefferson Yarce, Jenny Ramírez, Juan Carlos Olarte, María Belén Zea, Gabriela Buitrón, Maria Paula Werneck, Miluska Benavides, José Miguel Herbozo, Germán Alcalde, Juan Manuel García, Jesús Villalpando, Rowan Orellana, Lindsey Bugbee, Hernán Villanueva and Jorge Luis Barrera.

Contents

Chapter

Tables

Table

Figures

Figure

Chapter 1

Introduction

1.1 Background

In the past years, demand for wireless technologies and services has increased exponentially and this trend is expected to continue with the development of new standards and increasing amount of data traffic through the networks. However, spectrum is a scarce resource and some bands have become highly congested, while some others could potentially be used more efficiently. In this context, it becomes necessary to identify current uses of the spectrum and determine whether it can be utilized more efficiently.

In April of 2020, the Federal Communications Commission (FCC) made available the 6 GHz band, from 5.925 to 7.125 GHz, for unlicensed use in the United States, while sharing the spectrum with current terrestrial and satellite incumbents [39]. In Europe, only the low portion of the band, from 5.925 to 6.425 GHz is being considered for unlicensed use [21]. This decision will enable the development of new technologies and services that will help to satisfy the increasing demand for connectivity and capacity. This band could be used for new Wi-Fi standards such as 802.11ax, commercially known as Wi-Fi 6, 5G NR-U, which will allow using unlicensed spectrum for 5G networks, and increased number of Internet of Things (IoT) devices. Opening the 6 GHz band for unlicensed use will result in over $ 153 billion in economic value [88] in the United States. However, it is expected that the demand for unlicensed spectrum will continue to increase in the next years, and hence it is necessary to study additional bands to accommodate new technologies and services in the mid-band spectrum. The 13 GHz band, from 12.7 to 13.25 GHz is a good candidate due to

its allocation to the same incumbent services as in the 6 GHz band, the significantly lower number of incumbent links and higher frequency that causes higher propagation loss and lower interference. Coexistence in both bands, 6 GHz and 13 GHz, will be studied in this dissertation.

1.1.1 Spectrum sharing

Since spectrum is a limited resource, it should be used as efficiently as possible to allow for the operation of different technologies and services. The option that offers the lowest interference is band clearing or spectrum relocation, which has been used multiple times by the FCC to free up spectrum by moving incumbents to other bands. However, these are expensive, complex and relatively long processes and require that someone pays for the spectrum, which might not be feasible for unlicensed use. In this case, spectrum sharing is a more convenient alternative. It permits unlicensed users to utilize the spectrum more efficiently while protecting primary users from interference. To occur, the overall benefits that spectrum sharing produces in the economy should be higher than the potential harms it could cause.

A common term used in spectrum management is "harmful interference". In general, this term is defined by the FCC as the interference that "endangers the functioning of a radionavigation service or of other safety services or seriously degrades, obstructs, or repeatedly interrupts a radiocommunication service" [30]. With the aim of protecting primary allocation license holders from this "harmful" interference, spectrum management policies have been traditionally adopted based on worst-case scenarios. These scenarios are based on a single-value analysis for extreme cases that causes severe consequences, without considering the likelihood of occurrence. This analysis tends to be overly conservative and not representative of reality and, thus, its use can be counterproductive for efficient spectrum management. In many cases, this over-protection can cause the spectrum to be underutilized. Therefore, it is necessary to incorporate new approaches for spectrum policy that adopt market-oriented mechanisms which foster innovation and competition.

1.1.2 Incumbents in the 6 GHz and 13 GHz bands

There are four types of incumbents in these bands, which can be divided into terrestrial and satellite links. Terrestrial links are divided into Fixed Service (FS) and Mobile Service (MS) links. FS consists of fixed BAS, CARS and fixed microwave links. MS consists of mobile BAS and CARS. These incumbent services are described below and the spectrum allocation is summarized in Tables 1.1 and 1.2 for the 6 GHz and 13 GHz bands, respectively:

- Fixed microwave links are used for a variety of services, such as Operational Fixed Service (OFS), which includes public safety and industrial/business links, Common Carrier (CC) links, and Local Television Transmission Service (LTTS). It is regulated by the FCC [32] under the Code of Federal Regulations (C.F.R.), Title 47, Part 101. In the 6 GHz band, it is allocated in the 5.925-6.425 GHz, 6.525-6.875 GHz and 6.875-7.125 GHz bands. In the 13 GHz band, it is allocated to the 12.7-13.15 GHz band.

- Broadcast Auxiliary Service (BAS) links are used by TV and radio stations to relay broadcast television and aural signals between two locations. Mainly, it has one of the following configurations in the fixed mode: Studio-to-Transmitter Link (STL, fixed links used to transmit program material from the studio to the transmitter), InterCity Relay (ICR, used to relay signals between two stations, such as a main studio and an auxiliary studio), and Transmitter-to-Studio Link (TSL, less common, used as a return path for telemetry return links). Mobile BAS is used for remote pickup stations (signal is relayed from a remote location to the studio) and mobile TV pickup (such as electronic news gathering, ENG). An example of mobile BAS links used for live video transmission is illustrated in Figure 1.1. The BAS receiver can be located either on a central receive site, such as a tall building or a mountaintop, attached to a video camera mounted on a shoulder or, in the case of relay stations, on a truck or helicopter. BAS is regulated by the FCC under C.F.R., Title 47, Part 74 [29]. It operates in multiple bands, such as the 6.875-7.125 GHz, 12.7-13.15 and 13.2-13.25 GHz, both in fixed and mobile modes, and 6.425-6.525 and 13.15-13.2 GHz in

mobile mode only.

- Cable Television Relay Service (CARS) is used by cable TV and other MVPD (Multichannel Video Programming Distributor) operators to relay television and audio signals. It is used in the following configurations in the fixed mode: Local Distribution Service (LDS, from a fixed station to one or more receiving locations from where the signals are distributed to the public) and Cable Television Relay Service Studio to Headend Link (SHL, from a cable TV studio to the headend of a cable TV system). In the mobile mode, it can be used for Cable Television Relay Pickup Station, which consists of a mobile link from a remote location to the cable TV studio or headend. CARS is regulated by the FCC under C.F.R. Title 47, Part 78 [27]. It operates in multiple bands, such as 6.425-6.525 GHz, 6.875-7.125 GHz and 13.15-13.2 GHz in mobile mode only and 12.7-13.15 GHz and 13.2-13.25 GHz in fixed and mobile modes.

- Fixed Satellite Service (FSS) in the 6 GHz band is mainly used for Earth-to-space links (uplinks), from 5.925 to 7.075 GHz. The majority of FSS links in the 6 GHz band consist of uplinks in the conventional C-band, which corresponds to Earth-to-space frequencies between 5.925 GHz and 6.425 GHz. FSS is mainly used to distribute content to TV and radio broadcasters and as a backhaul for telephone and data traffic. Additionally, there are a few space-to-Earth nongeostationary mobile-satellite service (MSS) feeder downlinks between 6.7 GHz and 7.075 GHz with Earth stations within 300 meters of three specific locations in the United States. In the 13 GHz band, FSS is used for Earth-to-space links in 12.75 - 13.15 GHz and 13.2 - 13.25 GHz.

In addition to these incumbents, radio astronomy stations that operate in 6.650-6.6752 GHz in a few remote locations should also be protected. Unlicensed low-power wideband and ultra-wideband (UWB) systems also operate in the 6 GHz band at a maximum power spectral density of -41.3 dBm/MHz. They are regulated by the FCC under C.F.R. Title 47, Part 15, and, as unlicensed devices, they are not entitled any interference protection and should not cause harmful interference

to licensed services.

Table 1.1: Uses of the 6 GHz band [39]

6 GHz sub-band	**Frequency range (GHz)**	**Primary allocations**	**Predominant licensed services**
U-NII-5	5.925 - 6.425	Fixed	Fixed Microwave
		FSS	FSS (uplink)
U-NII-6	6.425 - 6.525	Mobile	Broadcast Auxiliary Service
			Cable Television Relay Service
		FSS	FSS (uplink)
U-NII-7	6.525 - 6.875	Fixed	Fixed Microwave
		FSS	FSS (uplink/downlink)
U-NII-8	6.875 - 7.125	Fixed	Broadcast Auxiliary Service
			Fixed Microwave
		Mobile	Broadcast Auxiliary Service
			Cable Television Relay Service
		FSS	FSS (uplink/downlink)

Table 1.2: Uses of the 13 GHz band

Band	**Frequency range (GHz)**	**Primary allocations**	**Predominant licensed services**
13 GHz	12.7- 12.75	Fixed	Fixed Microwave
		Fixed/ mobile	Broadcast Auxiliary Service
			Cable Television Relay Service
	12.75- 13.15	FSS	FSS (uplink)
		Fixed	Fixed Microwave
		Fixed/ mobile	Broadcast Auxiliary Service Cable Television Relay Service
	13.15 - 13.2	Mobile	Broadcast Auxiliary Service Cable Television Relay Service
	13.2 - 13.25	Fixed/ mobile	Broadcast Auxiliary Service
			Cable Television Relay Service (secondary)
		FSS	FSS (uplink)

1.1.3 Regulatory background

In August of 2017, the FCC published a Notice of Inquiry with the purpose of expanding licensed and unlicensed use in the mid-band spectrum, between 3.7 GHz and 24 GHz [34]. The

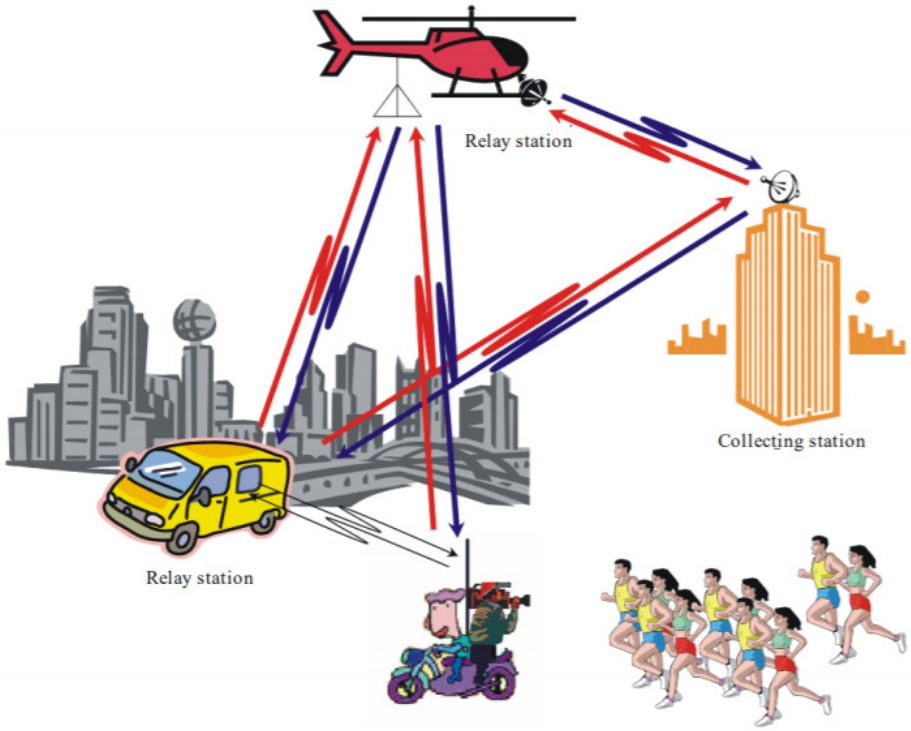

Figure 1.1: Mobile BAS example: live video transmission [52]

Commission focused on three bands: 3.7-4.2 GHz, 5.925-6.425 GHz, and 6.425-7.125 GHz, which are nationally and internationally considered by stakeholders as potential candidates to accommodate wireless broadband services. The FCC also announced to be open to hear comments to identify other bands. As a first step, in October of 2018, the FCC released a Notice of Proposed Rulemaking (NPRM) to allow unlicensed use in the 6 GHz band, while sharing the spectrum with current services [36].

1.1.3.1 The 6 GHz band

In April of 2020, the FCC published a Report and Order and Further Notice of Proposed Rulemaking to expand unlicensed broadband use in the 6 GHz band, while protecting incumbent operations [39]. In the Report and Order, the FCC authorized two types of unlicensed operations: low-power indoor and standard power. Low-power indoor (LPI) APs are authorized across the entire 6 GHz to connect multiple devices, such as laptops, tablets, cell phones and Internet-of-Things

(IoT) devices. Standard-power APs can operate at the same power as in the 5 GHz U-NII-1 (5.150-5.250 GHz) and U-NII-3 (5.725-5.850 GHz) bands and they require using an automated frequency coordination (AFC) system. These APs are used in outdoor and indoor scenarios for hotspots and rural broadband networks, as well as in deployments with increased network capacity. The FCC has specified a set of rules for 6 GHz RLAN devices to operate in this band and concludes that the risk of causing harmful interference to incumbents is minimal. The main RLAN technology is Wi-Fi and the 1200 MHz of additional spectrum will enable up to seven 160-MHz or three 320-MHz Wi-Fi channels and will enable new technologies and increased data capacity.

To facilitate sharing, the FCC divided the 6 GHz into four sub-bands, from U-NII-5 to U-NII-8, and, depending on the incumbents, proposed different EIRP limits and mitigation rules for each of them, as summarized in Table 1.3 [39]. The density of assignments per MHz in each sub-band for terrestrial incumbents is shown in Figure 1.2.

Table 1.3: Unlicensed use of the 6 GHz band proposed by the FCC [39]

Device class	**Operating bands**	**Maximum EIRP**	**Maximum EIRP power spectral density**
Standard-power AP (AFC controlled)	U-NII-5, U-NII-7	36 dBm	23 dBm/MHz
Client connected to standard-power AP		30 dBm	17 dBm/MHz
Low-power indoor (LPI) AP	U-NII-5, U-NII-6, U-NII-7, U-NII-8	30 dBm	5 dBm/MHz
Client connected to LPI AP		24 dBm	-1 dBm/MHz

U-NII-5 (5.925-6.425 GHz) and U-NII-7 (6.525-6.875 GHz) are allocated to fixed service (FS) and fixed satellite service (FSS) links, which use Geosynchronous Equatorial Orbit (GEO) satellites located at approximately 36000 km above the Equator. In addition to FS and FSS, U-NII-6 (6.425-6.525 GHz) is also allocated to Broadcast Auxiliary Service (BAS) and Cable Television Relay Service (CARS) on a mobile basis, while U-NII-8 (6.875-7.125 GHz) is also allocated to fixed and mobile BAS and mobile CARS [29][27].

In U-NII-5 and U-NIII-7, standard-power outdoor and indoor APs are required to use an AFC

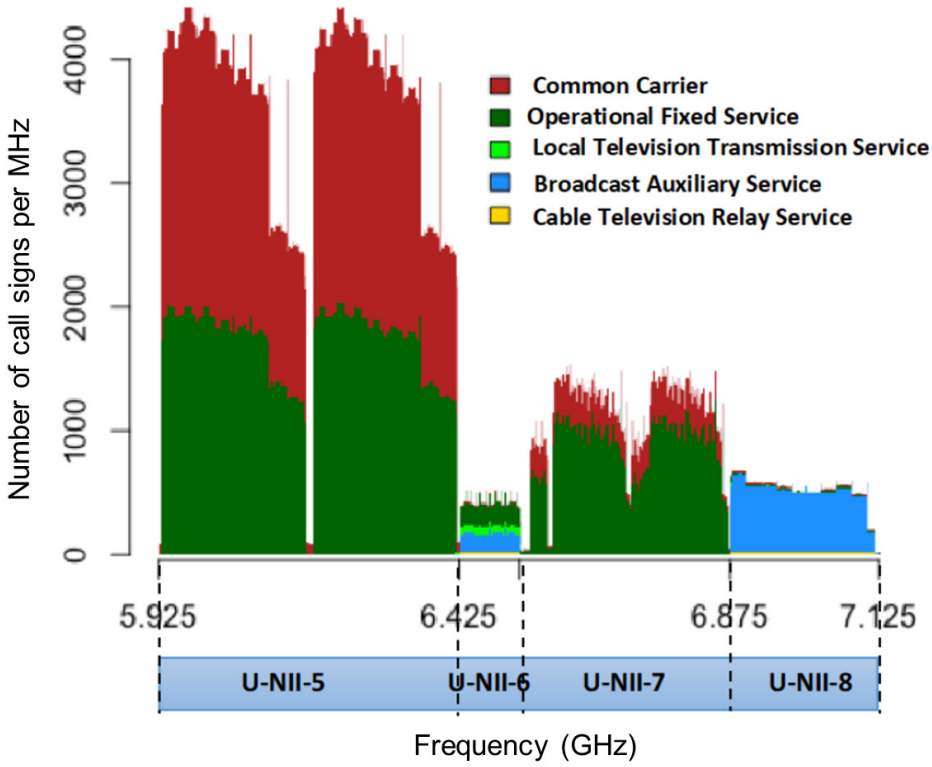

Figure 1.2: Incumbent terrestrial services in the 6 GHz band in the United States [36]

system to identify the frequency channels available and operate without causing harmful interference to incumbent FS receivers. The maximum EIRP in the APs should be 36 dBm, which corresponds to a maximum PSD of 23 dBm/MHz. Additionally, the EIRP should be limited to 21 dBm for elevation angles above 30° from the horizon to avoid interference to FSS satellites. Client devices are authorized to operate at a lower power level, at a maximum EIRP of 30 dBm, which corresponds to a maximum PSD of 17 dBm/MHz.

The purpose of the AFC system is to determine the exclusion zones required to protect incumbent licensed microwave links. The AFC should also protect incumbent radio observatories that operate between 6650 MHz and 6675.2 MHz in the U-NII-7 band in a few remote locations. This system is based on three components, as detailed below:

(1) Framework and database.- The FCC proposed a centralized AFC database that contains a list of available frequencies and maximum power limits that can be used to operate standard-

power APs. This centralized model defines the exclusion zones to protect incumbent FS links and is consistent with the framework used for TV white space databases and CBRS (Citizens Band Radio Service) spectrum access systems. The database will be based on the FCC's Universal Licensing System (ULS) database, which contains information of the incumbent FS links in the U-NII-5 and U-NII-7 bands. According to the Commission, this approach facilitates the management of the databases and reduces the complexity of the system.

(2) Operational requirements.- The FCC requires that standard-power APs include geolocation capabilities and automatically report their geolocation, mainly based on GPS, to the AFC to calculate the minimum separation distance from incumbent FS receivers. The AP antenna height should be provided either automatically or manually to the AFC. The frequency availability will be checked on a daily basis.

(3) Interference protection parameters.- The Commission recommends a set of propagation models depending on the distance between the standard-power AP and the incumbent FS receiver. Free-space path loss is suggested for distances lower than 30 meters and WINNER II for distances up to 1 km, including site-specific information regarding terrain and building data when available to determine line-of-sight (LOS) or non line-of-sight (NLOS). For distances beyond 1 km, the Commission proposed the irregular terrain model (ITM) combined with the ITU-R P.2108 [54] clutter model for urban and suburban environments and ITU-R P.452 [53] for rural environments. The interference protection criterion to be used is a maximum interference-to-noise power ratio (I/N) of -6 dB, as supported by incumbents and considered by Wi-Fi advocates in their studies. According to the FCC, in addition to the co-channel exclusion zone, it would be convenient to adopt a precautionary approach that requires the AFC to also determine the adjacent channel exclusion zone to protect fixed incumbents from out-of-band emissions (OOBE) from standard-power APs. In a more realistic scenario, according to the Commission, the adjacent channel interference should

not be a problem considering that incumbents already rely on filters and guard bands to suppress OOBE.

In the entire 6 GHz band, from U-NII-5 to U-NII-8, the FCC proposed to limit the maximum power spectral density (PSD) to 5 dBm/MHz for LPI APs and a maximum effective isotropic radiated power (EIRP) of 30 dBm for a maximum channel bandwidth of 320 MHz, considering future developments for unlicensed use. Client devices are authorized to operate 6 dB below the APs, at a maximum EIRP of 24 dBm and a maximum PSD of -1 dBm/MHz. Since the location of the MS stations is not predictable, AFC is not suitable and, instead, the FCC proposed that the APs are operated indoors only, at low power and using a contention-based protocol. The objective of this protocol is to enable fair spectrum sharing among multiple devices by ensuring that they do not transmit continuously. This mechanism is based on a spectrum sensing capability, so the unlicensed device senses the energy in the channel and only transmits if it determines that the channel is idle. Wi-Fi uses CSMA/CA (carrier sense multiple access with collision avoidance) as a contention-based protocol. Third-party interference analyses have been conducted in the past few years by different stakeholders. Many of them do not include the rules recently proposed by the FFC. They use different methodologies, parameters and assumptions, such as transmit power, antenna radiation pattern, propagation model, building entry loss, frequency overlap and RLAN activity factor. Advocates of unlicensed use usually base their studies on an statistical approach and they include the Wi-Fi Alliance and a coalition of hardware and software companies [87][10][75][62]. Their argument is also motivated by the need of more spectrum for unlicensed use and the economic importance of Wi-Fi. Through simulations, they claim that spectrum can be shared successfully with unlicensed devices in the 6 GHz band considering each incumbent service. One of the first and most representative studies was conducted by RKF consulting company, which uses real data of the active links in the contiguous US territory and calculates the probability of interference to each type of terrestrial and satellite incumbents [77]. According to the FCC, another relevant study is the one conducted by CableLabs, which consists of Monte Carlo simulations of interference

from low-power indoor APs in the 6 GHz band to FS and MS incumbents in New York City using a random distribution of parameters used in unlicensed devices, considering their probabilistic nature. The simulations show that there is no risk of harmful interference to FS incumbents, even after increasing the PSD to 8 dBm/MHz. The risk of interference to MS incumbents is very small and, if that occurs, the signal-to-interference-plus-noise ratio (SINR) indicates that the signal is still significantly stronger than the interference.

On the other hand, incumbents rely on worst-case scenarios where only one AP at a specific location and using certain parameters causes harmful interference, regardless of the likelihood of occurrence. Some of the incumbents are the National Association of Broadcasters, the Fixed Wireless Communications Coalition, electric, gas and water utilities companies, satellite companies, etc. [67][42][68][97][48]. A study conducted by AT&T [11] presents six examples of link budgets where potential RLAN devices can operate close to real FS receivers or within or close to the the main beam of the FS receiver at further distances. However, according to the FCC, the study is based on corner case assumptions with worst-case parameters instead of probabilistic quantities. A similar study has been performed by the CTIA [16], where it calculates five link budgets considering actual FS links using worst-case RLAN parameters. A study by Alion [6] focuses on the interference to MS receivers in a few locations using a similar approach as in the aforementioned studies.

Considering the studies and ex-parte reports submitted to the FCC, the Commission concluded that the two approaches suggested in [39] will enable spectrum sharing in the 6 GHz band while protecting incumbents: standard-power APs with AFC in U-NII-5 and U-NII-7 bands and low-power indoor APs with a contention-based protocol across the 6 GHz band. The risk of harmful interference to incumbents is minimal and can be significantly reduced considering the non-continuous nature of transmissions from unlicensed devices.

In the same document, the FCC includes a further notice of proposed rulemaking, through which it seeks comments about two options to expand unlicensed operations in the 6 GHz band without using an AFC system. The first proposal consists of authorizing very low-power APs that can operate indoor or outdoor in the entire 6 GHz band for high-speed and short-range applications.

The second one consists of increasing the PSD from 5 dBm/MHz to 8 dBm/MHz in low-power indoor APs in the entire 6 GHz band. Additionally, the Commission is evaluating whether to permit mobile standard-power APs with AFC and higher power levels in standard-power APs with AFC operating in a fixed point-to-point configuration.

1.1.3.2 The 13 GHz band

In the Unites States, the 13 GHz band has a bandwidth of 550 MHz and is allocated as follows, see Table 1.2: 12.7-13.15 GHz is allocated to BAS and CARS Fixed Service (FS) and Mobile Service (MS) links and fixed point-to-point links [31][27]; 13.15-13.2 GHz is allocated exclusively to MS (TV pickup and CARS pickup); 13.2-13.25 GHz is allocated to BAS on a primary basis and CARS on a secondary basis; and 12.75-13.25 GHz (except 13.15-13.2 GHz) is also allocated to FSS in a co-primary basis. FSS in this band corresponds to geosynchronous orbit (GSO) satellites at approximately 36000 km altitude and, recently, also to Non-GSO (NGSO) satellites at lower altitudes for broadband communications in Ku, Ka and V bands.

1.1.4 Risk-Informed Interference Assessment

In the United States, the historical approach for predicting the coexistence of competing uses of spectrum has been to rely upon a worst-case scenario analysis of single events of severe consequences, regardless of their probability of occurrence, which can lead to over-conservative use of the spectrum [18]. Consequently, the Technological Advisory Committee (TAC) of the Federal Communications Commission (FCC) proposed the use of Risk-Informed Interference Assessment (RIIA) as a quantitative methodology to analyze the probability and the consequence of interference when spectrum is shared between different uses [90] [41]. The objective is to offer the benefits of allowing flexibility in the use of spectrum without being overprotective. It has been applied to a few coexistence studies in the past years and has shown great potential in providing informed insight to spectrum sharing analysis.

RIIA is a new approach that complements the qualitative worst-case scenario analysis and

provides a quantitative assessment based on the probability and the consequences of the interference [41]. It is based on three questions associated with spectrum coexistence: What can happen? How likely it is to happen? And what are the consequences? When applied to spectrum sharing, it relies on statistical analysis of data, such as the distribution of the transmitted and received signal power, the aggregate interference model used, etc. [17] [98]. The FCC TAC has suggested a three step method for RIIA analysis [40]:

(1) Make an inventory of all significant harmful interference hazards

(2) Define a consequence metric to characterize the severity of hazards

(3) Analyze the likelihood and consequence of each hazard.

The RIIA approach has been applied to the following case studies:

(1) LTE/MetSat: In 2015, the FCC auctioned the AWS-3 spectrum (1695-1710 MHz) for Long-Term Evolution (LTE) technology, but a portion of it overlapped the spectrum used by Meteorological Satellite (MetSat) earth-station receivers, which could cause interference. Therefore, the FCC's TAC studied the interference from LTE cellular mobile transmitters operating in the AWS-3 band on MetSat receivers using the RIIA approach [40]. The study was further extended in 2017 and included a sensitivity analysis of the impact of different parameters [19]. The study provided useful insights, for example, identifying that the binding constraint for successful coexistence (i.e., the key technical issues most likely to cause harmful interference) was the short-term interference at 13° elevation angle instead of the long-term interference at 5° elevation angle that was considered before. It also included the analysis of out-of-band emissions (OOBE) and adjacent band interference (ABI), which is usually not considered in coexistence studies.

(2) NGSO-NGSO: In 2017, the FCC's TAC proposed a framework to assess the potential of RIIA for coexistence analysis between multiple Non-Geostationary Satellite Orbit (NGSO)

systems in the V-band (37.5 to approximately 51 GHz). It described a method to evaluate the quantitative risks of NGSO-NGSO interference, but it did not perform risk calculations [41]. In 2018, a new RIIA study analyzed NGSO-NGSO co-channel interference in the Ka-band and V-band [91]. It concluded that the degradation of throughput would not be substantial and, consequently, interference would be low and mitigation might not be required in most of the cases.

(3) DSRC-Wi-Fi: In 2017, NCTA (the Internet and Television Association) and CableLabs (Cable Television Laboratories) conducted a RIIA study to evaluate the potential quantitative risks of coexistence between DSRC (Dedicated Short-Range Communications) and Wi-Fi in the UNII-4 band (5.850-5.925 GHz) [89]. The study was based on a sensitivity analysis of different coexistence parameters and scenarios and it concluded that the probability of DSRC packet error rate due to adjacent channel interference from Wi-Fi was very small and below the threshold value. A new study using real-world traffic scenarios and DSRC lab measurements was conducted in 2018 and used RIIA and a sensitivity analysis to quantify the risk of interference [74]. The results found that DSRC was not impacted by adjacent channel Wi-Fi interference.

1.2 Objective

The purpose of this work is to determine the feasibility of spectrum coexistence between potential RLANs in the 6 GHz (5925 - 7125 MHz) and 13 GHz (12700 - 13250 MHz) bands and current terrestrial and satellite incumbents: fixed and mobile BAS and CARS links, fixed microwave links and FSS links. We conduct simulations and field measurements in both bands to determine the technical implications and possible risks that might be caused by allowing spectrum sharing for unlicensed use in these bands.

1.3 Research statement and methodology

The research question focus is on determining the feasibility and, if so, the technical implications of spectrum sharing in the 6 GHz and 13 GHz bands. The research question is the following:

Can we successfully allow RLANs (Radio Local Area Networks) to operate in the 6 GHz (5925 - 7.125 MHz) and 13 GHz (12700 - 13250 MHz) bands and ensure their coexistence with incumbent services: fixed and mobile Broadcast Auxiliary Service (BAS) and Cable Television Relay Service (CARS), Fixed Microwave Service and Fixed Satellite Service (FSS) links?

To answer this question, we use a methodology based on measurements and simulations, which consists of the steps summarized below in Figure 1.3.

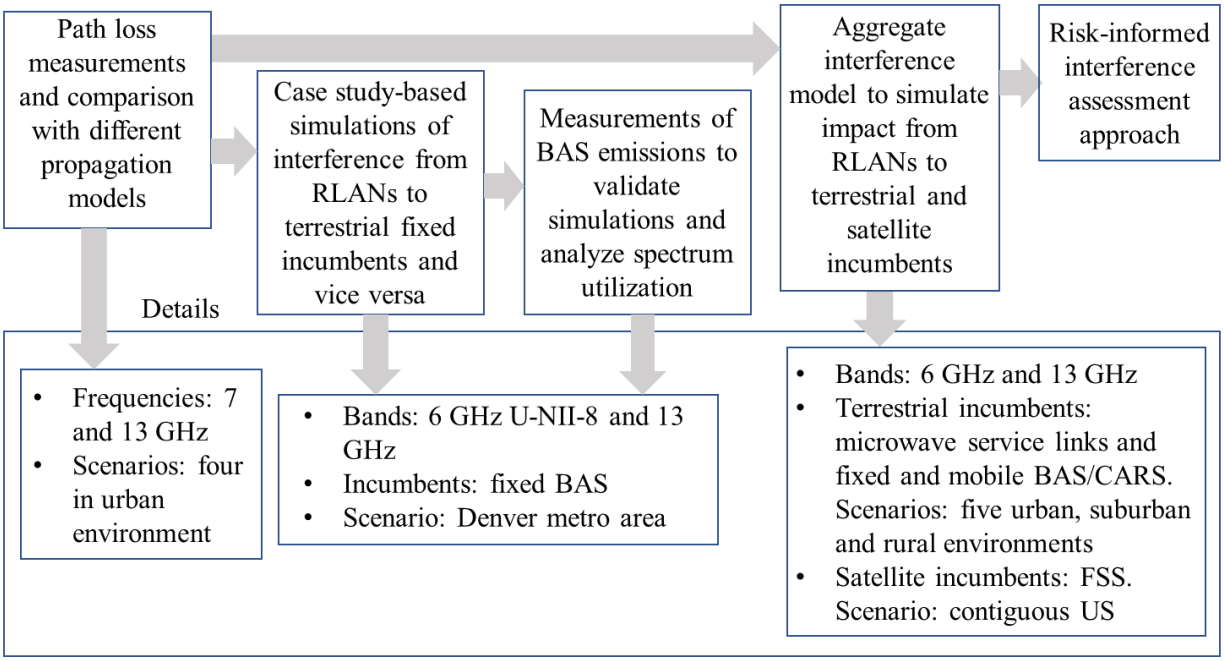

Figure 1.3: Methodology.

First, we conduct field measurements at 7 and 13 GHz to develop a propagation model to be used in the interference simulations. The path loss measurements are based on mixed line-of-sight (LOS) and NLOS conditions in four locations in an urban environment and are compared with different site-specific and empirical models.

Second, based on a case study approach, we simulate the aggregate interference from RLANs

to fixed BAS links and vice versa in the 6 GHz U-NII-8 band and the 13 GHz band in the Denver metro area. The simulations are based on real data about the location and parameters of the incumbent links in this area. The path loss is calculated using a site-specific propagation model that incorporates terrain and clutter information.

Third, we validate the simulations in the case study through measurements of fixed BAS emissions in the Denver metro area in the 6 GHz U-NII-8 band and the 13 GHz band. The measurements are also useful to study the real spectrum utilization by incumbents in this area.

Fourth, we develop an aggregate interference model to calculate the impact of Wi-Fi APs on terrestrial and satellite incumbents in the 6 and 13 GHz bands. The model is based on space, time and frequency-domain considerations and it uses an empirical propagation model. The simulation parameters are based on real data. Interference to terrestrial microwave service links and fixed and mobile BAS/CARS incumbents is calculated through Monte Carlo simulations in five urban, suburban and rural scenarios in the United States. Interference to FSS satellite incumbents is calculated considering Wi-Fi APs distributed across the contiguous United States (CONUS).

Finally, the likelihood and consequence of harmful interference on terrestrial fixed and mobile links is determined using the Risk-Informed Interference Assessment (RIIA) methodology instead of the more traditional worst-case scenario approach.

1.4 Research contributions

The main contributions of this dissertation are summarized in this section:

- Due to the limited amount of propagation measurements previously conducted at these frequencies, path loss measurements at 7 GHz and 13 GHz in an urban environment are conducted to determine the best propagation model to use in the coexistence simulations. A path loss model is generated for each frequency. The measurements are compared with empirical models used in the cellular industry, such as WINNER II, close-in (CI) free-space reference distance, ABG and 3GPP models, and with site-specific models, such as Anderson

2D, using terrain and clutter data with different levels of accuracy. Their advantages and limitations are evaluated in the context of coexistence analysis.

- A case study-based methodology is proposed to simulate the interference from RLANs to terrestrial fixed incumbents and vice versa. The simulations are based on real data of incumbent links in the simulated area. The path loss is computed based on a site-specific propagation model and includes terrain and clutter information to increase the accuracy of the interference calculation.

- Emissions from fixed terrestrial incumbents are measured in a few locations with the purpose of analyzing the real spectral occupancy in the 6 GHz and 13 GHz bands and determine whether the incumbents are transmitting at full spectrum and power, as authorized in their licenses.

- A new aggregate interference model is developed to calculate the impact from RLANs, specifically Wi-Fi APs, on terrestrial FS and MS links and FSS satellite incumbents. This model is applied to analyze coexistence in the 6 GHz, recently opened up by the FCC for unlicensed use, and the 13 GHz band, which has the same types of incumbents. This new model incorporates space, time and frequency considerations and RLAN parameters based on real data. In the case of terrestrial incumbents the simulations are conducted in different urban, suburban and rural environments. The simulations considering satellite incumbents include a sensitivity analysis considering different values of RLAN airtime utilization.

- Considering the impact caused by the RLAN airtime utilization on the interference calculation and the very different values proposed by Wi-Fi advocates and incumbents, this parameter is measured in three scenarios: home during the peak hour, office and classroom. The measurements have been conducted using a software-defined radio and are compared with other values used in 6 GHz coexistence studies.

- The risk-informed interference assessment methodology is used as an alternative to the

traditional worst-case scenario approach to determine the probability and consequence of interference on incumbent terrestrial links. The results using both approaches are presented to analyze the feasibility of spectrum sharing in the 6 GHz and 13 GHz bands.

1.5 Organization

The dissertation consists of six chapters. The remainder of this work has the following structure:

- Chapter 2 presents propagation measurements at 7 and 13 GHz conducted in mixed LOS and NLOS conditions in four urban locations. A path loss model is generated for each frequency and the measurements are compared with empirical models and site-specific models with different clutter and terrain resolutions.
- Chapter 3 conducts case study-based simulations of interference from RLANs to incumbent terrestrial links and vice versa. Measurements of incumbent emissions in a few locations in this area are collected to validate the simulations and analyze the spectrum utilization by incumbents.
- Chapter 4 presents an aggregate interference model to quantify the impact from RLANs to terrestrial and satellite incumbents in the 6 GHz band.
- Chapter 5 applies the aggregate interference model developed in the previous section to calculate the interference from potential RLANs in the 13 GHz bands to current incumbents, which are the same as in the 6 GHz band.
- Chapter 6 provides the conclusions and future work on this topic.

Chapter 2

Path loss measurements at 7 GHz and 13 GHz

2.1 Introduction

In the past, there has been little interest in studying propagation in the 6 and 13 GHz bands due to the traditional fixed spectrum allocation policy in these bands, which were reserved to licensed terrestrial and satellite links. Path loss measurements at 5.8 GHz have been reported in the literature as part of propagation studies in the 5 GHz U-NII-3 band (5.725-5.850 GHz) [20][82]. While path loss models at 5.8 GHz can be reasonably used for coexistence simulations in the lower part of the 6 GHz band, limited propagation studies have been conducted at or around 7 GHz and 13 GHz. One of them is the study by Salous et al. [80], which presents path loss measurements at multiple frequencies from 0.8 to 73 GHz with the purpose of deriving path loss models for 5G networks. It includes narrowband CW path loss measurements at 6 and 10 GHz in urban high-rise and urban low-rise/suburban environments. A recent study by Nabil [65] reports path loss measurements in an indoor environment for very short distances up to 2.5 m. However, none of these studies focus on path loss measurements in an urban scenario at 7 GHz and 13 GHz.

This chapter provides a better understanding on propagation on the 6 GHz and 13 GHz bands, which can be used for coexistence studies between RLANs and incumbent terrestrial links. For that purpose, we conduct narrowband drive tests with a moving receiver and fixed high-raised transmitter at both 7 and 13 GHz for urban and light urban environments. We report measurement results at 7 and 13 GHz in an urban environment and the corresponding fitted path loss model. The measured results are compared with existing deterministic and statistical path loss models. We

compare different terrain and clutter resolutions used in the deterministic model with respect to prediction error.

Deterministic propagation models are site-specific models that incorporate terrain and clutter information. Anderson 2D is a deterministic model based on the use of ray techniques for line-of-sight and obstructed paths. It has been designed to work from 30 MHz to 40 GHz [8][22]. This model is highly accurate, but requires using a software tool, having access to terrain and clutter information and demands higher amount of computation.

Empirical propagation models are statistical models based on large collections of field measurements conducted in different types of scenarios. They provide an average path loss based on the frequency of operation, distance and other parameters, such as height of the base stations and mobile stations, etc. They do not need to consider the terrain and clutter information. Some empirical path loss models that are applicable to these bands and will be analyzed in this chapter are WINNER II [59], close-in (CI) free-space reference distance [86][2], Alpha-Beta-Gamma (ABG) and 3GPP TR 38.901 [1].

There are four key contributions in this chapter. First, we conduct propagation measurements at 7 and 13 GHz in an urban environment and calculate the path loss, which includes the effects of shadowing due to terrain and building obstructions. Second, based on the measurements, we develop a fitted ABG path loss model for each of these frequencies. Third, we compare different terrain and clutter resolutions to determine the adequate resolution for deterministic propagation prediction. Fourth, we compare our measurements against existing empirical models and analyze their pros and cons.

2.2 Measurement system

A narrowband fixed-to-mobile measurement system is setup to measure the path loss at 7 and 13 GHz and analyze how the signal gets affected by variations in terrain and clutter along the path. The transmitter (TX) is fixed on top of a building. The receiver (RX) is mobile, mounted on a car roof and driven around the city, as shown in the block diagram in Figure 2.1.

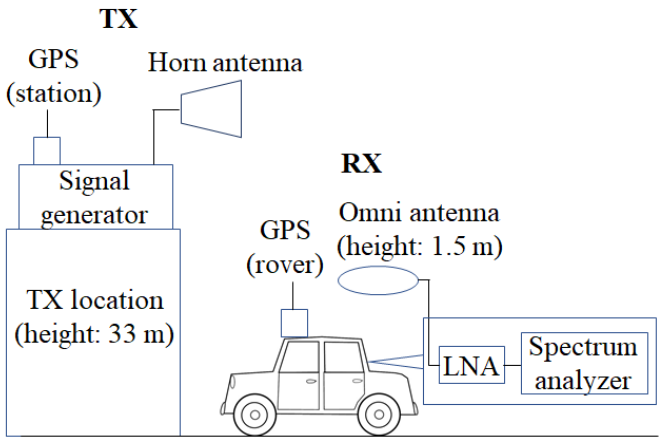

Figure 2.1: Measurement system diagram.

Device	Manufacturer	Model	Description
Signal generator	Agilent	E8267C	Frequency range: 250 kHz to 20 GHz. Transmit power: -130 dBm to +18 dBm
Horn antenna	A.H. Systems	SAS-571	Frequency range: 700 MHz to 18 GHz. Gain: 12dB @7GHz, 13dB @13GHz.

Table 2.1: TX equipment

The transmitter consists of a signal generator and a horn antenna and their characteristics are detailed in Table 2.1. The signal generator is an Agilent E8267C that transmits a continuous wave (CW) signal at 18 dBm. The vertical polarized horn antenna [3] has a maximum gain of 12 dBi at 7 GHz and 13 dBi at 13 GHz. It has a half power beamwidth (HPBW) of 50° on the E-field and 40° on the H-field for 7 GHz and 48° on the E-field and 36° on the H-field for 13 GHz.

The receiver consists of a portable Anritsu MS2760A spectrum analyzer, a low-noise amplifier (LNA) with 36.4 dB and 38.65 dB gain at 7 GHz and 13 GHz, respectively, and an omni-directional antenna with vertical HPBW of 39° for 7 GHz and 46° for 13 GHz [9], as detailed in Table 2.2. The antenna is placed on top of a 2010 Honda Civic that is 1.5 m above ground and the spectrum analyzer is controlled through a tablet, which displays the amplified received signal and records it for further processing. The frequency span of the spectrum analyzer is 20 kHz to tolerate the Doppler shift and the resolution bandwidth (RBW) is 100 Hz. This corresponds to a sweep time

Device	Manufacturer	Model	Description
Spectrum analyzer	Anritsu	MS2760A	Frequency range: 9 kHz to 110 GHz Reference level: -120 dBm to +30 dBm
LNA	Miteq	AFS6-02001800-23-S-6	Frequency range: 2 GHz to 18 GHz Gain: 36.4 dB @7GHz, 38.65 dB @13GHz Noise figure: 1.9 dB @ 7 GHz, 2 dB @ 13 GHz
Omni directional antenna	ARA	CMP-118	Frequency range: 1 GHz to 18 GHz Gain: 3.4dB @7GHz, 4.6dB @13GHz

Table 2.2: RX equipment

of approximately 90 ms. The cable loss and frequency offset for both transmitter and receiver are calibrated before the measurement. The total cable loss is 9.4 dB at 7 GHz and 19.4 dB at 13 GHz.

In order to determine the location of the receiver, an RTK (Real-Time Kinematic) system is used. RTK is a satellite navigation technique that uses two or more GPS receivers in order to provide increased spatial accuracy of up to 1 cm + 1 ppm. We use a fixed base station and a rover station to determine the location based on carrier phase tracking. This offers a comparative advantage over a single GPS receiver option, based on code-based positioning, which achieves an accuracy of approximately 10 m. Since the base station and the rover communicate through a wireless link, usually in the UHF band, the range is limited to approximately 10 to 20 km from the base station, which could decrease depending on the traffic on the these bands and the propagation conditions. Therefore, we also used a single GPS receiver as a backup, in case we notice that the RTK-based location is not consistent with the measurement path. Figure 2.2 shows the transmitter system and Figure 2.3 shows the section of the receiver system that is mounted on top of a car.

2.3 Measurement campaign

The measurements were conducted from November, 2018 to January, 2019 (no leaves on trees). Test data were collected at both 7 and 13 GHz at Boulder and Louisville, Colorado. The transmitter is placed on four locations, three at the University of Colorado (CU) Boulder main campus (urban environment) and one at CableLabs, Louisville (light urban environment), as indicated in Table 2.3.

Figure 2.2: TX system: signal generator, horn antenna and RTK GPS base station

Figure 2.3: Receiver system: omni directional antenna and RTK GPS rover station mounted on a car roof

The data considered in the analysis has a minimum signal-to-noise ratio (SNR) of 10 dB and the noise threshold is -100 dBm.

The first three scenarios in Boulder correspond to an urban residential and commercial area partially obstructed by 2 or 3-story buildings, houses and foliage (evergreen trees). The last scenario

Table 2.3: TX locations and parameters

Location	Latitude	Longitude	Height (m)	Antenna azimuth angle	Antenna elevation angle
CU Boulder, engineering tower, 7th floor	40°0′25.76″ N	105°15′48.16″ W	33	197°	0°
CU Boulder, engineering tower, 8th floor	40°0′26.83″ N	105°15′47.66″ W	27	0°	0°
CU Boulder, University Memorial Center (UMC), 5th floor rooftop terrace	40°0′23″ N	105°16′18.76″ W	17	122°	0°
CableLabs roof, 3rd floor	39°57′26.62″ N	105°9′38.34″ W	10	4°	0°

Figure 2.4: TX locations: a) CU engineering tower, 7th floor, b) CU engineering tower, 8th floor, c) CU University Memorial Center (UMC), and d) CableLabs roof.

is in Louisville, which is less densely populated and corresponds to a light urban area with 2 or 3-story commercial buildings, houses, large parking lots and foliage. The commercial buildings are made of concrete, brick and steel, while the residential buildings are primarily made of a combination of wood, metal studs, brick and concrete. The foliage consists of deciduous trees, such as oaks, maples and elms, which have already shed their leaves, and evergreen trees, such as pines and spruces. The first scenario incorporates hilly terrain and the other three consists of mainly flat terrain. In this work, only the data within the TX antenna HPBW in both azimuth and elevation are analyzed.

2.4 7 GHz Measurements Results

First, we focus on the results obtained for a transmitter placed on the 8th floor terrace of the engineering tower at CU Boulder main campus, at 33 meters above the ground, and transmitting at 7 GHz. The terrain is mostly flat in the measured area and it corresponds to a residential/commercial area partially obstructed by clutter consisting of houses, two or three-story buildings and foliage. The view from the transmit location is presented in Figure 2.5.

Figure 2.5: View from the TX location at the CU engineering tower 8th floor.

Figure 2.6 shows the received power level, P_r, along the driving route, which includes both line-of-sight (LOS) and non-line-of-sight (NLOS) conditions for three-dimensional (3D) TX-RX separation distances ranging from 90 m to 3.3 km. A noise threshold of -100 dBm was measured, which sets the system dynamic range of 160.4 dB. Based on this range, a log-distance path loss

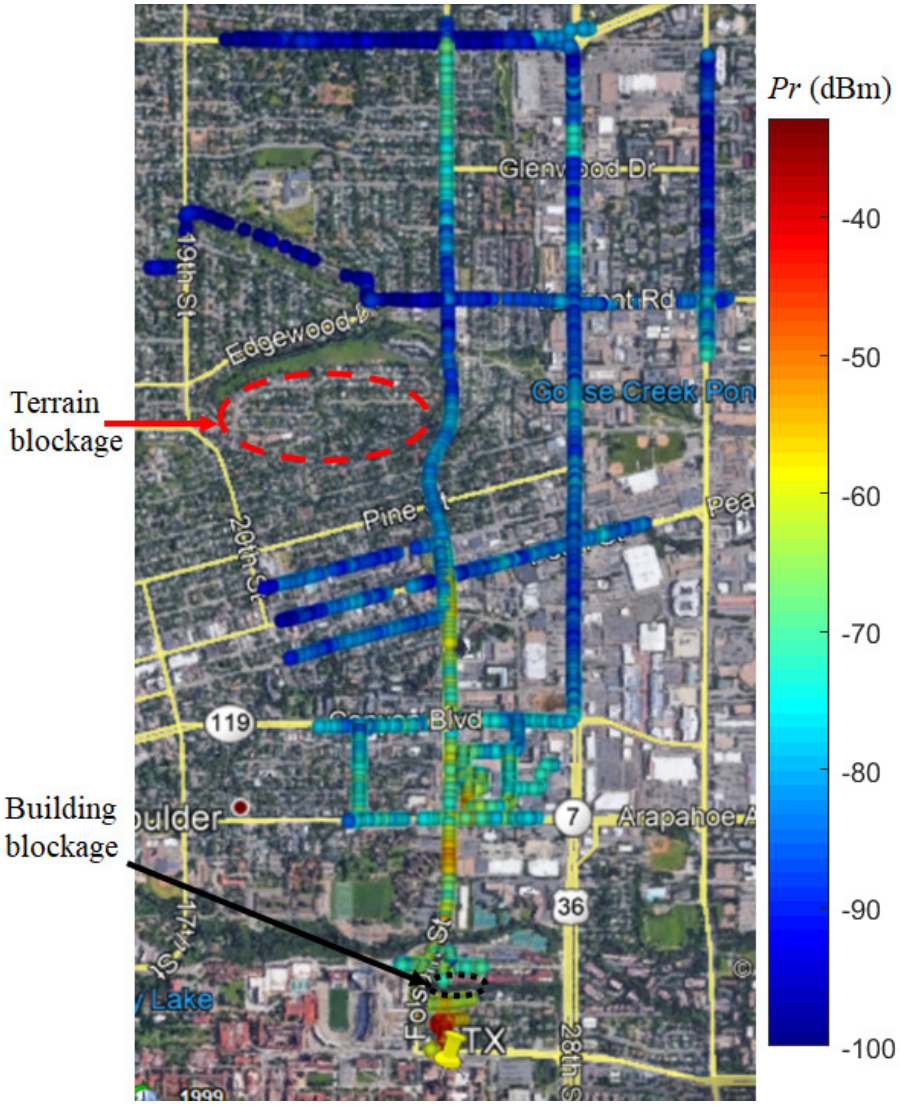

Figure 2.6: RX driving route and received power level within the main beam of the TX antenna, as well as examples of terrain and building blockage.

model is calculated which is then compared with a deterministic model using different terrain and clutter resolutions and empirical models.

2.4.1 Log-distance path loss model

The measured signal includes the effect of multipath fading and shadowing events. To remove multipath fading along the route while preserving large-scale fading for path loss calculation, Lee criterion [60] is used to estimate the local mean with a confidence of 1 dB around the real mean

value. Lee's method consists on averaging at least N samples for each running window $2L$, where $2L$ is between 20λ and 40λ and λ is the wavelength of the signal. Considering $2L$=40λ, the averaging length is 1.7 m. After the small-scale fading is removed, we apply a least-squares linear regression fit to obtain a log-distance path loss model:

$$PL(d) = PL(d_0) + 10nlog_{10}(d/d_0) + X$$

where d_0 is the reference distance of 1 m, n denotes the path loss exponent and X is a zero-mean Gaussian random variable with standard deviation of σ_X. Figure 2.7 presents the linear fit (light blue dashed line) of the measured data (blue dots). The path loss exponent n is 2.57 and the intercept $PL(d_0)$ is 56.7 dB. The shadow fading X has a standard deviation of $\sigma_X = 7.2$ dB, a max value of 25.5 dB and a min value of -27.2 dB.

By comparing Figure 2.6 and Figure 2.7, it can be observed that path loss fluctuations are correlated with terrain and clutter configurations. The terrain is mostly flat up to 2.1 km from the TX and, after that, the direct path is obstructed by a hill on the left side, indicated by the red-dashed circle in Figure 2.6, which causes two shadowing events. Terrain shadowing depth is up to 14 dB and the duration is up to 330 m, as the red-dashed circle indicates in Figure 2.7. More building obstructions are observed, e.g., the black-dotted circle in Figure 2.6. Building shadowing depth is up to 27 dB and the duration is up to 110 m in this shadowing event, which corresponds to a distance between 300 and 410 m from the TX, as indicated by the black-dotted circle in Figure 2.7.

2.4.2 Comparison with a deterministic model with different terrain and clutter resolutions

The simulations using Anderson 2D model have been developed using EDX SignalPro [22] RF planning software, which incorporates different propagation models, terrain and clutter data. Since this propagation model is site-specific and requires geographic information, we compare its performance using different terrain and clutter resolutions.

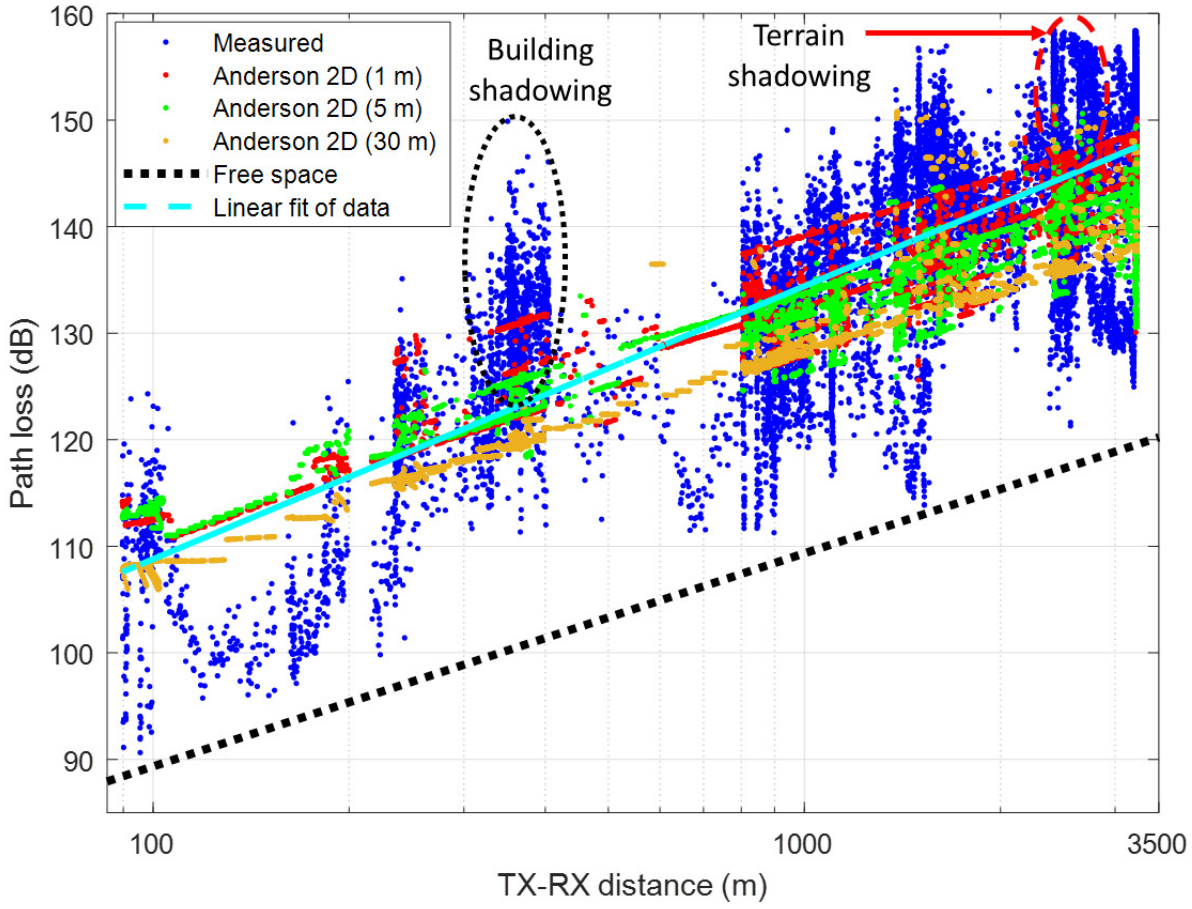

Figure 2.7: Measured path loss for a TX located on the 8th floor of the CU Boulder engineering tower, compared with simulations using Anderson 2D model with different terrain and clutter resolutions at 7 GHz.

For the terrain data, two possible accuracy levels are considered: 30-meter or 10-meter resolution. The Advanced Spaceborne Thermal Emission and Reflection Radiometer (ASTER) Global Digital Elevation Model (DEM) v2 is used for 30-m resolution, which is free for downloading through the Global Data Explorer (GDEx) data access interface [66]. A proprietary high-resolution subscription database [23] is used as the 10-m resolution terrain data based on geodata provided by [24].

Three clutter resolution options are used: 30-meter, 5-meter and 1-meter. For 30-m resolution data, we use the 2011 National Land Cover Database (NLCD) [64], which provides information of the land cover characteristics across the United States at a spatial resolution of 1 arc-second at no cost.

Table 2.4: Anderson 2D simulations using different terrain and clutter resolutions compared with 7 GHz path loss measurements considering a TX located at 33 m above the ground

Propagation model	**Terrain resolution (m)**	**Clutter resolution (m)**	μ**(dB)**	σ_X**(dB)**
Anderson 2D	10	1	-0.7	8
	10	5	-2.8	8.9
	30	30	-4.2	8.5

This database allows adding clutter loss depending on each of the 20-class land cover categories. The same subscription database [23] is used as the 5-m and 1-m resolution clutter data, which offers 64-class land cover classification based on high-resolution satellite imagery. Our simulations do not incorporate 3D building maps and, therefore, the results do not account for additional attenuation due to real buildings in this specific environment. As a result, the path loss simulated is considered conservative, which is useful for coexistence studies.

The following terrain and clutter resolution combinations are used, as indicated in Figure 2.7: a) 30-m terrain and clutter resolution (golden dots); b) 10-m terrain and 5-m clutter resolution (green dots); and c) 10-m terrain and 1-m clutter resolution (red dots). To improve the performance of the model, the clutter loss is tuned based on the data collected from the measurements. The “staircase" pattern in the simulated path loss plot is most noticeable when using the lowest resolution a). In this case, all the path loss measurements within an area of approximately 30 m x 30 m will correspond to only one point in the simulations which leads to the discontinuities. Comparison between measured data and Anderson 2D model with these three resolutions are listed in Table 2.4. As the resolution increases, the mean error reduced from -4.2 to -0.7. The negative sign indicates that the path loss is underestimated, this is likely due to foliage that is not considered in the simulations. Although the measurements were conducted in winter, bare branches of the trees and evergreen trees still slightly obstructed the signal.

Anderson 2D has smaller mean error than any empirical models, but it is complicated to be developed. It requires using a prediction software package and needs access of terrain and clutter databases. The most accurate results are obtained with the highest terrain and clutter resolutions,

10 m and 1 m, respectively, which provide the lowest μ of -0.7 dB and σ_X of 8 dB, but at an expense of higher computational complexity, limited availability and increased cost of high-resolution terrain and clutter databases.

2.4.3 Dual-slope fitted ABG path loss model

A dual-slope fitted ABG model is generated based on the measurements, as shown in Figure 2.8. This model sets a break-point (BP) distance d_{BP} of 100 m, considering that most of the data points measured correspond to distances beyond this value. Based on the ABG model, the intercept point at 100 m is used as an anchor point for the linear least-squares fit, which corresponds to the solid red line in the plot. The intercept point at $d0$=1 m is the free-space path loss value, which permits the model to be tied to physical meaning. The region between 1 m and 100 m is calculated based on a linear interpolation of free-space loss at 1 m and the ABG loss at 100 m and it corresponds to the dotted red line.

The equations that describe the fitted ABG model are detailed in Table 2.5 and the parameters and accuracy compared to the measurements are indicated in Table 2.6. The path loss exponent for distances shorter than d_{BP}=100 m is 2.86, which indicates heavily NLOS conditions. For distances beyond 100 m, the path loss exponent is 3.12. This higher value indicates that the path between transmitter and receiver is more obstructed.

2.4.4 Comparison with empirical models

The path loss measured in the four scenarios described is compared with the free space path loss, the fitted ABG model of the measured data, and empirical propagation models from the literature. Empirical models are validated by limited experimental data at specific conditions such as frequency range, distance range, antenna height and scenario. These empirical models and their limitations are detailed in Table 2.5. In some cases, these models are applicable for distances up to 5 km, TX antenna height of 25 m and, typically, RX antenna height of 1.5 m above the ground.

The accuracy of each model with respect to the measurements is compared in Table 2.6. This

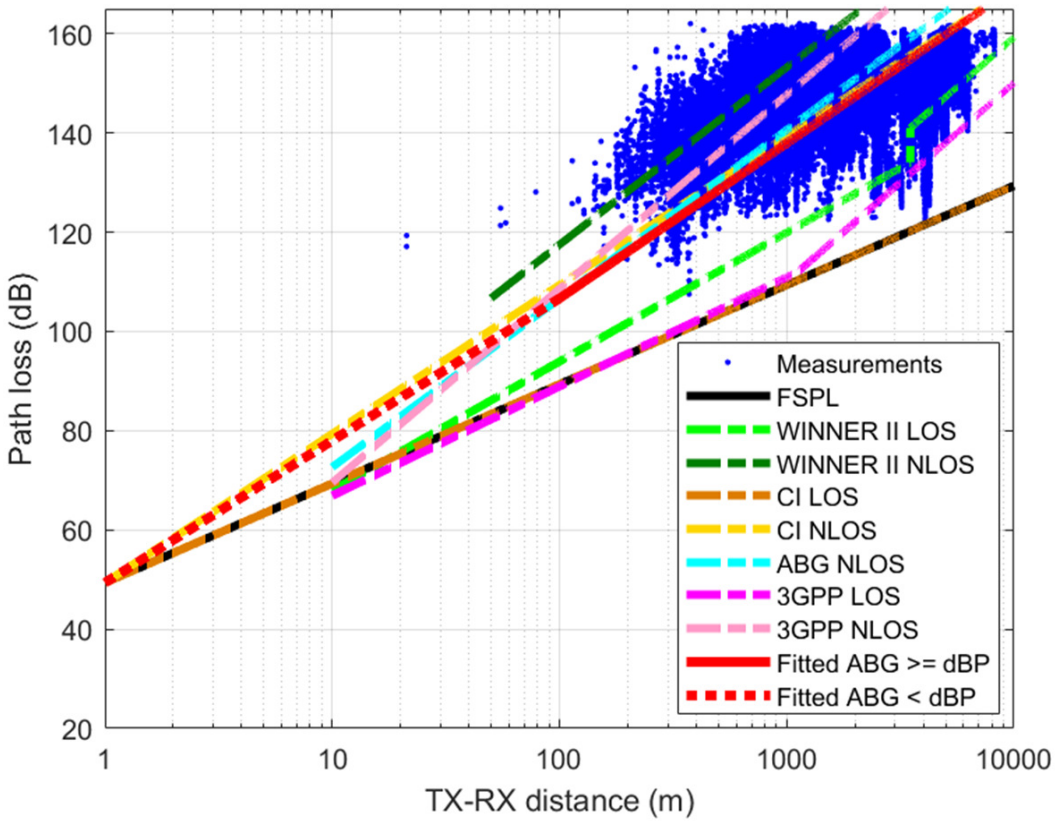

Figure 2.8: Measured path loss in the four scenarios at 7 GHz, compared with empirical propagation models for LOS and NLOS conditions.

table lists the distance range plotted, the path loss exponent n, intercept $PL(d_0)$, mean error μ and standard deviation σ_X of these models. The 7-GHz measurements and fitted ABG model are in mixed LOS and NLOS conditions with relatively high TX. As shown in Figure 2.8, these plots mostly fall between the LOS and NLOS empirical path loss curves. The fitted ABG model has a mean error of -2.5 dB and a standard deviation of 11.6 dB, and this model that represents the mixed LOS/ NLOS environment analyzed in the measurements. The negative sign indicates that the models underestimate the path loss, while the positive sign in the NLOS models show that they overestimate it. The significantly lower value of the standard deviation and lower absolute value of the mean error for NLOS conditions indicate that the RX is in NLOS with the TX for most of the driving path.

WINNER II has been widely used for 3G and 4G cellular design [59]. It is based on experi-

Table 2.5: Empirical Propagation Models for Urban Macrocell environment

Propagation model	**Condition**	**Path loss (dB)**	σ_X **(dB)**	**Applicability**		
				Distance	**Frequency**	**Antenna heights**
Fitted ABG	LOS/ NLOS	$PL = 49.3 + 28.6log_{10}(d) + X$	11.6	1m$<d<$100 m	7 GHz	17$<h_{TX}<$33m, h_{RX}=1.5m
		$PL = 44.1 + 31.2log_{10}(d) + X$		100m$<d<$8.2 km		
		$PL = 54.7 + 29.1log_{10}(d) + X$	10.3	1m$<d<$100 m	13 GHz	
		$PL = 66.4 + 23.2log_{10}(d) + X$		100m$<d<$5.3 km		
WINNER II	LOS	$PL = 39 + 26log_{10}(d) + 20log_{10}(f_c/5) + X$	4	10m$<d<d_{BP}$	2$<f<$6 GHz	h_{BS}=25m, h_{MS}=1.5m
		$PL = 40log_{10}(d) + 13.47 - 14log_{10}(h_{BS} - 1) - 14log_{10}(h_{MS} - 1) + 6log_{10}(f_c/5) + X$	6	$d_{BP}<d<$5 km		
	NLOS	$PL = (44.9 - 6.55log_{10}(h_{BS}))log_{10}(d) + 34.46 + 5.83log_{10}(h_{BS}) + 23log_{10}(f_c/5) + X$	8	50m$<d<$5 km		
Close-in (CI)	LOS	$PL = 20log_{10}(4\pi f/c)+20log_{10}(d)+X$	4.1	Not reported	0.5$<f<$100 GHz	Not reported
	NLOS	$PL = 20log_{10}(4\pi f/c)+30log_{10}(d)+X$	6.8			
ABG	NLOS	$PL = 34log_{10}(d) + 19.2 + 23log_{10}(f_c) + X$	6.5	Not reported	0.5$<f<$100 GHz	Not reported
3GPP	LOS	$PL = 28+22log_{10}(d)+20log_{10}(f_c)+X$	4	10m$<d_{2D}<d_{BP}$	0.5$<f<$100 GHz	h_{BS}=25m, 1.5m$<h_{MS}<$22.5m
		$PL = 28 + 40log_{10}(d) + 20log_{10}(f_c) - 9log_{10}((d_{BP})^2 + (h_{BS} - h_{MS})^2) + X$	4	$d_{BP}<d_{2D}<$5km		
	NLOS	$PL = max(PL_{LOS}, PL'_{NLOS})$, $PL'_{NLOS} = 13.54 + 39.08log_{10}(d) + 20log_{10}(f_c) - 0.6(h_{MS} - 1.5) + X$	6	10m $<d_{2D}<$5km		

Where:

f: central frequency [Hz]; f_c: central frequency [GHz]; $c = 3\times10^8 m/s$ is the propagation velocity in free space
d: 3D TX-RX separation; d_{2D}: 2D TX-RX separation; h_{TX} and h_{BS}: TX antenna height; h_{RX} and h_{MS}: RX antenna height
Break-point distance $d_{BP} = 4(h_{BS} - 1)(h_{MS} - 1)f_c/c$, assuming an effective environment height of 1 m for urban macrocell (UMa)

mental data collected at 2 and 5 GHz, but its range of operation has been extended up to 6 GHz, which is close to our 7-GHz applications. Based on the 7-GHz measured data, WINNER II LOS underestimates path loss by 19.4 dB and WINNER II NLOS overestimates path loss by 13.9 dB,

Table 2.6: Accuracy achieved with different propagation models compared with 7 GHz path loss measurements for the four scenarios considered

Propagation model	**Condition**	**Distance plotted**	**Path loss exponent (n)**	$\boldsymbol{PL(d_0)}$ **(dB)**	$\boldsymbol{\mu}$**(dB)**	$\boldsymbol{\sigma_X}$**(dB)**
Fitted ABG model of data	Mixed LOS/ NLOS	1m$<d<$100m	2.86	49.3	-2.5	11.6
		100m$<d<$8.2km	3.12	44.1		
WINNER II	LOS	10m$<d<$3.5km	2.6	41.9	-19.4	22.9
		3.5km$<d<$8.2km	4	-0.8		
	NLOS	50m$<d<$8.2km	3.57	46	13.9	18.6
Close-in (CI)	LOS	1m$<d<$8.2km	2	49.3	-33.4	34.5
	NLOS	1m$<d<$8.2km	3	49.3	-1.2	10.9
ABG	NLOS	10m$<d<$8.2km	3.4	38.6	1	11.9
3GPP	LOS	10m$<d<$1120m	2.2	44.9	-26.7	29.3
		1120m$<d<$8.2km	4	-10		
	NLOS	10m$<d<$8.2km	3.91	30.4	9.1	16.2

according to Table 2.6.

The CI [2] and ABG models [45] have been developed for 5G channels from 0.5 to 100 GHz, but they are based upon limited measurements in 28, 38, 60 and 73 GHz millimeter-wave bands [76] and ray tracing simulations at 5.6, 10, 18, 28, 39.3, and 73.5 GHz [45]. From Table 2.6, the CI NLOS model provides the lowest standard deviation of 10.9 dB and the second lowest magnitude of μ of -1.2 dB. The CI LOS model underpredicts path loss by 33.4 dB. ABG NLOS provides a standard deviation of 11.9 dB and the lowest magnitude of μ of 1 dB, which indicates that it overestimates path loss by 1 dB.

The 3GPP channel model is based on TR 38.901 [1] as an ongoing work to develop channel models from 0.5 to 100 GHz for 5G systems. However, the measurement parameters and frequency range that validate the 3GPP model are not reported. Based on our evaluation, the 3GPP LOS model underpredicts path loss by 26.7 dB and the 3GPP NLOS model overpredicts path loss by 9.1 dB.

After comparing the different path loss models in Table 2.6, the CI NLOS model and the dual-slope fitted ABG model are the ones that best represent the measurements, because they have the lowest standard deviation. They are both very similar and underpredict the path loss and, hence,

overpredict the interference, which provides a more conservative approach in coexistence studies. The third model that best fits the measurements is the ABG NLOS model, which underpredicts the path loss by 1 dB and, therefore, overpredicts the interference. These models are followed by the 3GPP models and the WINNER II models.

2.5 13 GHz Measurements Results

The 13 GHz measurements have been conducted in the same four scenarios as the 7 GHz measurements. However, it has a limited distance only up to 5.3 km due to the increased path loss at higher frequencies and limited LNA gain.

2.5.1 Dual-slope fitted ABG path loss model

The dual-slope fitted ABG model is calculated based on the 13 GHz path loss measurements. Figure 2.9 shows the measured path loss data (blue dots) at 13 GHz, the free-space path loss (black solid line), empirical path loss models and the dual-slope ABG fit of the data, which corresponds to the red dotted line and red solid line for distances shorter and longer, respectively, than the break-point distance (d_{BP}) of 100 m.

Table 2.5 presents the equations for each of these sections. The path loss exponent for a distance lower than 100 m is 2.91, which indicates that most of the data points are in NLOS conditions. For distances beyond 100 m, the path loss exponent gets reduced to 2.32, because the NLOS data points are affected by higher path loss at 13 GHz, which can produce received signal levels below the noise floor and, hence, cause a lower rate of NLOS data points with respect to LOS data. The accuracy of the model is measured using the standard deviation σ_X and the mean error μ_X, which have values of 10.3 dB and -2.5 dB, respectively, as indicated in Table 2.7.

2.5.2 Comparison with empirical models

The 13 GHz measurements in the four scenarios are also compared with empirical propagation models, as shown in Figure 2.9. Although the WINNER II model has been designed based on

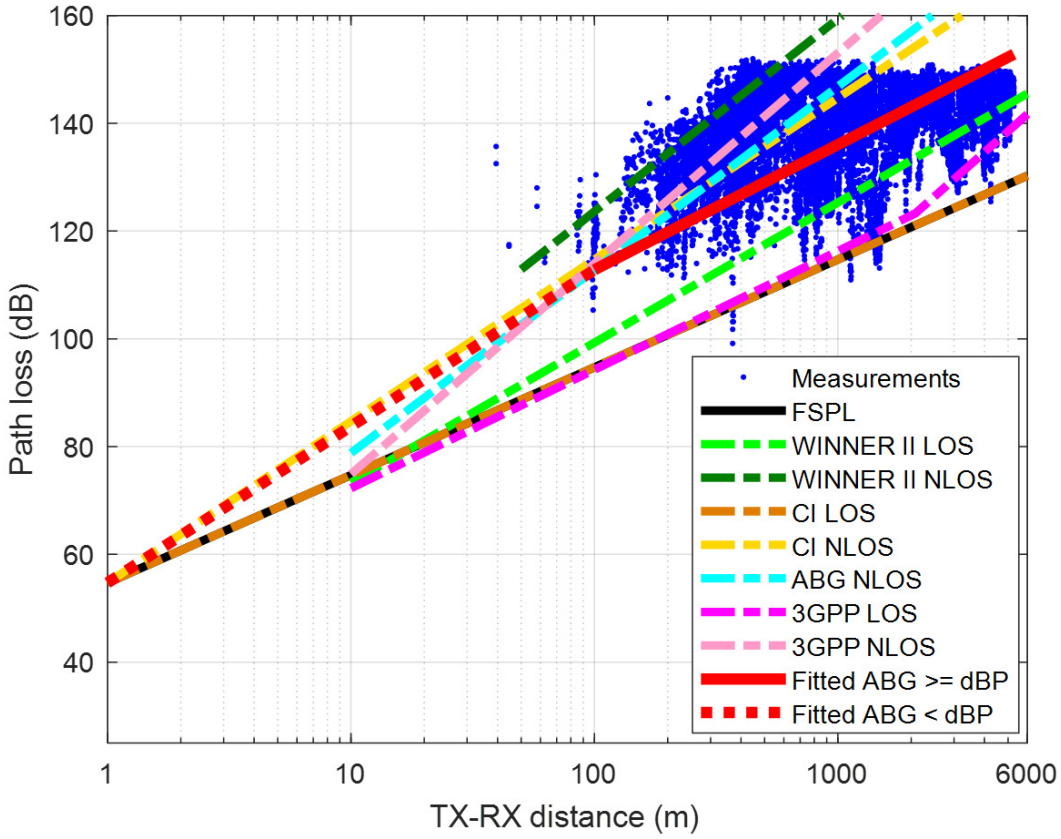

Figure 2.9: Measured path loss in the four scenarios at 13 GHz, compared with empirical propagation models for LOS and NLOS conditions.

measurements up to 6 GHz, it can be applied to the data at 13 GHz to analyze how well it performs outside its frequency range. Table 2.7 indicates the path loss exponent n and intercept $PL(d_0)$ for each empirical model in LOS and NLOS conditions, as well as the mean error μ and the standard deviation σ_X to quantify their accuracy. LOS models underestimates the path loss, as can be noted by the negative sign of μ, while NLOS overestimates the path loss, which underpredicts the interference.

Under LOS conditions, WINNER II, CI and 3GPP models underestimate the path loss by 13.2 dB, 23.8 dB and 21.3 dB, respectively. They show a higher absolute value of the mean error and a higher standard deviation compared with the NLOS case, which suggests that the signal is mostly affected by NLOS conditions. In NLOS conditions, WINNER II, CI, ABG and 3GPP models overestimate the path loss by 21 dB, 6.3 dB, 8.5 dB and 14.7 dB, respectively. Among the empirical

models and similarly to the 7 GHz measurements, the CI model is the one that has the lowest mean value and standard deviation, followed by ABG, 3GPP and the WINNER II models.

Table 2.7: Accuracy achieved with different propagation models compared with 13 GHz path loss measurements for the four scenarios considered

Propagation model	**Condition**	**Distance plotted**	**Path loss exponent (n)**	**$PL(d_0)$ (dB)**	**μ(dB)**	**σ_X(dB)**
Fitted ABG model of data	Mixed LOS/ NLOS	1m$<d<$100m	2.91	54.7	-2.5	10.3
		100m$<d<$5.3km	2.32	66.4		
WINNER II	LOS	10m$<d<$5.3km	2.6	47.3	-13.2	16.7
	NLOS	50m$<d<$5.3km	3.57	52.2	21	24.9
Close-in (CI)	LOS	1m$<d<$5.3km	2	54.7	-23.8	25.3
	NLOS	1m$<d<$5.3km	3	54.7	6.3	13.1
ABG	NLOS	10m$<d<$5.3km	3.4	44.8	8.5	15.3
3GPP	LOS	10m$<d<$2.1km	2.2	50.3	-21.3	23.6
		2.1km$<d<$5.3m	4	-9.4		
	NLOS	10m$<d<$5.3km	3.91	35.8	14.7	20.7

2.6 Discussion

We have developed empirical path loss models at 7 GHz and 13 GHz based on field measurements in four urban locations. This model corresponds to mixed LOS/NLOS conditions and is based on a dual-slope ABG linear least-squares fit of the measured path loss. This fitted ABG model has been compared with a deterministic model with different terrain and clutter resolutions and empirical path loss models in an urban environment. The deterministic model used is Anderson 2D, which is site-specific and incorporates terrain and clutter information through a RF planning software. We used 30-m and 10-m terrain resolution and clutter resolutions of 30 m, 5 m and 1 m, which have been tuned according to the experimental data. Anderson 2D provides more accurate prediction than the empirical models. Since it does not incorporate a building database nor simulate foliage loss, it underpredicts path loss by 0.7 to 4.2 dB for one specific scenario at 7 GHz. As expected, the highest terrain and clutter resolutions of 10 m and 1 m, respectively, provide the most accurate prediction at an expense of increased computation complexity and higher database costs. The empirical models include WINNER II, CI, ABG and 3GPP in both LOS and NLOS

conditions. LOS models underestimate the path loss and conservatively overpredict the interference, while NLOS models overestimate the path loss and underpredict the interference. In both frequencies, CI is the model that provides the closest prediction but all the other models can be used as well, including WINNER II in the 13 GHz band. These results are helpful for future spectrum sharing studies in these bands, with the ultimate purpose of evaluating the coexistence between incumbents and unlicensed devices.

Chapter 3

Coexistence simulations between RLANs and fixed microwave links in the 6 GHz and 13 GHz bands based on a case study

3.1 Introduction

The purpose of this chapter is to analyze coexistence between RLANs and current terrestrial fixed links in the 6 and 13 GHz bands based on a case study approach, which can be replicated to other parts of the country. The coexistence analysis uses information from real links and accounts for the terrain morphology and actual land use to calculate the potential interference. We have conducted interference simulations from low-power indoor (LPI) RLANs to terrestrial fixed links and vice versa, from terrestrial fixed links to LPI RLANs, in the Denver metro area. The simulations have been performed in the 6 GHz U-NII-8 band, from 6875 to 7125 MHz, and in the 13 GHz band, from 12700 to 13250 MHz. To validate the simulations, we measured the incumbent signal power detected on the ground in a few locations in this area.

Various stakeholders have provided comments to the FCC regarding coexistence in the 6 GHz band, as indicated in chapter 1. Most of these studies, however, do not incorporate real terrain and clutter information within the area of interest to calculate the interference, which would provide a more precise simulation of the sharing scenario. Some studies make very optimistic assumptions that favor spectrum sharing, while some others are based on a single realization of very unlikely scenarios, in both cases without considering site-specific information and real data from incumbents and unlicensed devices.

One of the main contributions of this chapter is the development of a case study methodology

based on data from real incumbent links and from real terrain and clutter information to simulate the interference from potential RLANs and vice versa. Additionally, our study complements previous reports submitted to the FCC by performing measurements to validate the simulations and analyze the actual use of the spectrum in these bands. Finally, we provide some guidelines for allowing spectrum sharing with fixed point-to-point links in these bands.

3.2 Methodology

Fixed microwave links use high-gain, narrow-beamwidth antennas and are usually placed at elevated heights. This indicates the possibility that little radiated energy from these links is detected on the ground and vice versa and, therefore, spectrum sharing with RLANs might be possible. Only indoor APs are considered, as suggested by the FCC for the U-NII-8 band. Fixed incumbent services in the 6 and 13 GHz bands are classified into fixed microwave and fixed BAS and CARS. Within these bands, fixed microwave operates in both, fixed BAS operates in the U-NII-8 and the 13 GHz band and fixed CARS operates in the 13 GHz band only.

In this chapter, we analyze the interference between fixed point-to-point links and future RLANs in the U-NII-8 band and the 13 GHz band based on a case study approach in the Denver metro area. The simulated area corresponds to a 70x70 km^2 area. The list of all active links in this area is obtained from the FCC's Universal Licensing System (ULS) database [28], which contains information such as the transmitter and receiver location, transmit power, frequency of operation, antenna heights and gains and azimuth and elevation angles. The FCC's Site/ Market/ Frequency database [26] was also queried to determine if CARS links were present, which was not the case. In the area analyzed, all the fixed 6 GHz U-NII-8 and 13 GHz links are BAS links and there are no fixed point-to-point links or fixed CARS links. There are 51 fixed BAS links in the U-NII-8 band and 45 fixed BAS links in the 13 GHz band in this area. Each BAS channel has a bandwidth of 25 MHz.

The point-to-point links are highly directional. The average antenna gain is 40.7 dBi for the U-NII-8 band and 43.8 dBi for the 13 GHz band, according to the ULS database. The transmit

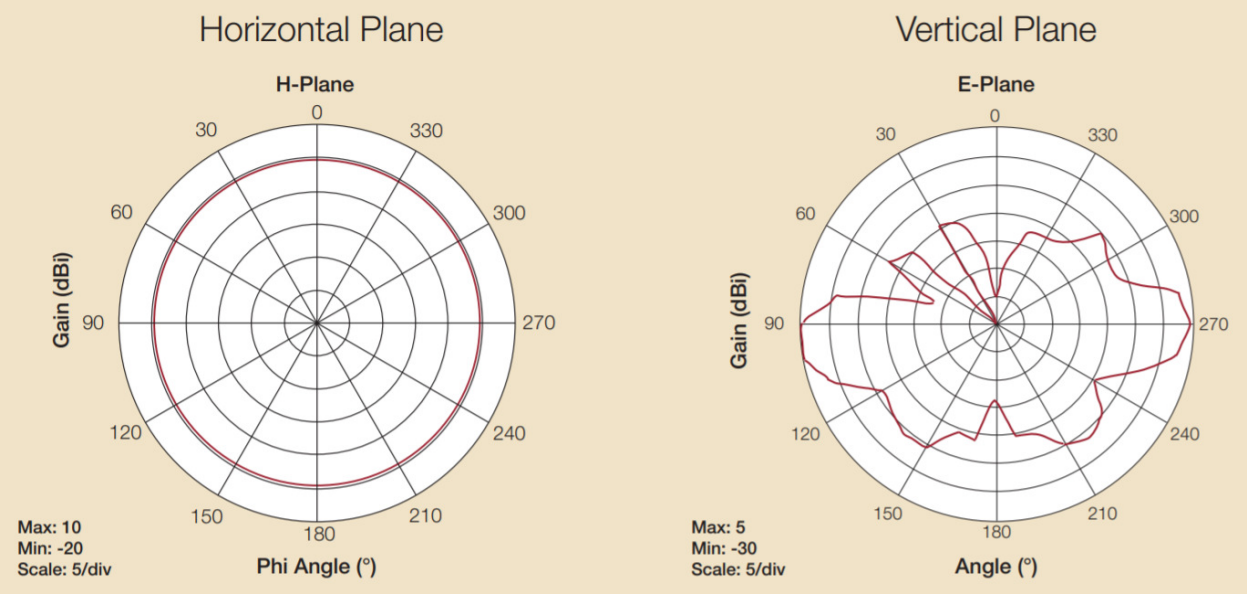

Figure 3.1: Antenna pattern of the Ruckus AT-0636-VP 5 GHz omni directional antenna

power ranges from 26 to 35 dBm for U-NII-8 and from -15 to 35 dBm for 13 GHz. The incumbent antenna can be located a few meters above the ground on a mountain or on top of a building, up to 244 meters height.

For simplicity and lack of complete antenna information in the ULS database for each BAS link, we only simulate one representative commercial antenna for each band. In the 6 GHz band, we consider Commscope HSX6-64/B antenna, which has 40 dB gain and 1.7° horizontal and vertical half-power beamwidth (HPBW). For the 13 GHz, we simulate Commscope P6-122G antenna, which has 45.4 dB gain and 0.9° horizontal and vertical HPBW. A representative 5 GHz Wi-Fi antenna is considered for the simulated RLANs. We have selected Ruckus AT-0636-VP 5.15 - 5.875 GHz omni-directional antenna [79], which has 5.5 dBi gain and has been used in previous interference studies [44]. The horizontal and vertical plane of the antenna pattern is shown in Figure 3.1.

EDX SignalPro planning software is used to calculate the interference received by either BAS links or RLAN devices in the Denver metro area. We select the Anderson 2D propagation model [8] because it is a physical, site-specific model that incorporates terrain and clutter information. For the terrain database, we use the Advanced Spaceborne Thermal Emission and Reflection Radiometer

(ASTER) Global Digital Elevation Model (DEM) v2 [66], which provides terrain information at 30-meter resolution. It can be downloaded for free using the Global Data Explorer (GDEx) data access interface. For the clutter database, we use the 2011 National Land Cover Database (NLCD) [64], which classifies the land use in the United States into 20 categories at a resolution of 1 arc-second, which is approximately 30 meters. To calculate the interference, we use Python, including Pandas data analysis library, and MATLAB.

First, the aggregate interference from indoor RLAN emitters to fixed BAS links is calculated. Then we simulate how much the potential indoor RLAN devices in these proposed bands will be affected by the incumbents. The interference results are mapped against the 2020 United Nations' World Population Prospects (UN WPP) Adjusted Population Density [14], calculated at a resolution of 30 arc-seconds (approximately, 1 km). Finally, to validate the simulations, the received signal power from fixed BAS transmitters is measured at a few locations in the Denver metro area. The measurements are also useful to study the actual spectrum utilization in the area of interest.

3.3 Simulations of Aggregate Interference from RLANs to terrestrial links

To estimate the interference to fixed incumbent links in the Denver metro area, we calculate the aggregate Wi-Fi emissions detected by each fixed BAS receiver in both the 6 GHz U-NII-8 and the 13 GHz bands. The Wi-Fi and propagation parameters assumed for these simulations are detailed in Table 3.1 and are based on statistical data and projections.

As indicated in Table 3.1, the Wi-Fi channel bandwidth considered in the simulations is the weighted average of the Wi-Fi channel bandwidth distribution indicated in Table 3.2, which is 142 MHz. This distribution is based on the ECC report 302 [21], which has been modified to include channel bandwidths up to 320 MHz, as suggested by the FCC [39].

A uniform probability of spectrum usage throughout all the current and proposed unlicensed bands for Wi-Fi is assumed. Current Wi-Fi spectrum is 563.5 MHz: 83.5 MHz in the 2.4 GHz band and 480 MHz in the 5 GHz band. The proposed expanded Wi-Fi spectrum will open additional 1750 MHz of spectrum: 1200 MHz in the 6 GHz band, from which 250 MHz corresponds to the

Table 3.1: Simulation parameters

Parameter	**Band**	
	6 GHz U-NII-8	13 GHz
Year simulated	2026	2028
Market penetration rate	68%	
Population per household	2.48	2.46
Internet usage ratio	88.7%	91.28%
Maximum power spectral density (dBm/MHz)	5	8
Weighted average EIRP (dBm)	17.3	17.68
RLAN airtime utilization	4%	
Channel bandwidth (MHz)	142	
Propagation model	Anderson 2D	
Terrain and clutter resolution	30 meters	
Building entry loss (dB)	22.5	24.1
Antenna polarization mismatch (dB)	3	
AP height (m)	1.5	

Table 3.2: Probability distribution of Wi-Fi channel bandwidth

Bandwidth (MHz)	20	40	80	160	320
Probability	0.1	0.1	0.3	0.3	0.2

U-NII-8 band, and, once the 6 GHz band is available for RLANs, 550 MHz in the 13 GHz band.

The maximum power spectral density is 5 dBm/MHz in the U-NII-8 band, as recently proposed by the FCC [39], and 8 dBm/MHz in the 13 GHz band, considering the higher path loss and, hence, lower interference. The simulations incorporate an EIRP distribution based on the ECC report 302 [21], that considers different types of AP, such as enterprise AP, consumer AP and high performance gaming router, which determines the conducted power, antenna gain and antenna radiation pattern. The weighted average EIRP is 17.3 dBm and 17.68 dBm for 6 GHz and 13 GHz, respectively.

The simulations are projected for 2026 in the case of the 6 GHz band and 2028 for the 13 GHz band, which corresponds to five years after the assumed opening of these bands for unlicensed use, in 2021 and 2023, respectively. The population number in 2026 and 2028 considers a population

growth of 1.04% and 1.06%, respectively, from 2020 [93]. The total number of APs is calculated assuming one AP per household with Internet access and an average of 2.48 people per household in 2026 and 2.46 people per household in 2028, as projected based on [95]. The Internet usage ratio will be 88.7% and 91.28% in 2026 and 2028, respectively, based on [72]. This is a conservative value that would overestimate the I/N, as the statistics refer to Internet access, not only through Wi-Fi, and the data considers people older than 3 years old instead of the entire population. The market adoption rate five years after making these bands available for unlicensed use is assumed to be 68%, based on the percentage of 5-GHz capable AP shipments per year since dual band Wi-Fi was introduced [4]. This value is conservative and overestimates the interference, as it only accounts for the percentage of new shipments instead of the total number of APs available.

The Wi-Fi airtime utilization provides a conservative estimate of the AP duty cycle, which is impacted by human-driven usage and the 802.11 protocol. The average airtime utilization in the busy hour used in the simulations is 4%, which is a conservative value supported by current incumbents [78]. According to empirical data from 2016 [99], it is expected that the airtime utilization will decrease with higher peak data rates due to lower channel occupation.

The average building penetration loss is computed according to 3GPP TR 38.901 [1]. Low-loss buildings consist of 30% standard glass windows and 70% concrete exterior walls, while high-loss, modern buildings have 70% energy efficient Infrared Reflective (IRR) glass windows and 30% concrete exterior walls. Loss through standard glass windows, IRR glass and concrete increase with the frequency. Considering a 50% probability for low-loss and high-loss buildings [1], the average building penetration is 22.5 dB at a central frequency of 7 GHz and 24.1 dB at 13 GHz. We assume a polarization mismatch of 3 dB between the incumbent receiver antenna and the RLAN antenna [87]. While RLAN antennas have dual polarization, BAS antennas have either horizontal or vertical polarization, which causes a coupling loss of up to half the power emitted.

The flowchart of the methodology is shown in Figure 3.2. First, all the APs are randomly assigned a 142-MHz weighted average Wi-Fi channel bandwidth and a weighted average EIRP of 17.3 dBm and 17.68 dBm for the 6 GHz and 13 GHz bands, respectively, according to Table

3.1. Using the parameters of the BAS receivers obtained from the ULS database, we calculate the frequency overlap between a weighted average Wi-Fi channel bandwidth of 142-MHz and a 25-MHz BAS channel. The operation of each AP is defined by the Wi-Fi parameters indicated in the previous section. Next, all the APs inside a $30m \times 30m$ area are assigned a unique location in the center of this square. This area corresponds to the resolution of the terrain and clutter databases used in the simulations and the number of APs in it is determined by the population density. Then, using EDX SignalPro and considering the propagation parameters indicated in the previous section, we estimate the path loss from all the Wi-Fi APs to each fixed BAS receiver and incorporate the building entry loss. This step generates large files used to calculate the path loss from each AP to each BAS receiver. Using the path loss, we calculate the aggregate Wi-Fi emissions from all the potential APs operating in the U-NII-8 and 13 GHz bands in this area to each BAS receiver. To simulate the variability due to the selection of random Wi-Fi channels, Monte Carlo simulations are conducted. Considering the intensive computation requirements, this process is repeated 50 times, which is enough to calculate the complementary cumulative distribution function (CCDF) of the aggregate interference from all the APs in the study area to each BAS receiver operating in these bands.

The interference protection criteria determine the maximum interfering signal level to allow a tolerable performance degradation of the incumbent link and maintain availability. The criteria depend on the type of service of the victim station, the type of interfering signal (noise-like, pulse, continuous wave, impulse, etc.) and how often it occurs. The maximum tolerable interference in the incumbent BAS receivers is calculated based on an interference protection criterion of I/N = -6 dB [70], as suggested by the FCC [39], which requires the interference to be at least 6 dB below the noise floor of the receiver. To calculate this noise floor, one representative radio was selected for each band, based on the information available at the ULS database. We select MRC DAR6 radio for the 6 GHz band and MRC DAR12 for the 13 GHz band [63], which have a noise figure of 3.5 dB and 4 dB in the 6 GHz and 13 GHz bands, respectively. Then, based on the 25-MHz BAS channels, the incumbent receiver noise floor is -96.5 dBm and -96 dBm in the 6 GHz and 13 GHz

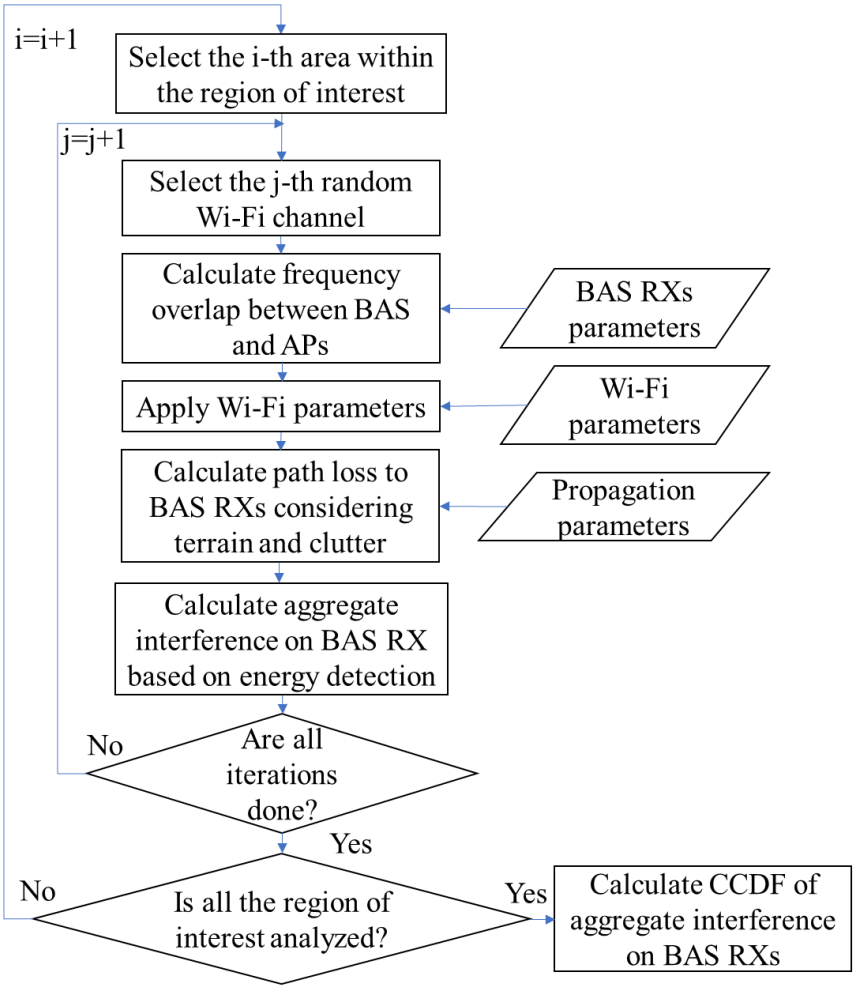

Figure 3.2: Flowchart used to calculate the aggregate interference from Wi-Fi APs to BAS receivers.

bands, respectively. Considering a aggregate I/N threshold of -6 dB, the maximum interference level allowed will be -102.5 dBm and -102 dBm for the 6 GHz and 13 GHz bands, respectively.

The total population in the Denver metro area in 2020 was approximately 3.2 million and, according to the simulation parameters, the estimated number of APs in 2026 and 2028 will be 1.17 million and 1.21 million, respectively. The results of the aggregate RLAN interference are shown in Figure 3.3. The maximum I/N in all the BAS links is -18 dB in the U-NII-8 band and -29 dB in the 13 GHz band. The I/N threshold of -6 dB is not exceeded in the simulation, which will guarantee the availability of the BAS links in this area.

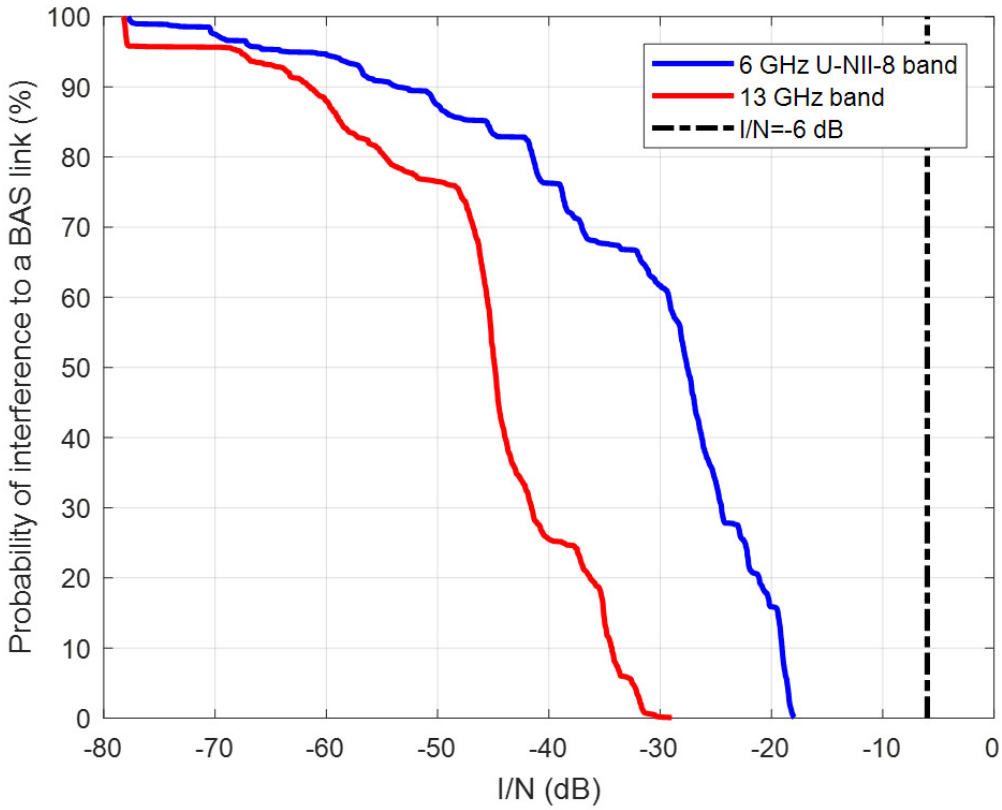

Figure 3.3: Percentage of BAS links impacted by aggregate interference from indoor RLANs at 1.5 meters height in the Denver metro area.

3.4 Simulations of Interference from terrestrial fixed links to RLAN devices

This section calculates the percentage of population that will be potentially affected by interference from fixed BAS links in the Denver metro area. Figure 3.4 presents the flowchart used, which follows a similar method as the one in the previous section. The main difference is that this simulator considers the BAS transmitters instead of the receivers to calculate their impact on the APs. The path loss calculation is also based on simulations using EDX SignalPro, which estimates the terrestrial coverage of all the fixed BAS links operating in U-NII-8 and 13 GHz bands in the Denver metro area. Next, based on the population density, we calculate the amount of people that will be potentially affected by this interference. Then, we estimate the CCDF of the population that will be affected by BAS emissions in the Denver metro area. Since additional indoor wall loss is not considered in the simulations, the energy detected by future indoor APs is expected to be

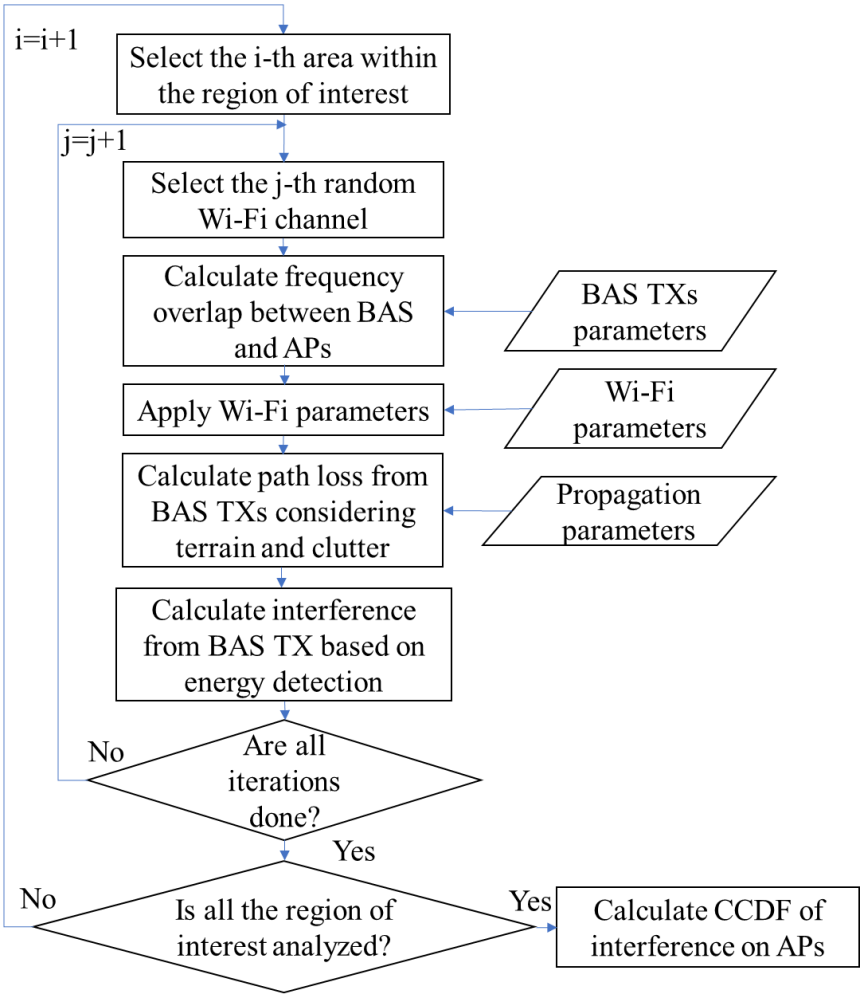

Figure 3.4: Flowchart used to calculate the interference from BAS TXs to Wi-Fi APs.

lower.

Interference affects the throughput and latency in Wi-Fi devices. To assess the impact of incumbent BAS links on them, we use Clear Channel Assessment (CCA) sensitivity thresholds and Modulation and Coding Scheme (MCS) tables. For 802.11ac, the CCA energy detection (ED) threshold of -62 dBm indicates the minimum interference level at which the Wi-Fi device will sense a 20 MHz channel as busy and back off data transmission. A CCA signal detection (SD) threshold of -82 dBm for a 20 MHz channel indicates the minimum 802.11 received signal power that can be decoded using BPSK modulation, which is the lowest modulation scheme. The analysis presented considers a 20 MHz Wi-Fi channel bandwidth because it provides the lowest CCA signal

detection threshold, which determines the maximum interference allowed based on bit-error rate (BER) curves. For example, a BER of 10^{-6} corresponds to a Eb/N0 of 10.5 dB for BPSK in an AWGN channel. Higher modulation schemes require higher Eb/N0 values. Using these parameters, the maximum interference allowed to maintain a BER of 10^{-6} using BPSK should be -92.5 dBm. Higher Wi-Fi channel bandwidths require higher CCA signal detection thresholds. Using a Wi-Fi channel bandwidth of 160 MHz and maintaining the other parameters, the CCA signal detection threshold is -73 dBm, which determines a maximum interference of -83.5 dBm.

Figure 3.5 presents the percentage of population that might be impacted by BAS emissions in the Denver metro area, considering 20-MHz Wi-Fi channels. The maximum level of interference to an AP operating in a 20-MHz channel is -95 dBm in the U-NII-8 band and -116 dBm in the 13 GHz band, which are lower than the -92 dBm value calculated before for BPSK with maximum BER of 10^{-6}. For higher modulation schemes considering the same Eb/N0, the BER will increase. Consequently, incumbent BAS links could potentially cause a small impact on indoor Wi-Fi networks in the U-NII-8 band and, considerably less likely, in the 13 GHz band, but they would still be able to operate either at a lower throughput or with an increased BER. However, it should be noted that these simulations are very conservative and do not consider additional loss due to internal walls and vegetation.

3.5 Measurements of Potential Interference from Incumbent Fixed Links

BAS emissions were measured at a few locations in the Denver metro area for both the U-NII-8 and the 13 GHz bands. The purpose is to validate the simulations and estimate the potential interference from fixed BAS links. Most of the measurements were conducted at a relatively small distance to the BAS transmitter and in line-of-sight with it. These measurements are useful to study how much power and bandwidth are effectively used by these incumbents. The measurement system consists of an Anritsu MS2760A spectrum analyzer and a vertical polarized horn antenna of 12 dBi and 13 dBi gain at the 6 GHz and 13 GHz bands, respectively, which were described in the previous chapter.

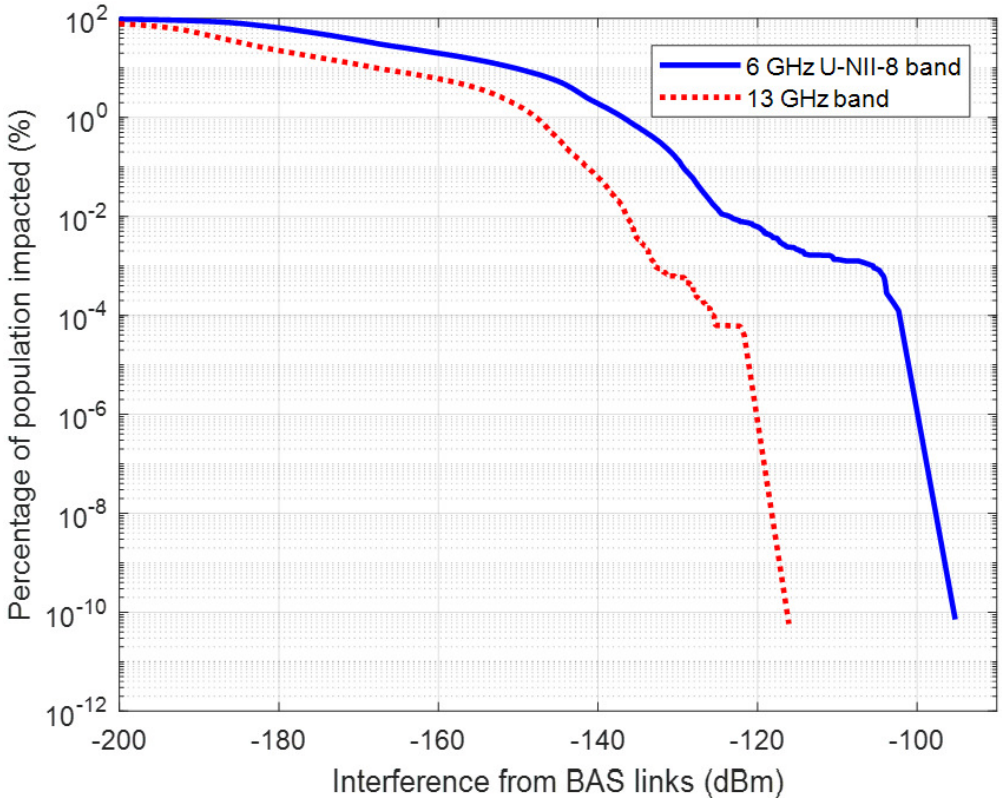

Figure 3.5: Flowchart used to calculate the aggregate interference from APs to incumbent FS and MS links.

Different measurement locations were identified in the Denver metro area and the received signal level was measured at 1.5 meters above the ground. Figure 3.6 shows an example of a measurement location 116 meters away from the BAS transmitter station with callsign KTZ95. This link operates in the 7062.5 MHz channel and is licensed for TI (TV Intercity Relay). We are positioned along the direct path between the transmitter and the receiver, but below the height of the main beam. The transmit antenna used in BAS links is highly directional (40.5 dB gain and 1.3° HPBW). The receiver station is on top of Lookout Mountain. Figure 3.7 shows the spectrum of the signal measured at this location. According to its emission designation, 25M0F8W, it is a FM signal that can occupy a maximum bandwidth of 25 MHz. We observe that the received signal power is low, approximately -90 dBm in the street without any obstacle. The bandwidth used is less than 1 MHz, which is significantly lower than the 25 MHz licensed by the FCC. We repeated this

Figure 3.6: BAS fixed link and measurement location.

measurement three times in different months and the bandwidth occupation was the same, which would indicate that the spectrum assigned is not being used at its full capacity. Out of the six BAS transmitters for which their measured emissions were above the noise floor of the spectrum analyzer, only in one case the broadcasters were using the full 25 MHz bandwidth, as shown in Figure 3.8. The other five links were using significantly less spectrum than that. This indicates that it is likely that a significant amount of licensed links might not be actively used.

A summary of the measurements results is presented in Table 3.3. It indicates the location of each fixed BAS transmitter, the measurement location and, for each of them, it compares the received signal power obtained from the simulations with the average measurements. The same measurement locations were considered for both bands, but due to the limited range at 13 GHz, the measured signal was above the noise floor in only one case. Measured BAS emissions are always lower than the values obtained from the simulations and they are up to 22 dB lower in the U-NII-8 band, which indicates that the simulations are very conservative. The reason could be due

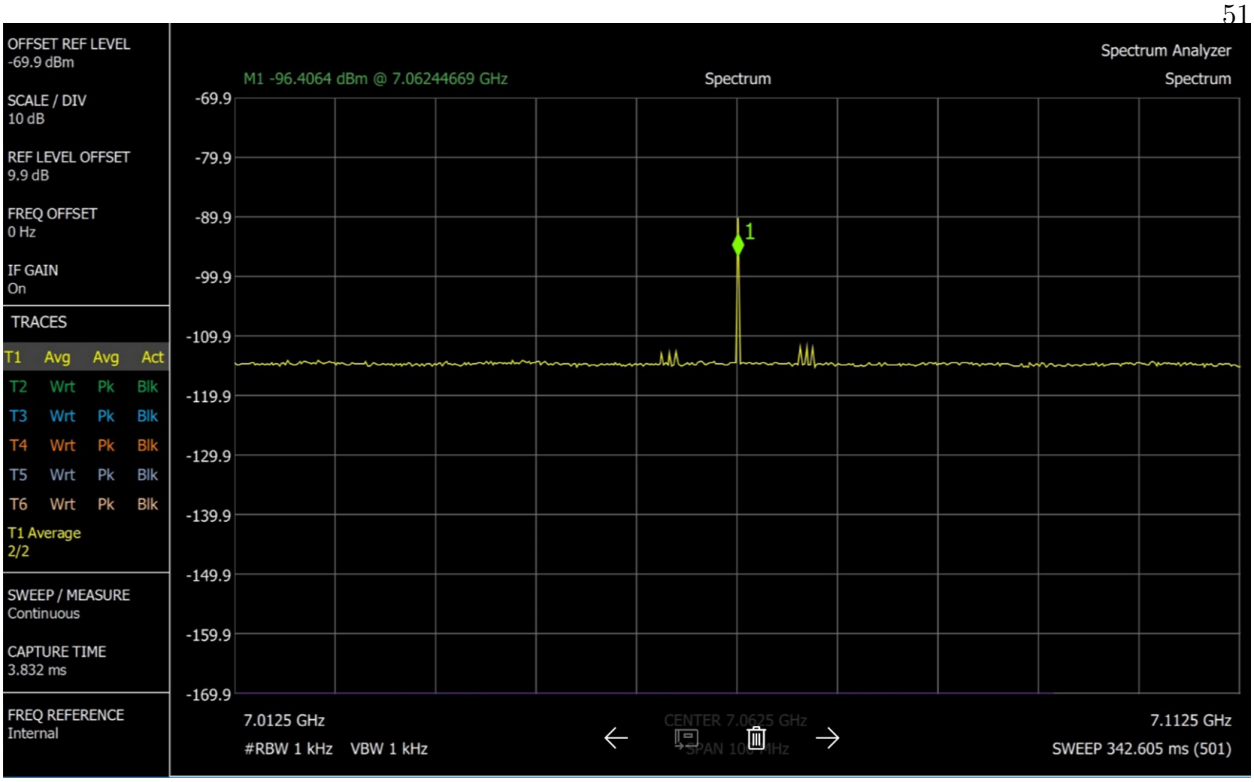

Figure 3.7: BAS emissions at 7062.5 MHz.

to partial or total obstructions by buildings, trees and other structures, which are not included in the simulations. This difference could also be due to a lower BAS transmission power than the maximum allowed in its license.

3.6 Discussion

In this chapter, we have analyzed the coexistence between low-power indoor RLANs and fixed microwave links in the 6 GHz U-NII-8 band and the 13 GHz band as a case study in the Denver metro area. In this area, all the fixed microwave links in these bands are BAS links. We have developed a simulator that uses real information of all the incumbent links in this area and incorporates terrain and clutter information to calculate the interference between them. Our simulations show that coexistence in the 6 GHz U-NII-8 band is possible for low power indoor APs operating at a maximum power spectral density of 5 dBm/MHz in U-NII-8 and 8 dBm/MHz in 13 GHz and a maximum Wi-Fi channel bandwidth of 320 MHz, according to the FCC. A interference

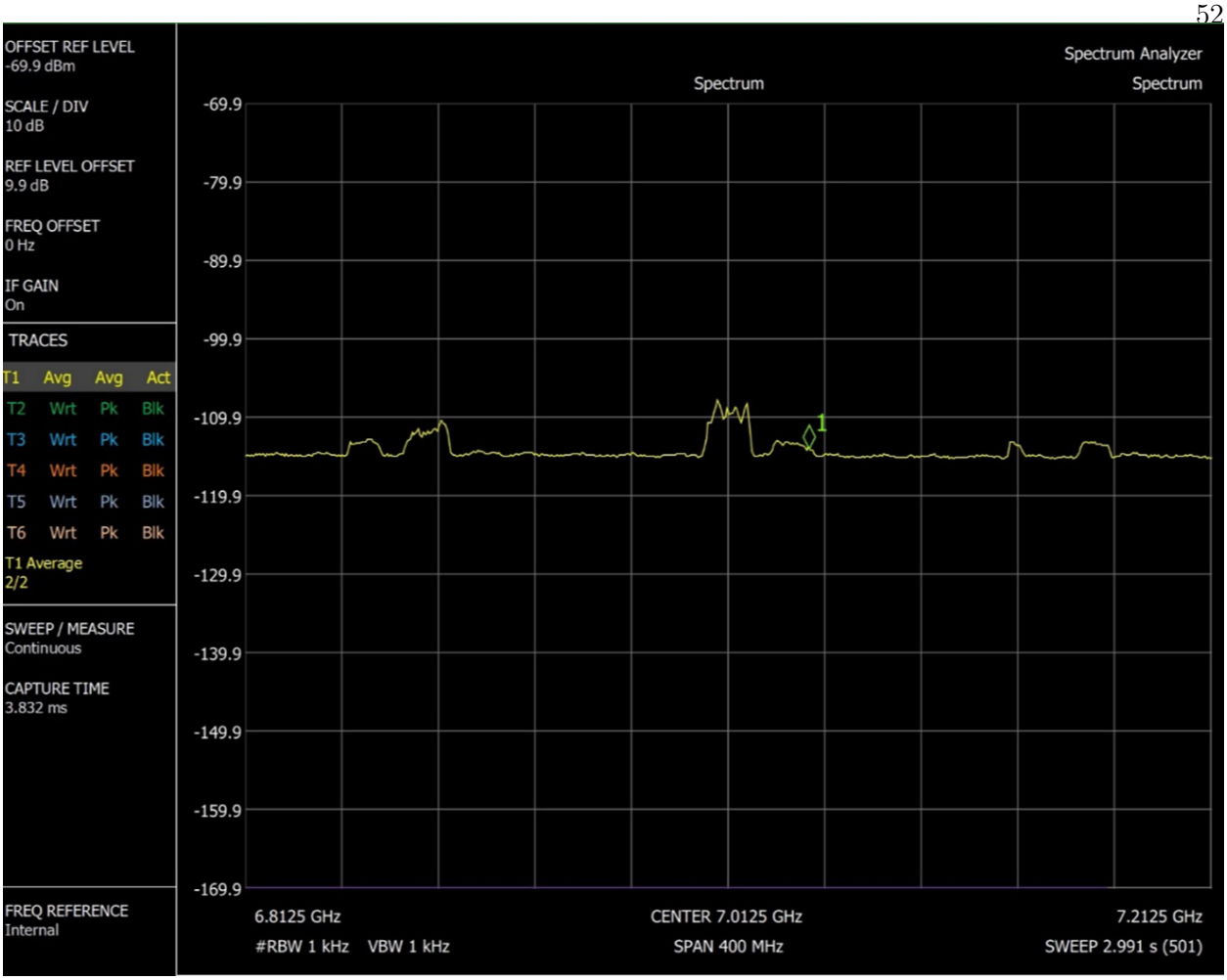

Figure 3.8: BAS emissions at 7012.5 MHz.

to noise ratio (I/N) of -6 dB is used as an interference protection criterion. In both bands, I/N is below -6 dB, which indicates that no harmful interference to BAS links is expected. Additionally, interference from current BAS links may cause a small impact on the performance of indoor Wi-Fi APs, especially in the U-NII-8 band, but the Wi-Fi protocol should be able to adapt its modulation scheme or allow a BER increase. These simulations were validated by measuring BAS emissions in the Denver area. The simulations are conservative and predict more interference than the measured value, which provides increased flexibility for spectrum sharing. This case study approach can be used in other parts of the country to study coexistence in these bands.

Table 3.3: Simulations and measurements of BAS emissions in the Denver Metro area

BAS transmitter	**Measurement location**	**6 GHz band**		**13 GHz band**	
		Simulations (dBm)	Measurements (dBm)	Simulations (dBm)	Measurements (dBm)
Lookout Mountain	Kalamath & 5^{th}	-95	-117	-94	-127
9News - KUSA (NBC)	Grant & 4^{th}	-100	-102	-	-
	Sherman & 3^{rd}	-93.7	-115	-	-
	Lookout Mountain	-99.5	-117	-	-
7News - The Denver Channel (ABC)	Lincoln & Speer Blvd.	-101.2	-113	-	-
KCNC (CBS)	Lincoln & 11^{th}	-92.9	-110	-	-
	Broadway & 11^{th}	-112.7	-118	-	-
Colorado Public Television (KBDI-TV)	Welton & 29^{th}	-94.2	-111	-	-
Spanish Television of Denver	Federal & 19^{th}	-114.7	-126	-	-

Chapter 4

Aggregate interference model for coexistence simulations in the 6 GHz band

4.1 Introduction

Multiple coexistence studies in the 6 GHz band have been conducted by incumbents and Wi-Fi advocates in the past three years, but they consider different approaches and parameters and do not include the latest rules proposed by the FCC [39]. In this chapter, we present aggregate interference models based on a space, time and frequency-domain approach to analyze the impact of RLANs on terrestrial and satellite incumbents in the 6 GHz band.

4.2 Coexistence with terrestrial incumbents

This section presents an aggregate interference model to simulate the coexistence with terrestrial FS and MS incumbents. The risk of harmful interference is quantified by conducting Monte Carlo simulations and, using the Risk-Informed Interference Assessment approach, we calculate the probability and consequences of aggregate interference to FS (fixed BAS and CARS and fixed microwave links) and MS (mobile BAS and CARS) incumbents.

Multiple aggregate interference models have been developed in the past. Many of them assume that the location of the interferers is modeled according to a Poisson Point Process in a two-dimensional plane [84]. Some of these studies include propagation effects such as shadowing and multipath [46]. In many of them, the interferers are assumed to be synchronously transmitting [100], which might not be realistic depending on the interferer. Many of these models simulate full co-channel interference, but only a few of them compute the frequency overlap with the incumbent

[71].

The model developed in this chapter is based on a three-dimensional distribution of the interferer transmitters. In the 2D plane, they are uniformly distributed in a circle. The height of the interferers is determined by Lidar data in each of the five scenarios simulated, following a deterministic approach based on real data. The interferers simulate asynchronous transmission of packets based on a Poisson distribution with exponentially-distributed interarrival time, which provides a more realistic approach for independent Wi-Fi transmissions. To simulate random propagation effects, Rayleigh fading is incorporated to add multipath if the propagation path is obstructed. Additionally, the model assigns random frequency channels to the incumbent and interferers and computes the frequency overlap between them.

There are five key contributions of this section. First, we develop a novel aggregate interference model to analyze the coexistence between RLANs and terrestrial incumbents in the 6 GHz band. The model incorporates the probabilistic component of unlicensed transmissions through randomized realizations of system parameters. Second, the simulations include the rules recently proposed by the FCC and use realistic assumptions based on data. Third, based on airtime utilization measurements using a software-defined radio, we estimate the Wi-Fi airtime utilization in different environments and compare them with the values used in other studies. Fourth, we use our model to estimate the interference to FS and MS in five representative scenarios in the United States and compare the results. Fifth, using the RIIA approach, we quantify the likelihood and impact of the interference. This model can be extended to coexistence studies in other countries and bands.

4.2.1 Aggregate interference model

The aggregate interference model incorporates a three-dimensional approach based on space, time, and frequency-domain considerations. The block diagram is presented in Figure 4.3. In the spatial domain, the model simulates multiple APs uniformly distributed in a circle, as illustrated in Figure 4.1. The incumbent receiver is located at the center of a circle of area equal to the area of the city simulated. The APs are placed at different heights based on the building height distribution

extracted from LiDAR data, as will be detailed in section 4.2.2.5. Exclusion zones of 10 m and 20 m are applied to MS indoor receivers and MS outdoor receivers, respectively.

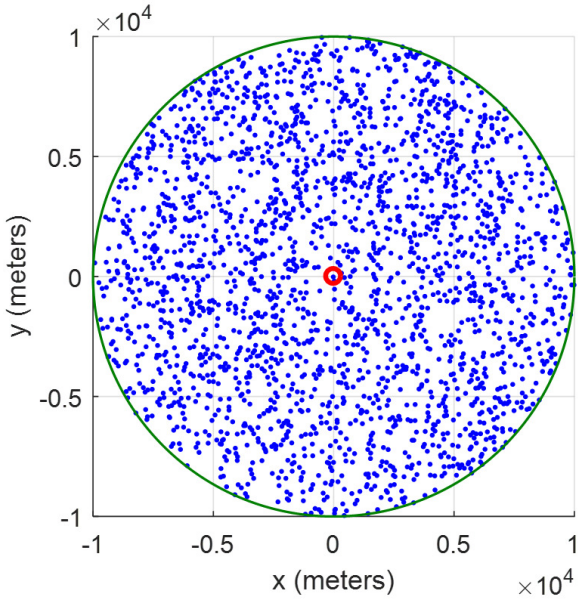

Figure 4.1: Incumbent receiver (red circle in the middle) and uniform distribution of APs (blue dots) within a circle.

In the time domain, Wi-Fi traffic is simulated in each AP that overlaps with the incumbent link. The number of Wi-Fi packets per second is modeled as a Poisson process with exponentially-distributed interarrival time. For each fixed time $t > 0$, the distribution of packets $N(t)$ is Poisson with mean λt:

$$P_r(N(t) = k) = \mathrm{e}^{-\lambda t}. \ \frac{(\lambda t)^k}{k!}, \ k \geq 0,$$

where λ is the mean interarrival rate per unit time. The interarrival times are independent and follow an exponential distribution exp(λ):

$$\mathrm{P}(\text{interarrival time} > \mathrm{t}) = \mathrm{e}^{-\lambda t}$$

Figure 4.2 illustrates the Wi-Fi packet generation as a Poisson process. The simulation time is 10 milliseconds, which is sufficient to represent the Wi-Fi traffic.

The mean interarrival time ($1/\lambda$) is calculated based upon three parameters: airtime utilization, throughput and the 802.11 maximum transmit unit (MTU). The last parameter consists of

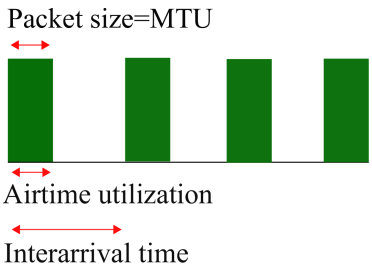

Figure 4.2: Packet generation modeled as a Poisson process

the MAC service data unit (MSDU) of 2304 bytes, the MAC header of 34 bytes and the encryption overhead of up to 20 bytes for WPA (TKIP) encryption. The packet size in the simulations will be equal to this MTU of 2358 bytes. The throughput assumed is 1 Gbps, based on new 802.11 standards and Wi-Fi channel bandwidths up to 320 MHz. The calculation is shown in the equation below:

$$\textit{Mean interarrival time} = \textit{Time per packet} / \textit{Airtime utilization},$$

where the airtime utilization is randomly selected from a distribution, as will be detailed in section 4.2.2.2, and the time per packet is calculated as follows:

$$\begin{aligned} &\textit{Time per packet} = (MTU/packet)/Throughput \\ &= \frac{2358 bytes}{1\ packet} \times \frac{1s}{1 Gbit} \times \frac{8 bits}{1 byte} = 18.9 \mu s/packet \end{aligned}$$

For example, for an airtime utilization of 1% and a time per packet of 19 μs, the mean interarrival time is 1.9 ms.

In the frequency domain, the frequency overlap between each AP and the incumbent is calculated to compute the aggregate interference. For each AP, the model assigns a random frequency of operation within the U-NII band of interest and a random Wi-Fi channel bandwidth. The incumbent frequency of operation is also randomly assigned. The model considers an equal probability of spectrum usage throughout the current unlicensed bands of 2.4 GHz and 5 GHz and the new 6 GHz band.

To simulate the transmission through a wireless channel, the path loss is calculated between each AP and the incumbent receiver. If there are obstructions in the propagation path, the model incorporates Rayleigh fading. The probability density function of the Rayleigh distribution is presented below:

$$p(r_0) = \frac{r_0}{\sigma^2} \exp(-\frac{r_0^2}{2\sigma^2}), \text{ when } r_0 \geq 0,$$

where r_0 is the envelope amplitude of the signal and σ^2 is the variance of the random variable.

The Rayleigh fading channel is simulated by generating a complex number whose real and imaginary parts are two independent random variables that follow a standard normal distribution, X$\sim$N(μ,σ^2) and Y$\sim$N(μ,σ^2), with zero mean (μ=0) and unit variance (σ^2=1). The envelope is a Rayleigh-distributed random variable that represents the multipath fading: Z $\sim$ Rayleigh(σ), Z=$\sqrt{X^2 + Y^2}$.

Next, the interference from each AP is calculated based on energy detection using the following equation [51]:

$$I_j = P_t + G_t + G_r - PL - L_{pol} - L_f - FDR(\Delta f),$$

where:

I_j = Interference level from the j-th AP at the incumbent receiver

P_t = Interferer (RLAN) transmit power

G_t= Gain of interferer (RLAN) antenna in the direction of the receiver

G_r= Gain of receiver (incumbent) antenna in the direction of the interferer

PL= Path loss

L_{pol}= Polarization mismatch loss

L_f= Feeder loss

FDR= Frequency dependent rejection caused by the receiver selectivity with respect to the interferer's emissions

and $FDR(\Delta f) = 10log\frac{\int_0^\infty P(f)\,df}{\int_0^\infty P(f)|H(f+\Delta f)|^2\,df}$,

where:

$P(f)$ = Power spectral density of the interfering signal equivalent intermediate frequency

$H(f)$ = frequency response of the victim receiver

$\Delta f = f_t - f_r$, where f_t is the interferer tuned frequency and f_r is the receiver tuned frequency

This process is repeated for all the N APs located in the circle to estimate the aggregate interference I for one Monte Carlo iteration:

$$I = \sum_{j=1}^{N} I_j$$

The impact caused by the randomness of the packet generation, the location and height of the APs, their EIRP, frequency overlap with the incumbent, the building entry loss for indoor APs and the Rayleigh fading can be simulated by implementing Monte Carlo simulations. This permits to generate the Complementary Cumulative Distribution Function (CCDF) of the aggregate interference from all the APs to an incumbent receiver.

Two interference protection criteria are used in the simulations. The first one is the aggregate interference to noise ratio I/N. This metric compares the aggregate interference power I and the receiver noise power N, which is calculated as follows:

$$N = 10log10(k * T_0 * 1000) + NF + 10log10(BW),$$

where:

k = Boltzmann's constant $1.38 * 10^{-23}$ joules per Kelvin

T_0 = Receiver temperature (Kelvin)

BW = Receiver IF bandwidth (MHz)

NF = Receiver noise figure (dB)

The maximum I/N to avoid harmful interference is -6 dB [70], which corresponds to 1 dB increase in the receiver noise, as suggested by the FCC [39]. If I/N>-6, the signal-to-interference-plus-noise ratio SINR is calculated to estimate the impact of the interference compared to the received signal level.

$$SINR = \frac{S}{I + N},$$

where S is the received signal power.

For FS links, the minimum SINR required is calculated based on a representative radio, Alcatel-Lucent 9500 Microwave Packet Radio [5]. The receiver noise level is -94.2 dBm and is calculated based on a BER of 10^{-6}, a bandwidth of 30 MHz, a noise figure of 5 dB, and 256QAM modulation, which is the highest-rate modulation scheme available in that radio. Considering these parameters for outdoor operations with static modulation, the minimum received signal power should be -65.5 dBm, which determines a minimum SINR of 28.7 dB. For a lower-rate modulation scheme of 128QAM, the minimum received signal power should be -69.3 dBm, which requires a minimum SINR of 24.9 dB. For MS incumbents, a minimum SINR of 10 dB is required to guarantee the link quality, according to measurements in [12] for Electronic News Gathering (ENG) operations. Both metrics are calculated and the results are compared for different scenarios to estimate the risk of harmful interference on the incumbents.

4.2.2 Simulation parameters

The aggregate interference model includes parameters related to the incumbent FS or MS links, characteristics and usage of the Wi-Fi APs, and the radio propagation assumptions. The simulations consider five representative scenarios in the United States.

4.2.2.1 Incumbent parameters

The parameters of the incumbent FS links are summarized in Table 4.1. The incumbent bandwidth is 25 MHz for fixed BAS/CARS and from 2.5 MHz to 60 MHz for FS links [28]. A mobile BAS video link system can utilize a channel bandwidth of 9 MHz or 18 MHz [52]. In this work, FS BAS/CARS links in U-NII-8 and MS BAS/CARS links in U-NII-6 and U-NII-8 are simulated with a bandwidth of 25 MHz and 18 MHz, respectively, while fixed microwave links in U-NII-5 and U-NII-7 are simulated with a bandwidth of 30 MHz.

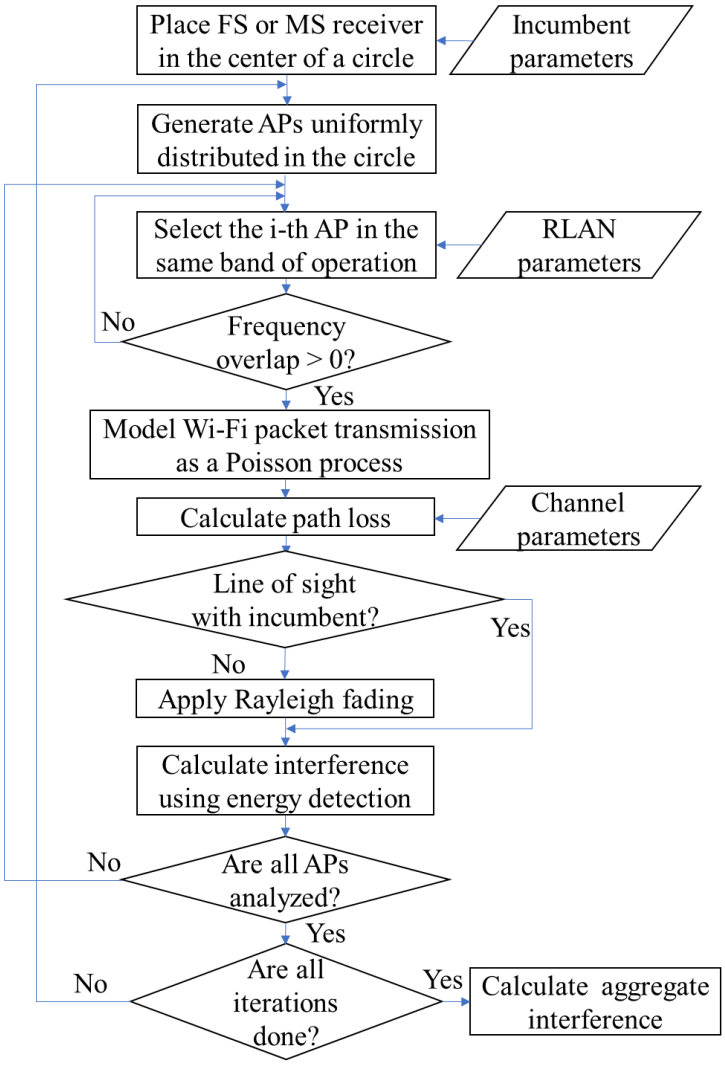

Figure 4.3: Flowchart used to calculate the aggregate interference from APs to incumbent FS and MS links.

Incumbent FS links are highly directional. A representative FS antenna is simulated based on information from the ULS database [28]. The antenna simulated is Commscope UHX6-59, which has 38.8 dBi gain and 1.8° horizontal and vertical half-power beamwidth (HPBW). It has a diameter of 6 ft, which is the most common one in this band [15], and has been mentioned as a reference in a previous coexistence study [77]. The parameters and antenna pattern are detailed in [69]. The radiation pattern is shown in Figure 4.4. The noise figure in the FS receiver is 5 dB [56] [21].

For MS incumbents, two antennas are simulated, based on [6]. For camera-back ENG trans-

Table 4.1: Parameters of terrestrial incumbents in the 6 GHz band

Parameter	**Incumbent service**			
	FS: fixed microwave	FS: fixed BAS/CARS	MS: mobile BAS/CARS (outdoor)	MS: mobile BAS/CARS (indoor)
Band	U-NII-5, U-NII-7	U-NII-6	U-NII-6, U-NII-8	
Bandwidth (MHz)	30	25	18	
Antenna type	Parabolic		Sector	Omnidirectional
Antenna manufacturer and model	Commscope UHX6-59		Vislink 9003561	Vislink L3535
Antenna gain (dBi)	38.8		12	3
Antenna HPBW	1.8° horizontal and vertical		120° horizontal, 19° vertical	360° horizontal, 76° vertical
Noise figure (dB)	5		4	
Feeder loss (dB)	2		1	

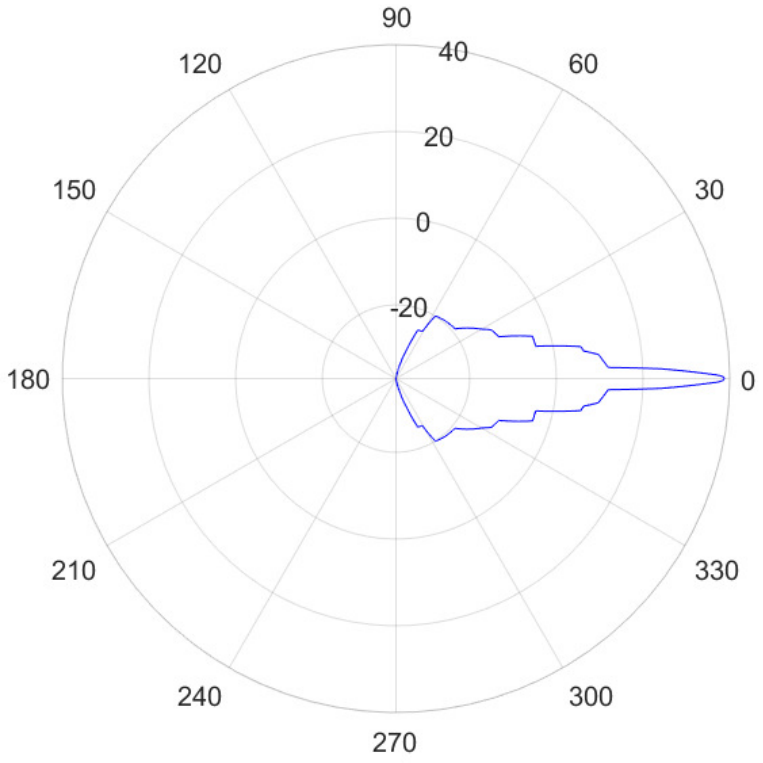

Figure 4.4: Azimuth radiation pattern for UHX6-59 antenna used for FS links

mitters and indoor ENG receivers, the antenna simulated is Vislink L3535, which is an omnidirectional antenna with 3 dBi gain. Its elevation radiation pattern is illustrated in Figure 4.5. For

outdoor ENG receivers, we simulate Vislink 9003561 sector panel antenna, which has 12 dBi gain, 120° horizontal HPBW and 19° vertical HPBW. The radiation patterns have been modeled based on ITU-R F.1336-5 [55] and they are shown in Figure 4.6. The receiver noise figure and the feeder loss used in the simulations is 4 dB [56] and 1 dB [52], respectively.

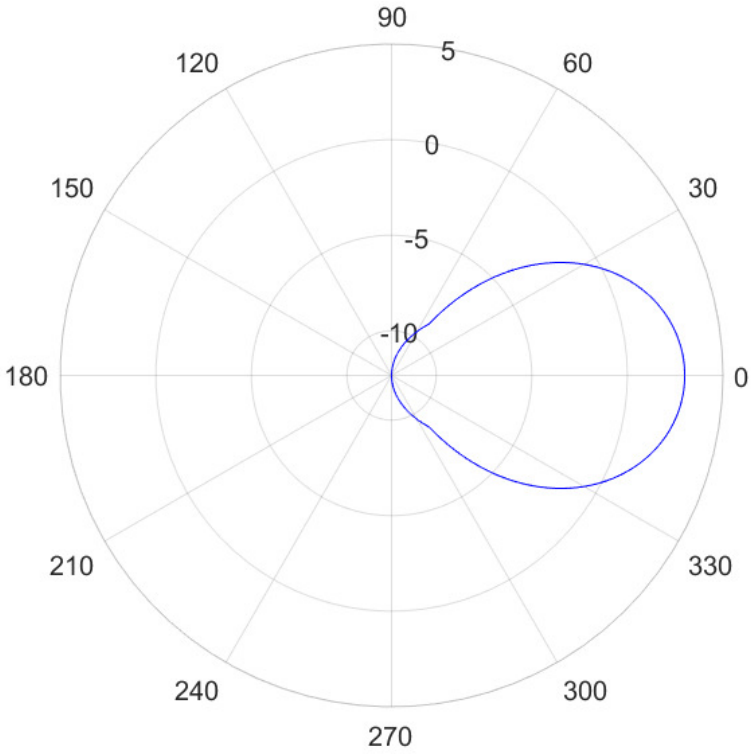

Figure 4.5: Elevation radiation pattern for Vislink L3535 omnidirectional antenna

4.2.2.2 RLAN airtime utilization

The RLAN airtime utilization represents the time during which the Wi-Fi channel is occupied and provides a conservative estimate of the AP transmission time. This parameter has been measured using the ADALM-PLUTO software-defined radio (SDR) from Analog Devices [7], which is a low-cost learning module, and GNU radio software to setup the device and save the data. This SDR has been configured to operate up to 6 GHz, which allowed measuring the Wi-Fi usage in the 5 GHz band in three scenarios, home, class and office, for one hour.

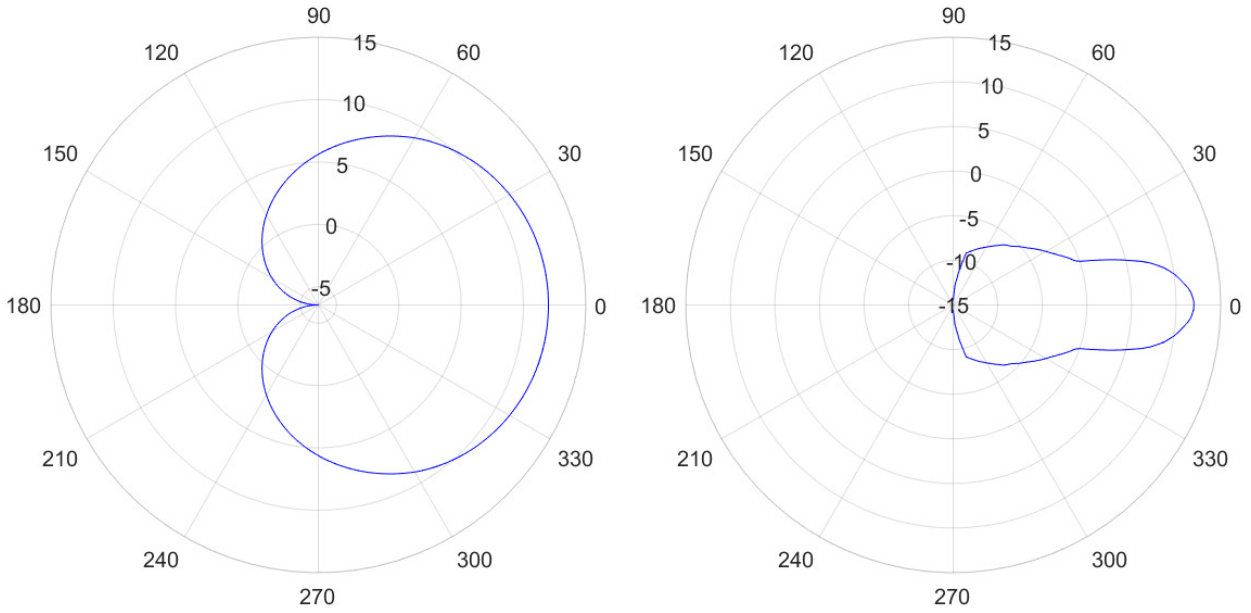

Figure 4.6: Azimuth (left) and elevation (right) radiation patterns for Vislink 9003561 sector panel antenna

The first scenario corresponds to a home environment in an apartment in a multi-floor building at 8 pm during the busy hour. The traffic consisted of simultaneous Netflix and YouTube streaming, in addition to web browsing generated by two laptops. The class environment consisted of a laboratory session in an engineering class at the University of Colorado Boulder, during which approximately 60 students were solving an assignment. The office environment is a research facility and the airtime utilization was measured in the morning. The main traffic source of the last two scenarios was web browsing.

Figure 4.7 compares the airtime utilization distribution for these measurements. The weighted average airtime utilization is 1.38%, 0.33% and 0.3% in the home, classroom and office environments, respectively, while the maximum measured airtime utilization is 33.5%, 27% and 19.9%, respectively. These results show that the average airtime utilization is relatively low and the RLAN devices are not transmitting most of the time. The airtime utilization values measured for classroom and office environments are similar and considerably lower than in the home environment due to the type of traffic. These measurements are compared with an airtime utilization distribution collected from

approximately half-million 5-GHz APs over 10 days across the United States in 2019 [13], which has a weighted average of 0.4%. To be conservative, the airtime utilization considered in these simulations correspond to the one in the home environment during the busy hour, which provides the highest weighted average airtime utilization in our measurements.

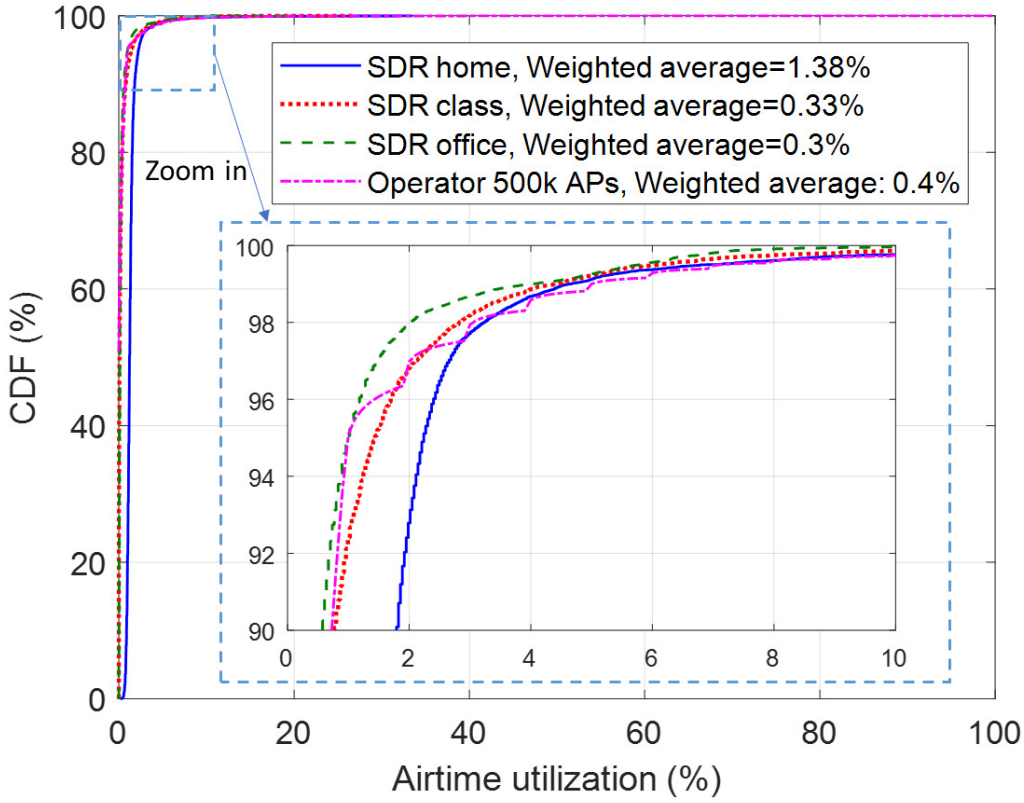

Figure 4.7: CDF of 5-GHz Wi-Fi airtime utilization measured by a software-defined radio in home, classroom and office environments, compared with the airtime utilization measured by an operator.

4.2.2.3 RLAN parameters

The RLAN simulation parameters are summarized in Table 4.2. The simulations consider the projected number of 6-GHz capable APs in 2026 as calculated in the previous chapter, assuming that the first 6-GHz capable APs will be available in 2021. The market penetration rate of APs in this band is expected to be 68% in 2026 based on data about the adoption rate of 5-GHz APs [4]. The average number of people per household will be 2.48 [95] and it is projected that 88.7%

of people older than 3 years old will use the Internet [72], which could be through Wi-Fi or other technologies. To calculate the total number of APs, one AP per household with Internet access is assumed.

Table 4.2: RLAN simulation parameters in the 6 GHz band

Parameter	**Band**	
	U-NII-5, U-NII-7	U-NII-6, U-NII-8
Year simulated	2026	
Market penetration rate	68%	
Population per household	2.48	
Internet usage ratio	88.7%	
Power restriction	Maximum EIRP=36 dBm	Maximum PSD=5 or 8 dBm/MHz
EIRP	Distribution based on Tables 4.5 and 4.4 [77]	Distribution based on Table 4.3 [21]
RLAN airtime utilization	Distribution based on measurements (Figure 4.7)	
Channel bandwidth	Distribution based on Table 3.2	
Outdoor APs	2%	0
Propagation model	WINNER II	
Building entry loss (dB)	Distribution based on ITU-R P.2109	
Antenna polarization mismatch (dB)	3	
AP height (m)	Distribution based on Lidar data	

As proposed by the FCC [39], all APs in the U-NII-6 and U-NII-8 bands are LPI APs. We simulate two maximum power spectral density (PSD) EIRP values of 5 and 8 dBm/MHz. A PSD of 5 dBm/MHz is limited by a maximum EIRP of 30 dBm and a maximum Wi-Fi channel bandwidth of 320 MHz, as proposed by the FCC. A PSD of 8 dBm/MHz has also been evaluated based on the further notice of proposed rulemaking contained in the same document, in which the FCC seeks comments about increasing the PSD to this value. The EIRP values are based on the EIRP distribution proposed in the ECC report 302 [21] and shown in Table 4.3, which are based on five types of APs with different maximum conducted powers and antenna radiation patterns. In our simulations, only the APs are considered, not the client or STA devices, which transmit at a significantly lower power.

In U-NII-5 and U-NII-7 bands, the maximum EIRP is 36 dBm, as indicated by the FCC.

Table 4.3: EIRP distribution used for low-power indoor APs [21]

Indoor use case	Weight	Weighted EIRP distribution (mW)					
		1000	250	100	50	13	1
Client/STA (*)	26.32%	0	0	1.82%	12.03%	12.47%	0
Enterprise AP/small cell	2.63%	0	1.06%	0.9%	0.58%	0.09%	0.01%
Consumer AP/small cell	66.31%	0	7.9%	2.76%	11.2%	38.94%	5.51%
High performance gaming router	4.74%	0.71%	0.2%	0.73%	1.97%	0.97%	0.16%
Subtotal	100%	0.71%	9.15%	6.21%	25.79%	52.47%	5.68%

*No client/STA devices are simulated in this work, only APs

However, since the ECC report 302 only considers EIRP values up to 30 dBm [21], the EIRP distribution in the RKF report [77] is used in this case. The EIRP distributions for standard-power indoor and standard-power outdoor devices are presented in Tables 4.4 and 4.5, respectively.

Table 4.4: EIRP distribution used for standard-power indoor APs [77]

Indoor use case	Weight	Weighted EIRP distribution (mW)						
		4000	1000	250	100	50	13	1
Client/STA (*)	26.32%	0	0	0	1.82%	12.03%	12.47%	0
Enterprise AP/small cell	2.63%	0	0	1.06%	0.9%	0.58%	0.09%	0.01%
Consumer AP/small cell	66.31%	0	0	7.9%	2.76%	11.2%	38.94%	5.51%
High performance gaming router	4.74%	0.67	0.42%	1.43%	1.01%	0.83%	0.34%	0.04%
Subtotal	100%	0.67%	0.42%	10.39%	6.49%	24.64%	51.84%	5.56%

*No client/STA devices are simulated in this work, only APs

Table 4.5: EIRP distribution used for standard-power outdoor APs [77]

Indoor use case	Weight	Weighted EIRP distribution (mW)						
		4000	1000	250	100	50	13	1
High power AP	20%	2.83%	1.77%	6.04%	4.21%	3.55%	1.44%	0.17%
Low power AP	30%	0	0.25%	3.41%	1.33%	5.73%	16.89%	2.41%
Client	50%	0	0	0	3.46%	22.85%	23.68%	0
Subtotal	100%	2.83%	2.02%	9.45%	9%	32.13%	41.99%	2.58%

*No client devices are simulated in this work, only APs

The ECC report 302 presents a Wi-Fi channel bandwidth distribution only up to 160 MHz.

Our simulations take this report as a reference for channel bandwidths of 20 and 40 MHz with a probability of 10% each. We conservatively assume that channel bandwidths of 80 MHz, 160 MHz and 320 MHz will have a probability of 30%, 30% and 20%, respectively, as indicated in Table 3.2 in the previous chapter.

The percentage of outdoor APs in the U-NII-5 and U-NII-7 bands is considered to be 2%. Based on real data and estimations considered in the ECC Report 302 for spectrum sharing in the 6 GHz band [21], there will be 0.6% of outdoor AP shipments in 2021. This value would increase to 1% after including small cell outdoor equipment and, to be conservative, this analysis considers 2% of outdoor units in 2026 [77].

4.2.2.4 Channel parameters

The interference is calculated using the WINNER II propagation model [59], which is based on measurements up to 6 GHz. This model has also been used in other 6 GHz coexistence studies [21][77] and its applicability has been validated through measurements at 7 GHz [101]. The WINNER II model has been selected because it incorporates the heights of both transmitter and receiver, as opposed to the other models, which do not include them. Another advantage of this model is that it is classified into different types of scenario, such as urban, suburban, rural and large indoor, which are simulated here. For indoor APs, WINNER II NLOS is used considering that the propagation path between the APs and the incumbent receiver is obstructed by internal and external walls. For outdoor APs, a probability of LOS/NLOS is used to calculate the path loss in the absence of site specific information, as recommended by the FCC in [39].

For coexistence with indoor APs, the indoor-to-outdoor interference is calculated based on ITU-R P.2109 [57], which estimates the building entry loss through traditional and thermally-efficient buildings considering the incidence angle of the path. In the simulations, the scenarios consist of 50% of each type of building, except for New York City, which is assumed to have 30% of thermally-efficient buildings due to their older construction.

A polarization mismatch loss of 3 dB is added due to the large number of RLAN emitters,

the absence of a dominant source of interference and the polarization in the incumbent receiver [21]. An average feeder loss of 2 dB and 1 dB is considered for FS and MS incumbents, respectively [56] [52].

4.2.2.5 Scenarios

Five representative scenarios in the United States are considered in the analysis, which correspond to different types of environments, areas and population densities: New York City (New York), Los Angeles (California), Boulder (Colorado), Louisville (Colorado) and Leon (Kansas). New York City (NYC), Los Angeles (LA) and Boulder correspond to urban scenarios, while Louisville is considered suburban and Leon is rural.

Table 4.6 shows the parameters per each scenario, such as the population number, the area simulated and three FS incumbent receiver heights per each of them. In NYC and LA, these FS incumbent receiver heights are determined by the 90th, 50th and 10th percentile of all the heights at which the FS incumbent receivers are located in each of these cities, according to the ULS database [28]. Due to the limited number of actual FS links in Boulder, Louisville and Leon, the values of these heights are assumed in these scenarios. To be conservative, the FS incumbent receiver heights simulated are the 10th percentile of the incumbent receiver heights in each scenario. The antenna elevation angle simulated on the receiver is 1° for FS incumbents and 0° for MS incumbents.

Table 4.6: Scenarios

Parameter		**NYC**	**LA**	**Boulder**	**Louisville**	**Leon**
Population		8398748	3990456	107353	21163	701
Area simulated (km^2)		784	1214	100	100	1.9
Receive antenna height of FS incumbent (m)	90th percentile	262	104	45	30	30
	Median	115	55	30	22	22
	10th percentile	85	42	15	15	15

In the rural scenario, indoor APs are located at 1.5 m height. In urban and suburban scenarios, indoor APs are distributed in buildings of different heights and located at an average height of 1.5 m above each floor. The buildings are assumed to be at least 3 m high and each floor is separated

by 3 m in each building. Building heights are based on 3D elevation maps of a few representative areas per each scenario, which are obtained through LiDAR data from the U.S. Geological Survey (USGS) [96]. The CDF of the building height distribution in NYC, LA, Boulder and Louisville is shown in Figure 4.8.

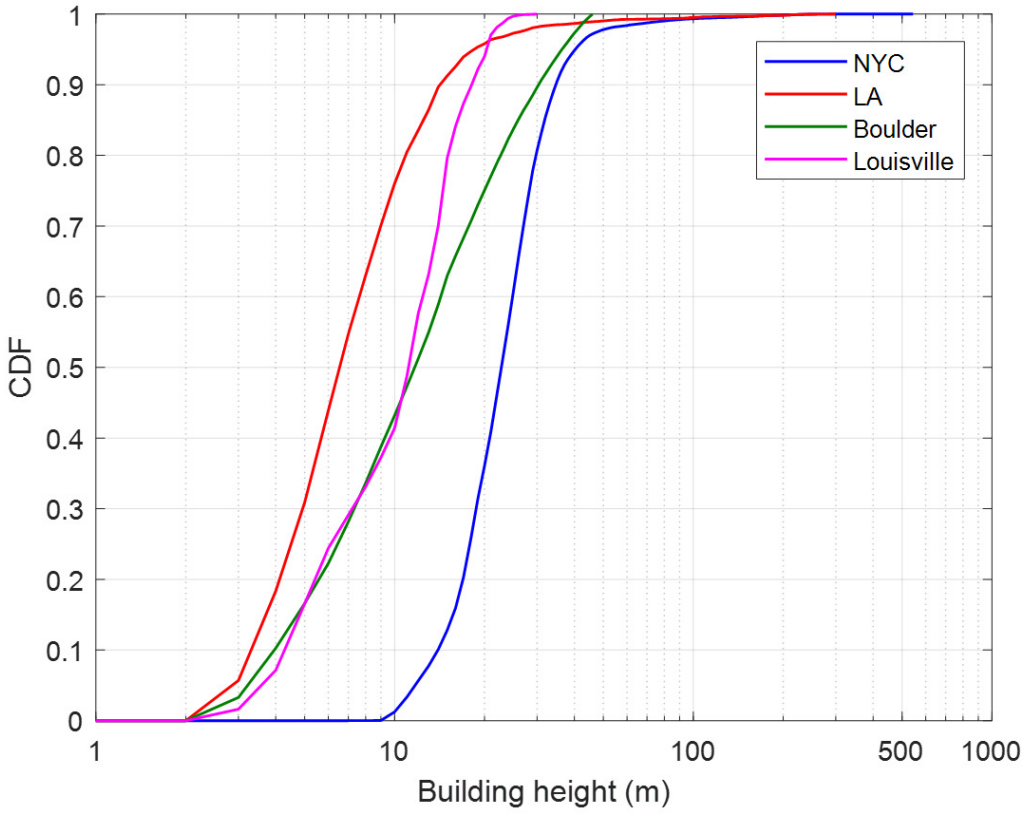

Figure 4.8: Distribution of building heights based on Lidar data in the urban and suburban environments simulated

Outdoor APs are assumed to be distributed at different heights from 4.5 m to 28.5 m in urban scenarios, according to data estimated for outdoor public access APs in [58]. Approximately 70% of them are mounted on a pole at 7.5 m height, 5% are placed on a rooftop at 10.5 m height, 5% are mounted on a wall at 4.5 m and the remaining 20% is uniformly distributed between 13.5 and 28.5 m height. In suburban and rural scenarios, the distribution of outdoor AP heights is similar to the urban case, but it is assumed to be limited to 7.5 m and 4.5 m, respectively, due to lower building heights. The probability distribution of outdoor AP heights for each environment is detailed in

Table 4.7.

Table 4.7: Probability distribution of outdoor AP heights for urban, suburban and rural scenarios [58]

Height (m)	**Probability distribution (%)**		
	Urban	Suburban	Rural
4.5	5	6.7	100
7.5	70	93.3	
10.5	5		
13.5	3.3		
16.5	3.3		
19.5	3.3		
22.5	3.3		
25.5	3.3		
28.5	3.3		

4.2.3 Results

We conducted Monte Carlo simulations of aggregate interference from Wi-Fi APs to incumbent FS and MS links based on the model developed in this chapter and the parameters and scenarios described in the previous section. Each iteration corresponds to an independent random system realization and each of them has been repeated 100000 times. Due to the intensive computation requirements, the simulations have been conducted on Intel Xeon E5-2680 CPUs. In the simulations, the conducted power is 22.5 dBm for FS using 256QAM modulation [5], and 20 dBm for MS, which is the maximum value for a representative camera-back ENG transmitter [73]. The results are compared and analyzed in this section.

4.2.3.1 Interference to FS

The results of the aggregate I/N to an incumbent FS link considering a maximum PSD of 5 dBm/MHz for LPI APs are shown in Figure 4.9. Aggregate I/N is lower than the -6 dB threshold for all the scenarios in U-NII-8 due to the use of LPI APs only. Aggregate I/N is higher for U-NII-5 and U-NII-7 bands due to standard-power APs, including outdoor APs, which can produce

higher interference caused by the lack of building entry loss and the higher probability of being in LOS with the incumbent. The probability of I/N>-6 dB is 0.001%, 0.003%, 0.004% and 0.002% for NYC, LA, Boulder and Louisville, respectively. These higher aggregate I/N values come from comparatively fewer simulations that do not necessarily reflect the statistics. In all cases, they are caused by outliers where only one AP with a combination of worst-case parameters, such as location of the AP within the HPBW of the receiver FS antenna, high EIRP, high frequency overlap with the incumbent, low building entry loss and high airtime utilization, causes aggregate I/N>-6 dB. In Leon, the probability that I/N exceeds this threshold is significantly higher, up to 0.44%, due to the lower path loss in a rural environment and the higher probability of LOS conditions.

Additionally, in cases where I/N>-6 dB, SINR has been calculated. The propagation model used to estimate the path loss between the incumbent transmitter and receiver is WINNER II for distances up to 5 km and free space path loss for distances of up to 100 km. As detailed in Table 4.8, the minimum SINR in urban and suburban scenarios is significantly higher than 28.7 dB, which indicates that Wi-Fi will not cause harmful interference. In the rural scenario, FS links will not exceed a BER of 10^{-6} using 256QAM for distances up to 1 km, considering a minimum SINR of 28.7 dB. Using 128QAM modulation will require a minimum SINR of 24.9 dB, which can be achieved in FS links up to 10 km [5].

Table 4.8: Minimum SINR (dB) if I/N>-6 dB for 6 GHz FS incumbent

Sub-band	**Scenario**	**Distance FS transmitter - receiver**			
		1 km	10 km	50 km	100 km
U-NII-5&7	NYC	63.6	54.2	40.2	34.2
	LA	63.9	54.4	40.5	34.4
	Boulder	64.1	54.6	40.7	34.6
	Louisville	67.7	53.9	39.9	33.9
	Leon	43.4	25.7	11.7	5.7

Figure 4.10 compares the distribution of aggregate I/N using maximum PSD EIRP values of 5 and 8 dBm/MHz in LPI APs in the U-NII-8 band. Using a maximum PSD of 8 dBm/MHz causes an aggregate interference of up to 1 dB higher due to the use of an EIRP distribution instead of a

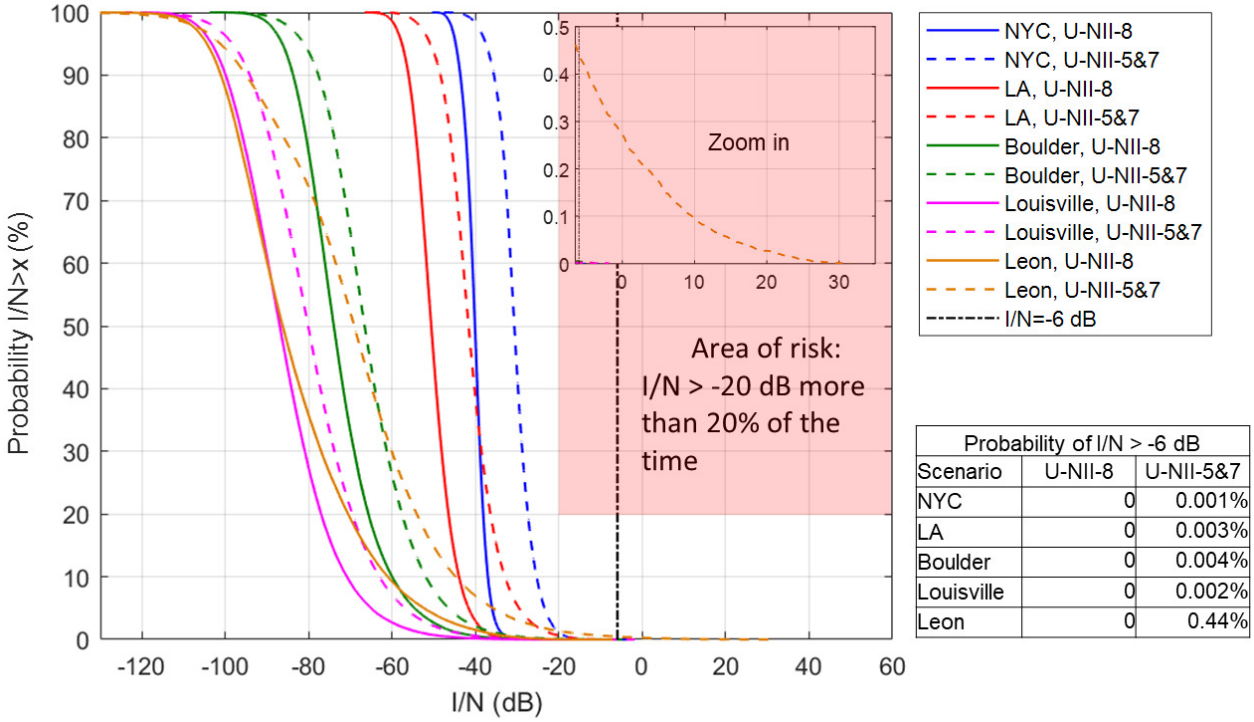

Probability of I/N > -6 dB		
Scenario	U-NII-8	U-NII-5&7
NYC	0	0.001%
LA	0	0.003%
Boulder	0	0.004%
Louisville	0	0.002%
Leon	0	0.44%

Figure 4.9: Probability of aggregate I/N on a FS incumbent exceeding values on the X-axis. APs are LPI operating at a maximum PSD of 5 dBm/MHz

fixed maximum PSD value in the simulations. Consequently, there is no significant impact of using a maximum PSD of 8 dBm/MHz instead of 5 dBm/MHz for LPI APs.

4.2.3.2 Interference to MS

The aggregate I/N to an incumbent MS link has been simulated for two MS configurations: indoor-to-indoor and outdoor-to-outdoor. In these cases, the MS transmit system consists of an ENG transmitter (Tx) and an antenna attached to a video camera mounted on a shoulder at 1.8 m height. The indoor receiver (Rx) is located at 4.9 m height, as proposed in [6]. The outdoor receiver is located on a truck, at a height between 1.5 m and 15 m, and both heights are considered in the simulations. The simulations do not calculate the interference to an ENG central receive site, which corresponds to a tall building or mountaintop, because the configuration is similar to the FS case already simulated. Figure 4.11 shows the probability of aggregate I/N considering a maximum PSD EIRP of 5 dBm/MHz, as proposed by the FFC. The I/N is higher for a MS receiver at 15 m

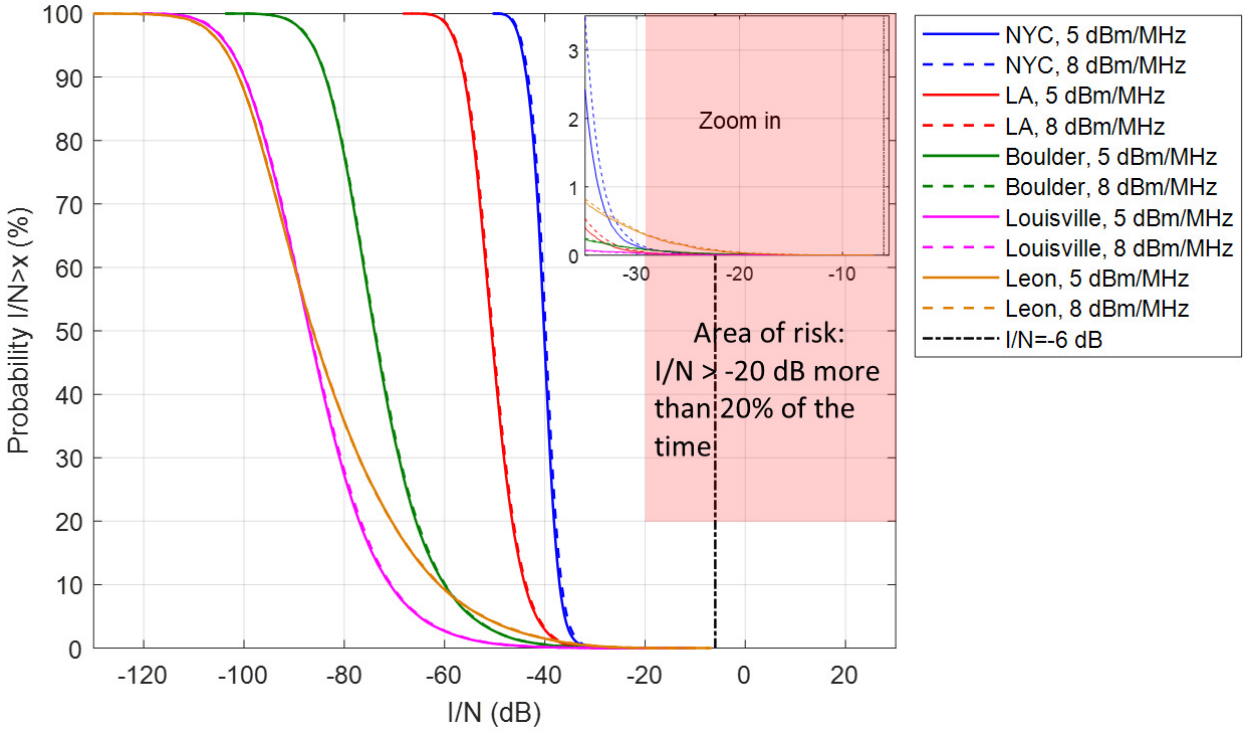

Figure 4.10: Probability of aggregate I/N on a FS incumbent in the U-NII-8 band exceeding values on the X-axis. APs are LPI with maximum PSD values of 5 dBm/MHz or 8 dBm/MHz

height in urban and suburban cases, because the AP heights are closer to 15 m than to 1.5 m, as opposed to the rural scenario, where all the APs are simulated at 1.5 m.

Considering a maximum PSD of 5 dBm/MHz, Table 4.9 shows that, in the cases where the aggregate I/N is higher than the -6 dB threshold, outdoor-to-outdoor configurations permit a SINR higher than the 10 dB threshold, which indicates that the APs will not cause harmful interference on MS. The same applies to the indoor-to-indoor scenario for distances up to 46 m. For higher distances, the SINR will be lower than 10 dB, but these indoor links can be easily improved for optimal signal reception by adapting the incumbent receiver location and changing the frequency of operation.

Figure 4.12 shows the probability of aggregate I/N on incumbent MS links considering a maximum PSD of 8 dBm/MHz in LPI APs. Using a higher PSD causes higher maximum I/N values, as can be compared with Figure 4.11, which corresponds to a maximum PSD of 5 dBm/MHz in the

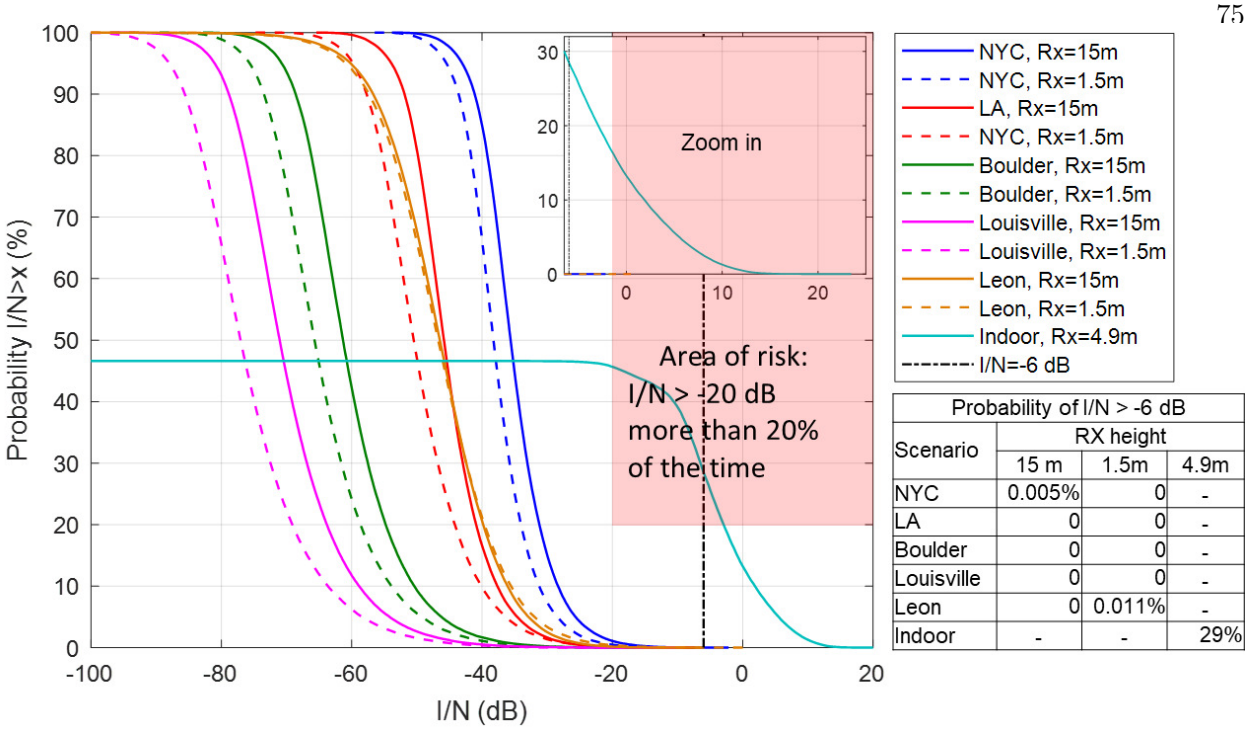

Probability of I/N > -6 dB			
Scenario	RX height		
	15 m	1.5m	4.9m
NYC	0.005%	0	-
LA	0	0	-
Boulder	0	0	-
Louisville	0	0	-
Leon	0	0.011%	-
Indoor	-	-	29%

Figure 4.11: Probability of aggregate I/N on a MS incumbent exceeding values on the X-axis. APs are LPI operating at a maximum PSD of 5 dBm/MHz.

Table 4.9: Minimum SINR (dB) if I/N>-6 dB for MS incumbent using a maximum PSD of 5 dBm/MHz in LPI APs

Configuration		**Scenario**	**Distance MS transmitter - receiver**			
Tx	Rx		20 m	50 m	70 m	100 m
Indoor (1.8 m)	Indoor (4.9 m)	All	14.5	9.6	7.6	5.5
Outdoor (1.8 m)	Outdoor (15 m)	NYC	33.7	35.9	36.1	33.8
Outdoor (1.8 m)	Outdoor (1.5 m)	Leon	53.7	57.9	52.1	45.9

APs. In cases the I/N exceeds the -6 dB threshold, the minimum SINR is computed, as indicated in Table 4.10. Similar to 4.9, only indoor-to-indoor MS links for distances up to approximately 20 m are not degraded. However, it is realistically not expected that a Wi-Fi device would transmit in a busy channel.

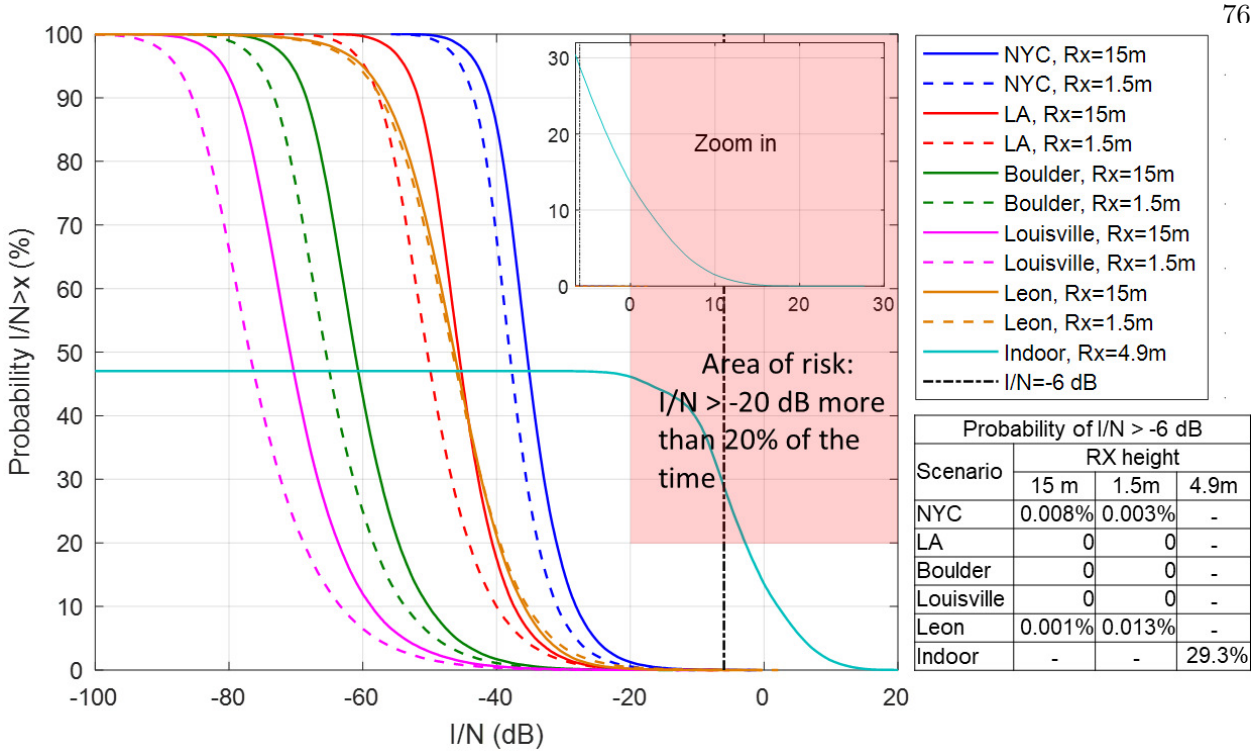

Probability of I/N > -6 dB			
Scenario	RX height		
	15 m	1.5m	4.9m
NYC	0.008%	0.003%	-
LA	0	0	-
Boulder	0	0	-
Louisville	0	0	-
Leon	0.001%	0.013%	-
Indoor	-	-	29.3%

Figure 4.12: Probability of aggregate I/N on a MS incumbent exceeding values on the X-axis. APs are LPI operating at a maximum PSD of 8 dBm/MHz

Table 4.10: Minimum SINR (dB) if I/N>-6 dB for MS incumbent using a maximum PSD of 8 dBm/MHz in LPI APs

Configuration		**Scenario**	**Distance MS transmitter - receiver**			
Tx	Rx		20 m	50 m	70 m	100 m
Indoor (1.8 m)	Indoor (4.9 m)	All	10.4	5.4	3.4	1.3
Outdoor (1.8 m)	Outdoor (15 m)	NYC	33.6	35.8	36	33.7
Outdoor (1.8 m)	Outdoor (1.5 m)	NYC	52.9	40.7	34.9	28.7
Outdoor (1.8 m)	Outdoor (15 m)	Leon	34.3	38.1	38.9	37.3
Outdoor (1.8 m)	Outdoor (1.5 m)	Leon	55.6	59.9	54	47.8

4.2.3.3 Risk-Informed Interference Assessment approach

The methodology used in this subsection adopts the Risk-Informed Interference Assessment (RIIA) approach to quantitatively analyze the implications of spectrum sharing in the 6 GHz band. We identify the potential sources of interference for each of the current incumbents in both bands, define the interference protection criterion as a metric to characterize the severity of the interference

and quantify the probability and consequence of the potential interference.

The methodology follows the four-step RIAA method proposed in [17][18]:

(1) Identify the hazards. We identify the parameters of the interferers (Wi-Fi APs) and how they can affect the incumbents (FS and MS links). This is affected by the characteristics and locations of both systems and the coupling between them, which determines the amount of interfering energy that enters the receiver (e.g. propagation loss, antenna gain and antenna radiation pattern). The parameters were identified in section 4.2.2.

(2) Define a consequence metric. To set the maximum tolerable interference on incumbents, an interference protection criterion based on NTIA's recommendations is considered. The area of risk is determined by an aggregate I/N higher than -20 dB for more than 20% of the time for long-term interfering signals from non-primary allocated services [70]. This is based on ITU-R F.1094 [50], which allocates 1% of the total performance and availability degradation to non-primary services.

(3) Assess likelihood-consequence values. An interference risk analysis is conducted for each type of incumbent using the coexistence simulator developed in this chapter. Using Monte Carlo simulations, we generate risk curves, which show the probability that the maximum allowed interference is exceeded.

(4) Aggregate the results. The results of the likelihood-consequence analysis are aggregated and compared for different scenarios, depending on the total population, population density and environment.

Figures 4.9, 4.10, 4.11 and 4.12 show in pink the areas of unacceptable risk to the incumbent, which occurs when I/N is higher than -20 dB for more than 20% of the time. To avoid harmful interference, I/N should not exceed -20 dB more than 20% of the time or, in other words, I/N should be below this threshold for at least 80% of the time. In the case of a FS incumbent in Figures 4.9 and 4.10, this threshold is never exceeded due to the low probability of occurrence. In the case of

a MS incumbent, the threshold is only exceed for indoor-to-indoor configurations. However, due to Wi-Fi's Clear Channel Assessment (CCA) mechanism, it will not be very likely that the AP will select an occupied channel, so this case represents a worst-case, conservative scenario.

4.2.4 Discussion

We have developed an aggregate interference model to simulate the impact of RLAN devices on current FS and MS incumbents in the 6 GHz band, according to the rules recently proposed by the FCC and using realistic assumptions in urban, suburban and rural environments. The RLAN airtime utilization has been measured using software-defined radio for home, class and office environments. Our model has space, time and frequency considerations and can be applied to other scenarios and bands to estimate the potential risks of spectrum sharing on terrestrial incumbents. Considering the interference protection criterion of a maximum interference-to-noise ratio (I/N) of -6 dB, the results show that low-power indoor (LPI) APs can coexist with current FS links in the U-NII-8 band. Standard-power APs, including outdoor units, can coexist with FS incumbents in the U-NII-5 and U-NII-7 bands using mitigation techniques or, alternatively, considering the minimum required SINR for a representative radio with a BER of 10^{-6} and using the highest modulation scheme available, 256QAM. In the case of MS incumbents, coexistence is possible for indoor-to-indoor distances up to 46 m and outdoor-to-outdoor MS configurations considering I/N<-6 dB and SINR>10 dB. For indoor-to-indoor MS links beyond 46 m distance, the incumbent receiver location should be adapted for optimal signal reception. Increasing the maximum power spectral density EIRP in LPI APs from 5 dBm/MHz to 8 dBm/MHz does not cause significant impact on the results, considering that the AP transmission power is based on an EIRP distribution. Alternatively, the Risk-Informed Interference Assessment Approach has also been used in the coexistence study, as it does not focus on the worst-case scenario, but on the likelihood and consequence of the interference. It considers a maximum I/N of -20 dB for more than 20% of the time, according to NTIA's criterion for long-term interfering signals from non-primary allocated services. According to this criterion, RLANs do not cause harmful interference on FS incumbents and outdoor-to-outdoor MS links. It

could only degrade indoor-to-indoor MS links if the APs were transmitting in the same band as the incumbent, but, in reality, it is not very likely that the APs will be transmitting on a busy channel.

4.3 Coexistence with satellite incumbents

Different stakeholders have submitted multiple coexistence studies, most of them focused on spectrum sharing between RLANs and FS or MS services, but only a few analyses have been conducted to calculate the impact on FSS space stations. One of them is the study developed by RKF Engineering Solutions prepared for Wi-Fi advocates in 2018 [77]. This study calculates the interference to FSS without considering any mitigation rules, which were later proposed by the FCC [36] [39]. The path loss estimation is based on the Irregular Terrain Model (ITM) and incorporates terrain information. They conclude that the interference to noise ratio (I/N) from RLANs to FSS is always below -20 dB, which is significantly lower than the maximum I/N of -4.7 dB from current terrestrial FS transmitters and, consequently, the impact of RLANs would be negligible. In 2019, Intelsat and SES, two satellite companies, argued that a higher satellite antenna gain should be considered, based on their Intelsat 35e satellite, which is relatively new and one of the most sensitive ones on orbit [48]. The simulations are based on free space path loss. Considering a maximum I/N of -13.5 dB, they conclude that AFC would be needed to avoid harmful interference from outdoor APs on the FSS space stations. However, the parameters are conservative and do not consider terrain and clutter loss, frequency overlap with the incumbent and the satellite footprint does not cover the entire United States.

The objective of this section is to calculate the aggregate interference from RLAN devices, specifically Wi-Fi APs, across the contiguous United States on FSS uplinks. There are three key contributions of this section. First, considering the rules proposed by the FCC, we simulate the aggregate interference to FSS incumbents considering two scenarios, one with only LPI APs in the entire 6 GHz band and the other including standard-power outdoor APs in U-NII-5 and U-NII-7 bands. Second, we conduct a sensitivity analysis to estimate the impact of different Wi-Fi airtime utilization values. Third, the results of the sensitivity analysis are compared considering different

I/N thresholds as interference protection criteria to determine the best sharing scenarios between RLANs and FSS links

4.3.1 Aggregate interference model

The simulations estimate the aggregate interference from all Wi-Fi APs in the Contiguous United States (CONUS) territory to a GEO satellite that can be located at different longitudes on top of the Equator, which is shown in Figure 4.13. The simulator is based on the population density in each census tract in the CONUS. The geometry considered in the simulations and the look angle from AP to GEO satellite is illustrated in Figure 4.14.

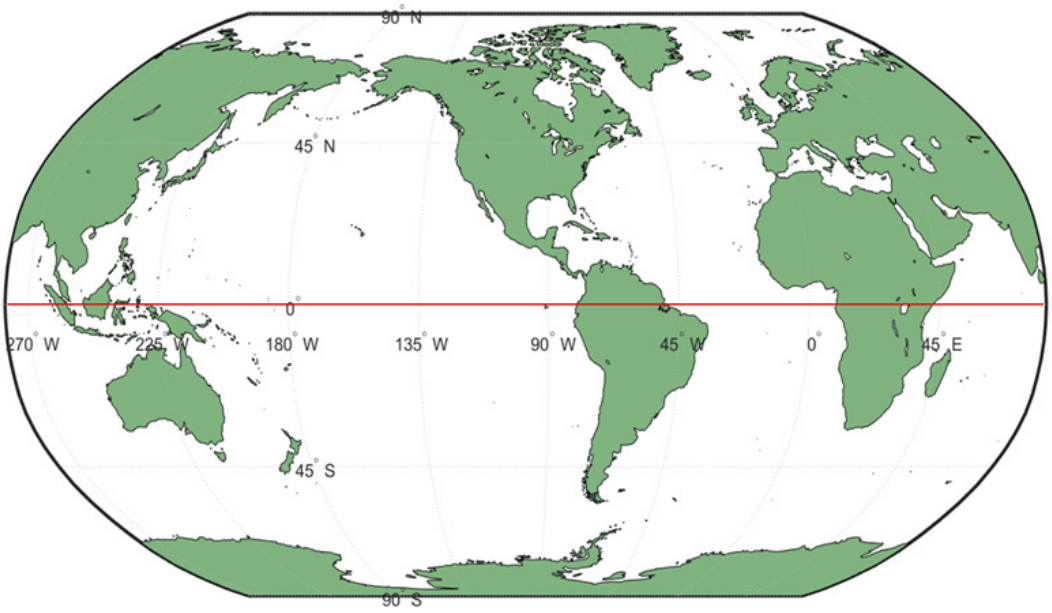

Figure 4.13: Geostationary orbit: 36000 km above the Equator (red line).

The flowchart of the simulator is presented in Figure 4.15. The path loss estimation in the simulation is conservative, as the model does not include terrain information and corresponding shadowing loss, therefore, the practical interference level should be lower than the results presented in this chapter.

A census tract is a relatively small geographic subdivision of a county. The demographic information in the census tracts is based on the 2010 United States Census [92] and projected

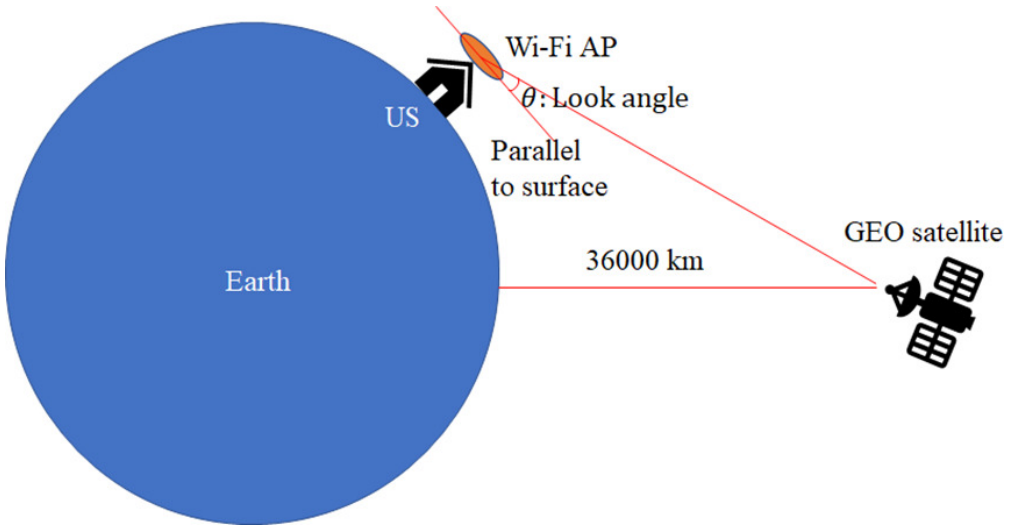

Figure 4.14: Look angle from Wi-Fi AP to GEO satellite.

to 2026, as in the previous section. There are 74002 census tracts in the US and the amount of population per census tract in the CONUS is illustrated in Figure 4.16. Census tracts have been classified into urban, suburban and rural. According to the US Census Bureau, urban and suburban environments have more than 1000 people per square mile [94]. Considering only the census tracts within the 48 contiguous states, the total population in this region will be approximately 330.7 million in 2026.

4.3.2 Simulation parameters

The FSS and RLAN parameters used in the simulations are described in this section.

4.3.2.1 Satellite parameters

The FSS incumbent parameters are summarized in Table 4.11. The simulations consider a satellite antenna gain of 26.1 dBi, which is based on the SES-2 satellite that covers the entire CONUS. The satellite uplink coverage is determined by the orbital location of the satellite and its antenna gain-to-noise temperature (G/T). After analyzing the G/T contours in [81] and [61], it was found that SES-2 is the satellite that has the maximum average G/T over CONUS of 2 dB/K and

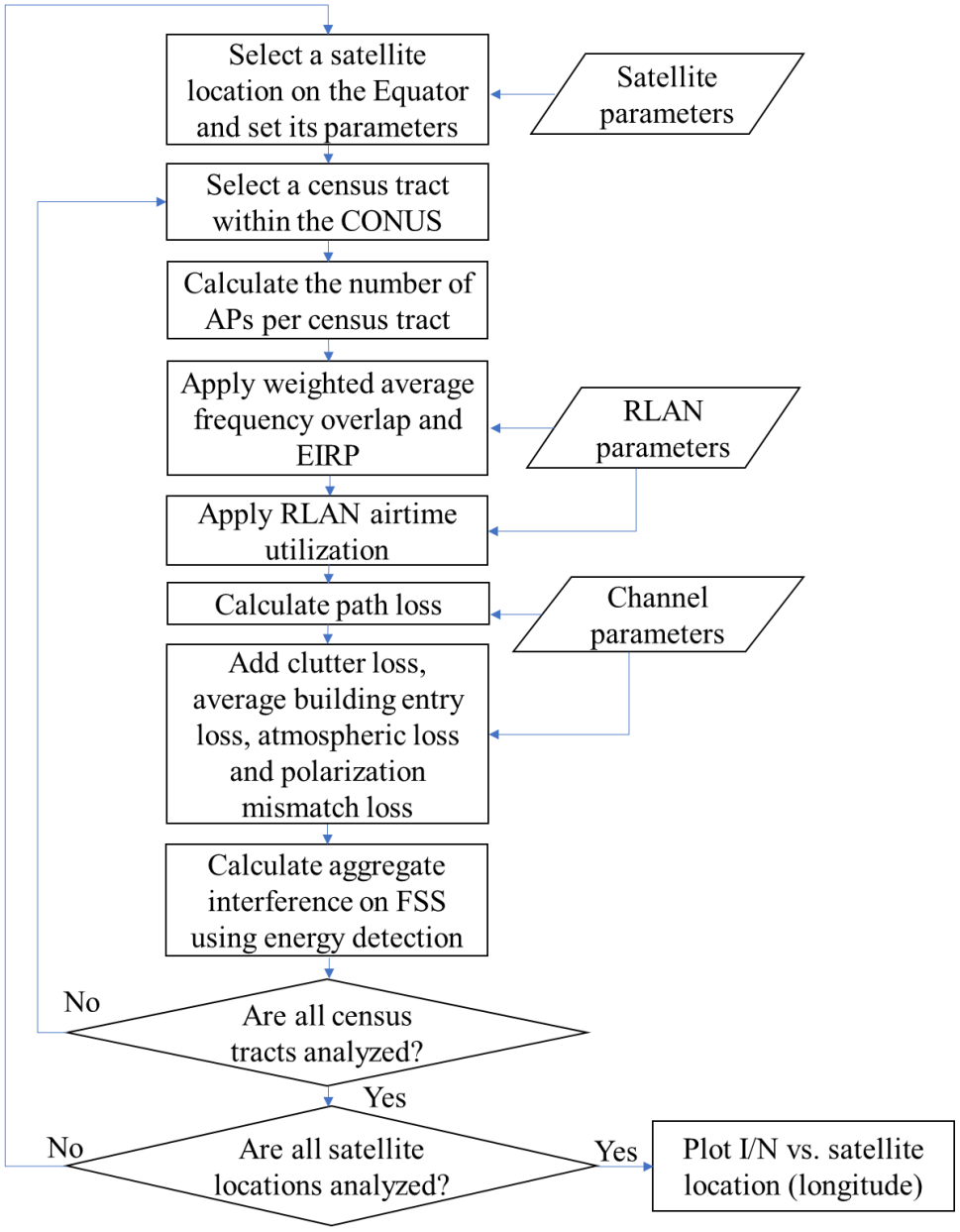

Figure 4.15: Flowchart used to simulate the aggregate interference from Wi-Fi APs to an FSS incumbent.

it has a peak G/T of 3.39 dB/K [83]. Although other satellites have spot beams with higher G/T, they do not cover the entire CONUS and, therefore, they would only be affected by a fraction of the APs, so they are not considered in the simulations.

In the satellite, the bandwidth occupied by each transponder is 36 MHz and, additionally, 4 MHz are used as guard band. The satellite receiver noise temperature used in the simulations is

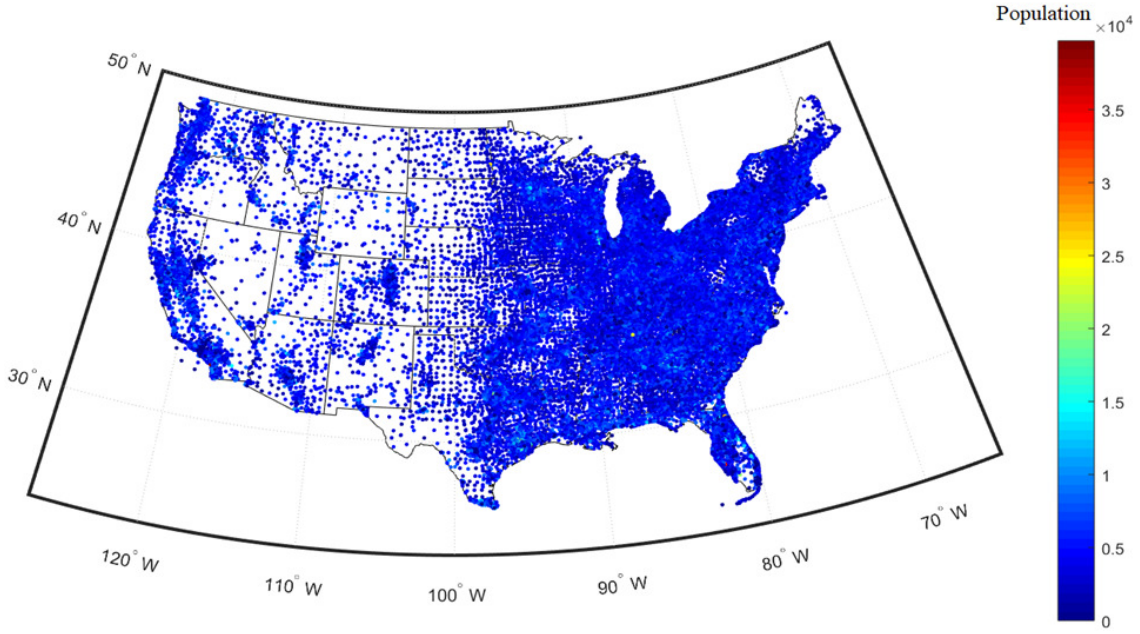

Figure 4.16: Distribution of population according to census tracts.

Table 4.11: Parameters of FSS incumbents in the 6 GHz band

Parameter	**Incumbent service**
	FSS
Transponder bandwidth (MHz)	36
Satellite simulated	SES-2
Antenna gain (dBi)	26.1
Average G/T over CONUS (dB/K)	2
Peak G/T over CONUS (dB/K)	3.9
Receiver noise temperature (K)	257 (*)
Noise floor (dBm)	-98.48 (*)

*Based on Intelsat 35e satellite

257° K, based on Intelsat 35e satellite [48], which is one of the most sensitive satellites on orbit that operates in the 6 GHz band, although it only covers the CONUS partially. Considering these parameters, the noise floor in the satellite receiver is -98.48 dBm.

4.3.2.2 RLAN parameters

The RLAN parameters used in the simulations are indicated in Table 4.12. We simulated more than 80 million 6-GHz capable APs in the entire CONUS in 2026. The number of APs per census tract has been estimated considering the same parameters as in the simulations of interference to a terrestrial incumbent indicated in the previous section. The APs are simulated at 20 m, 7.5 m and 1.5 m height for urban, suburban and rural census tracts, respectively.

The FCC proposal considers Wi-Fi channel bandwidths of up to 320 MHz to allow future expanded performance and capabilities in the next years [39]. The weighted average Wi-Fi channel bandwidth is based on a distribution previously presented in Table 3.2 and has a value of 142 MHz, which is used in each census tract. The EIRP limitations align with the FCC proposal [39] and are the ones assumed in chapter 3. In case of LPI APs only, the maximum PSD is 5 dBm/MHz, according to the FCC rules. The EIRP used in each census tract is the weighted average based on the ECC report 302 [21], as indicated in Table 4.3. For standard-power outdoor APs in U-NII-5 and U-NII-7, we use the EIRP distribution indicated in Table 4.5 presented in the RKF report [77], because it provides a maximum EIRP of 36 dBm, which is the maximum value allowed in the FCC rules [39]. The ECC report 302 only considers EIRP values up to 30 dBm for outdoor APs.

We have developed a numerical method to estimate the weighted average EIRP to consider in the simulations. The method consists of simulating 1 million APs and assigning a random EIRP based on the distributions mentioned before and the weighted average Wi-Fi channel bandwidth. The simulations assume that their antennas are randomly oriented, which is a conservative approach, since most of the energy is usually radiated downwards and the antenna gain tends to decrease for higher elevation angles with respect to the ground. Using the maximum PSD of 5 dBm/MHz for LPI APs in the 6 GHz band, the weighted average EIRP is 17.3 dBm. For standard-power outdoor APs, the simulations assume that the elevation angle of the AP antenna is randomly distributed between -90° and 90°. Applying the EIRP limitation of 21 dBm for elevation angles greater than 30° indicated by the FCC [39], the weighted average EIRP for standard-power outdoor APs is 24.28

Table 4.12: Simulation parameters

Parameter	**Scenario**	
	LPI APs only	Including standard-power outdoor APs
Band	6 GHz	U-NII-5 and U-NII-7
Year simulated	2026	
Market penetration rate	68%	
Population per household	2.48	
Internet usage ratio	88.7%	
Power restriction	Maximum PSD=5 dBm/MHz	Maximum EIRP=36 dBm
Weighted average EIRP (dBm)	17.3	17.63
RLAN airtime utilization	0.4%, 1.38% and 4%	
Weighted average channel bandwidth (MHz)	142	
Outdoor APs	0	2%
Propagation model	Free space path loss	
Clutter loss (dB)	Median value based on ITU-R P.2108 for urban and suburban and on ITU-R P.452 for rural environments	
Building entry loss (dB)	Median value based on ITU-R P.2109	
Antenna polarization mismatch (dB)	3	
AP height (m)	20, 7.5 and 1.5 in urban, suburban and rural scenarios, respectively	
Atmospheric loss (dB)	0.1 dB for high elevation angles, $<$ 1 dB for elevation angles $<$ 5°	

dBm. Considering 2% of outdoor APs, the weighted average EIRP in the U-NII-5 and U-NII-7 bands is 17.63 dBm.

APs with spectrum fully or partially overlapping with an FSS channel contribute to the aggregate interference. An equal probability of spectrum usage throughout all the current and proposed unlicensed bands for Wi-Fi is assumed. The current total Wi-Fi spectrum is 563.5 MHz: 83.5 MHz in the 2.4 GHz band and 480 MHz in the 5 GHz band. The 6 GHz band will add 1200 MHz of spectrum. The weighted average frequency overlap between the incumbent and each Wi-Fi channel is calculated. For an FSS bandwidth of 36 MHz and the weighted average Wi-Fi channel bandwidth of 142 MHz, the estimation of the total frequency overlap is illustrated in Figure 4.17. For example, considering APs operating within the 1200 MHz of the 6 GHz band, if the channel

overlap occurs in the regions 1 or 3 indicated in Figure 4.17, the frequency overlap is $\frac{36}{2}$ and the probability of overlap is $\frac{36}{1200}$. If the channel overlap occurs in region 2, the frequency overlap is 36 and the probability of overlap is $\frac{106}{1200}$. Then, the weighted average frequency overlap within the 6 GHz band will be $\frac{36}{2} \times \frac{36}{1200} + \frac{36}{1} \times \frac{106}{1200} + \frac{36}{2} \times \frac{36}{1200}$ =4.26 MHz. Similarly, considering U-NII-5 and U-NII-7 bands only, the frequency overlap would be 6 MHz.

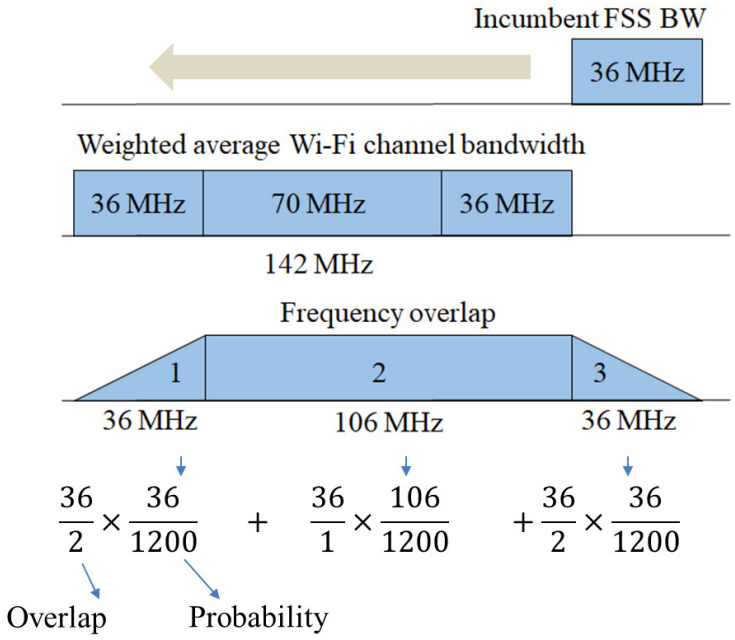

Figure 4.17: Calculation of total frequency overlap between incumbent satellite and Wi-Fi device.

Since the airtime utilization causes a considerable impact on the simulations, a sensitivity analysis is conducted to simulate three AP airtime utilization values. Their weighted averages are 1.38%, 0.4% and 4% and they consider different assumptions. The first one corresponds to the airtime utilization measured in a home environment for 5-GHz Wi-Fi traffic using the ADALM-PLUTO software-defined radio during the peak hour, as indicated in section 4.2.2.2. The second one corresponds to the measurements collected from approximately 0.5 million 5-GHz APs during 10 days in the United States in 2019 [13]. This value is similar to the airtime utilization of 0.44% proposed in [77], which is supported by Wi-Fi advocates. The third airtime utilization is 4% [78], which is supported by current incumbents. This value is based upon a technical analysis that

considers the transmission of 4K video and 160 MHz channel bandwidth. The airtime utilization values of 0.4%, 1.38% and 4% used in the simulations represent ordinary, bad and worst-case scenarios, respectively. In all these cases, it is assumed that the airtime utilization is the same throughout the CONUS and, in case it corresponds to the peak hour, it indicates that it is simulated at 7 pm Pacific Time and 10 pm East Time.

4.3.2.3 Channel parameters

The propagation model used is the free space path loss and, depending on the look angle from the Wi-Fi antenna to the satellite, a median clutter loss has been added. For urban and suburban environments, the clutter loss is based on ITU-R P.2108, section 3.3 [54], which is designed for frequencies above 10 GHz, but it will still be used due to its relative closeness in frequency to the 6 GHz band and similar propagation characteristics. This recommendation provides a cumulative clutter distribution for different look angles. For rural environments, we use ITU-R P.452, section 4.5.3 [53]. It estimates an average nominal clutter height of 5 m at 70 m from a Wi-Fi antenna in a village center, which produces an elevation angle of 4.1°. Considering an antenna height of 1.5 m above the ground, the resulting clutter loss is 18.4 dB for look angles below 4.1°.

Atmospheric attenuation at 6 GHz is very small, approximately 0.1 dB for high elevation angles, and it increases up to 1 dB for elevation angles lower than 5° [85]. No attenuation due to rain and fog is considered in the simulations. For the APs located indoors, the building entry loss (BEL) is estimated based on ITU-R P.2109 recommendation, which models the penetration loss through traditional buildings and thermally-efficient buildings depending on the incidence angle [57]. Figure 4.18 plots the probability of BEL for both types of buildings considering horizontal and vertical incidence angle. The BEL is significantly higher for a vertical incidence angle and thermally efficient buildings. In the simulations, we consider 50% of each type of building per census tract, which causes a median BEL between 24.5 and 36.8 dB for the satellite locations considered. Finally, the loss due to polarization mismatch between the satellite receiver antenna and each of the Wi-Fi AP antennas is 3 dB.

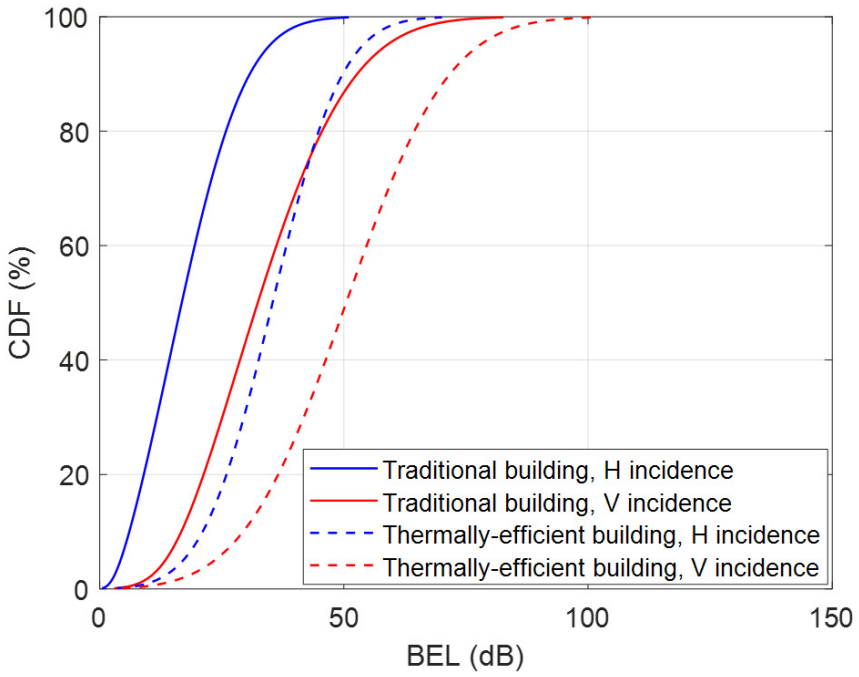

Figure 4.18: Building entry loss at horizontal (H) and vertical (V) incidence according to ITU-R P.2109 recommendation (frequency=6.525 GHz)

4.3.3 Results

We have conducted a sensitivity analysis that estimates the aggregate interference to an FSS incumbent considering different parameters. Figure 4.19 presents the results of the aggregate interference from all the APs in the CONUS to a GEO satellite for airtime utilization values of 1.38%, 0.4% and 4%, considering a satellite antenna gain of 26.1 dBi. This analysis has been conducted for both cases, considering all low-power indoor APs on the entire 6 GHz band and, alternatively, considering 2% of standard-power outdoor APs in U-NII-5 and U-NII-7. The results are compared for different I/N thresholds of -5.7 dB, -7 dB, -12 dB and -20 dB, proposed by the International Telecommunications Union (ITU) and compiled by the National Telecommunications and Information Administration (NTIA) [70], as detailed in Table 4.13. Since the maximum tolerable value of I/N has not been defined by the FCC yet, the results are compared against all these thresholds.

In the simulations, the incumbent GEO FSS satellite is located at different longitudes between

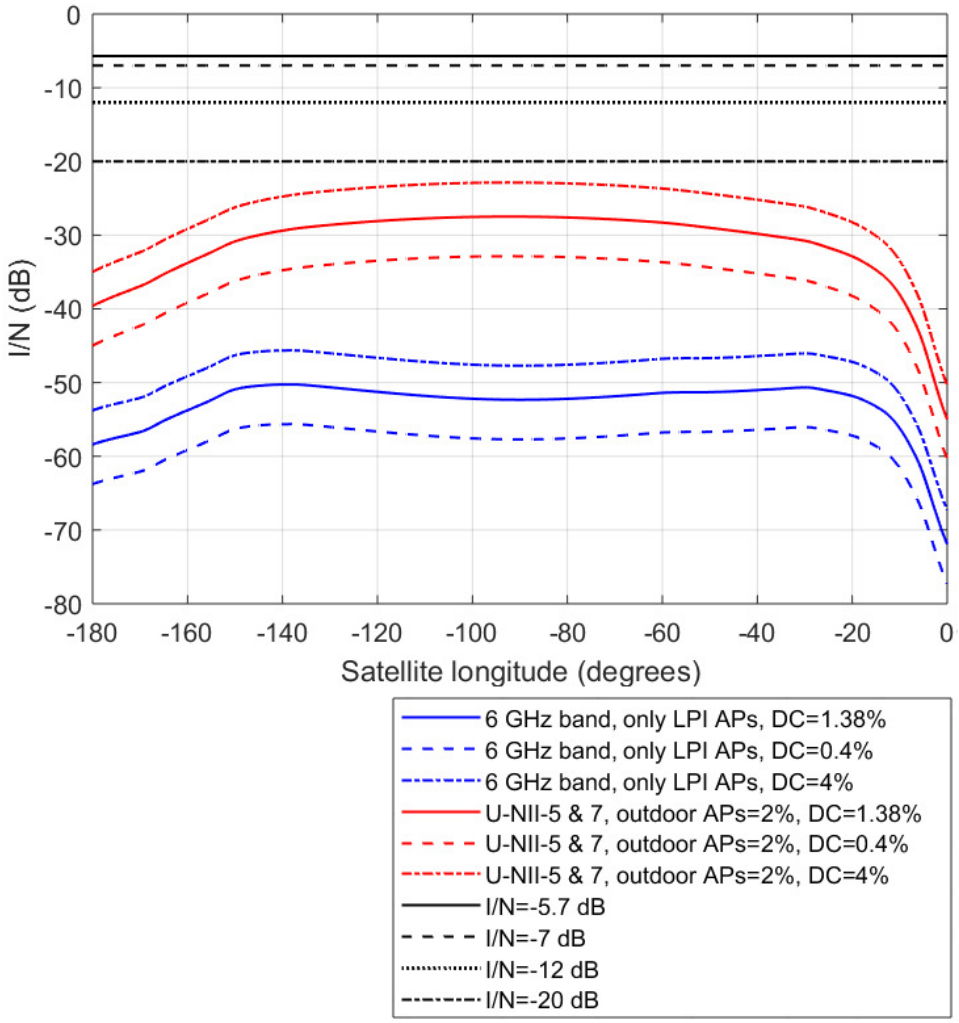

Figure 4.19: Interference from WLANs to a GEO satellite at different longitudes for the U-NII-5 band considering a satellite antenna gain of 26.1 dBi.

-180° and 0° with 0.5° increments. The simulations are based upon an EIRP distribution considering the rules recently proposed by the FCC [39]. As expected, the highest airtime utilization of 4% considering 2% of standard-power outdoor APs in U-NII-5 and U-NII-7 provides the highest I/N of -22.9 dB at a longitude of -92°, which is lower than all the I/N thresholds. Among the simulations that include standard-power outdoor APs, the RLAN airtime utilization of 0.4% provides the lowest I/N of -32.9 dB. For the simulations considering only low-power indoor APs in the entire 6 GHz band, the I/N will always be below -45.6 dB, which is also below all the I/N thresholds indicated.

The I/N ratios for all the cases analyzed in this work are always below the most conservative

Table 4.13: Interference Protection Criteria for FSS Receiver [70]

Interference protection criteria	**Reference bandwidth**	**% time**	**Source document**
$I_{total}/N_{BER} \leqslant$ -5.7 dB	IF passband	20 (of any month)	ITU- S.523
$I_{agg,FSS}/N_{BER} \leqslant$ -7 dB			ITU- S.671
$I_{se,FSS}/N_{BER} \leqslant$ -12 dB			ITU- S.735
$I_{co-prim}/N_{BER} \leqslant$ -12 dB			ITU- S.1323
$I_{others}/N_{BER} \leqslant$ -20 dB			ITU- S.1432
I_{total}: total interfering signal power			
$I_{agg,FSS}$: total interfering signal power from other FSS systems			
$I_{se,FSS}$: interfering signal power from another FSS system			
$I_{co-prim}$: total interfering signal power from services of co-primary status			
I_{others}: total interfering signal power from all other sources			
N_{BER}: total clear sky noise power giving rise to the BER objective			

I/N threshold of -20 dB, which applies to the total interference signal power from all sources, as indicated in Table II. These I/N ratios are considerably lower than the I/N caused by existing terrestrial FS links in this band calculated in [77], which has a maximum value of -4.7 dB. Therefore, even considering the most conservative parameters evaluated in this study, most of the interference to FSS will be caused by current FS links and the amount of interference caused by RLANs will be minimal. Consequently, the results indicate that spectrum sharing with FSS incumbents is possible in the entire 6 GHz band considering the FCC rules recently proposed.

4.3.4 Discussion

We have developed a simulator to model the aggregate interference from Wi-Fi APs in the United States to an incumbent GEO satellite in the 6 GHz band according to the rules proposed by the FCC. The simulator implements space, time and frequency-domain considerations and compares the aggregate I/N for three different airtime utilization values and considering low-power indoor APs only or including standard-power outdoor APs operating in U-NII-5 and U-NII-7, where the percentage of outdoor APs is 2%. The results show that, for a satellite antenna gain of 26.1 dBi, the aggregate I/N caused by the Wi-Fi APs is always significantly lower than the different I/N

thresholds considered by the ITU as interference protection criteria to incumbent FSS links. Since most of the interference will be produced by existing FS links, the impact of RLANs will be minimal considering the FCC rules and, therefore, coexistence with FSS should be possible without causing harmful interference to incumbents.

Chapter 5

Aggregate interference model for coexistence simulations in the 13 GHz band

5.1 Introduction

Current coexistence studies to expand unlicensed spectrum focus on defining rules to operate in the 6 GHz band. However, due to the exponential demand for spectrum, it becomes necessary to explore new bands that can potentially be used for unlicensed devices in the next years. This chapter presents the first coexistence study in the 13 GHz band, which has the same types of incumbents as the recently opened 6 GHz band. We present simulations of aggregate interference from RLANs on each type of incumbent: FS and MS terrestrial links and GSO (geostationary satellite orbits) and NGSO (non GSO) FSS links. Since MS links are allocated in the entire band, only Low-Power-Indoor (LPI) Access Points (APs) are simulated to be consistent with the mitigation rules proposed by the FCC in the 6 GHz band. Based on the methodology we previously developed for 6 GHz coexistence studies, we apply novel aggregate interference models for terrestrial and satellite incumbents. The simulations incorporate a space, time and frequency-domain approach. The risk of interference is quantified by calculating the interference to noise ratio (I/N) as an interference protection criterion and, in cases where I/N exceeds a threshold of -6 dB for terrestrial incumbents, the signal-to-interference-plus-noise ratio (SINR) is also calculated. Alternatively, the Risk-Informed Interference Assessment (RIIA) approach is also used to quantify the likelihood and consequence of the interference to terrestrial FS and MS incumbents.

There are three key contributions of this chapter. First, we conduct coexistence studies in the 13 GHz band and calculate the aggregate interference to terrestrial FS and MS links in urban,

suburban and rural scenarios and to satellite GSO and NGSO links in the entire United States and compare the results. Second, we propose RLAN parameters consistent with the FCC criteria for the 6 GHz band. The RLAN and incumbent parameters simulated are based on real data and projections. Third, using the RIIA approach, we conduct a quantitative risk assessment instead of the traditional worst-case scenario to evaluate the likelihood and impact of the interference to terrestrial incumbents.

5.2 Coexistence with terrestrial incumbents

This section studies the coexistence between RLANs and incumbent FS and MS links in the 13 GHz band.

5.2.1 Aggregate interference model

The coexistence with terrestrial links is based on the model detailed in section 4.2.1. The aggregate interference to terrestrial FS and MS links is calculated in five representative scenarios in the United States and it incorporates space, time, and frequency-domain considerations. In the spatial domain, the model simulates an incumbent receiver located in the center of a circle and multiple APs uniformly distributed around it at different heights, which are based on the building heights obtained from LiDAR data. The model considers exclusion zones of 10 m and 20 m for MS indoor and MS outdoor receivers, respectively. In the time domain, Wi-Fi traffic in each AP is simulated as a Poisson process with exponentially-distributed interarrival time, which is calculated based on an estimated throughput of 1 Gbps in 2028, the 802.11 maximum transmit unit (MTU) assuming WPA (TKIP) encryption and the airtime utilization, which provides an estimate of the AP transmission time. In the frequency domain, the frequency of operation for the incumbent and APs is randomly generated and only the APs with frequency overlap with the incumbent are considered. The path loss between each AP and the incumbent is calculated and, if the propagation path is obstructed, Rayleigh fading is incorporated to simulate multipath environments. The aggregate interference from all the APs is calculated and, using Monte Carlo simulations, a Complementary

Cumulative Distribution Function (CCDF) is generated to estimate the probability of aggregate I/N to an incumbent terrestrial receiver. According to the FCC, the maximum I/N to allow coexistence is -6 dB [39].

5.2.2 Simulation parameters

The simulations include parameters related to the incumbent links, APs and Wi-Fi protocol, and the radio propagation environment.

5.2.2.1 Incumbent parameters

The parameters of the FS and MS incumbents are summarized in Table 5.1. According to the FCC Universal Licensing System (ULS) database [28], the bandwidth for fixed BAS and CARS is 25 MHz and, for fixed point-to-point links, it goes up to 50 MHz. For mobile BAS video, the channel bandwidth is 9 MHz or 18 MHz [52]. In this section, incumbent FS and MS links are simulated with bandwidths of 30 MHz and 18 MHz, respectively.

Table 5.1: Parameters of terrestrial incumbents in the 13 GHz band

Parameter	**Incumbent service**			
	FS: fixed microwave and BAS/CARS		MS: mobile BAS/CARS (outdoor)	MS: mobile BAS/CARS (indoor)
Bandwidth (MHz)	30		18	
Antenna type	Parabolic		Sector	Omnidirectional
Antenna manufacturer and model	Commscope P6-122	Commscope P4-122	MRC Megahorn MH13-20	Vislink L3535 (*)
Antenna gain (dBi)	45.1	41.5	20	3
Antenna HPBW	0.9° horizontal and vertical	1.4 ° horizontal and vertical	17° horizontal and vertical	360° horizontal, 76° vertical
Noise figure (dB)	10		4	
Feeder loss (dB)	1		1	

*It operates only from 6 to 8 GHz, but its parameters will be used in the simulations

Two representative FS antennas have been selected based on all the 13 GHz links in the United States extracted from the ULS database [28]. The most common antenna diameter is 6 ft (47.8%)

and the second one is 4 ft (25.7%). The most common 6 ft and 4 ft antennas are Commscope P6-122 and P4-122, respectively, and both of them are simulated here. P6-122 is more directive and has 45.1 dBi gain and 0.9° HPBW, while P4-122 has 41.5 dBi gain and 1.4° HPBW. Their azimuth antenna radiation patterns are compared in Figure 5.1. The noise figure in the FS receiver is 10 dB and the feeder loss is 1 dB [56].

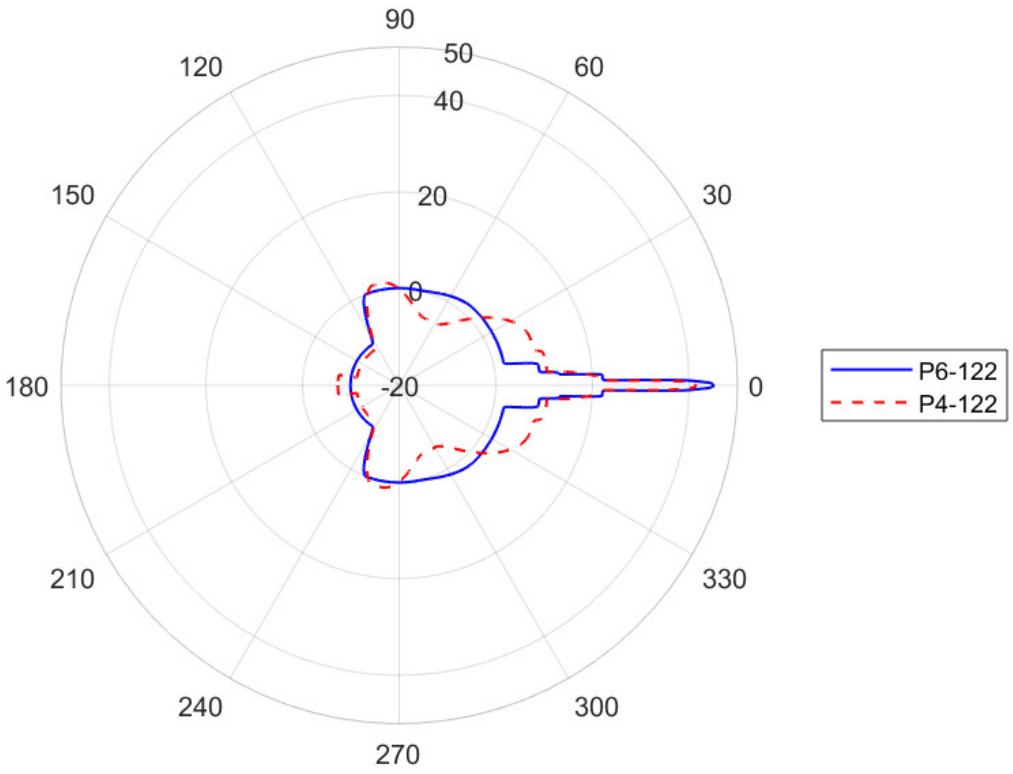

Figure 5.1: Azimuth radiation patterns for P4-122 and P6-122 FS antennas

For MS incumbents, two antennas are simulated based on assumptions used in coexistence studies in the 6 GHz band [6]. For camera back Electronic News Gathering (ENG) transmitters and indoor receivers, a 3 dBi gain omnidirectional antenna is simulated, based on Vislink L3535 antenna for 6 GHz. This antenna has been selected as a representative omnidirectional MS BAS antenna in the absence of datasheets for 13 GHz antennas. For outdoor ENG receivers, we simulate a MRC Megahorn MH13-20 sector panel antenna, which has 20 dBi gain in the 13 GHz band and 17° horizontal and vertical HPBW. The azimuth and elevation radiation patterns have been modeled

based on ITU-R F.1336-5 [55] and they are shown in Figure 5.2. The MS receiver noise figure used in the simulations is 4 dB, as indicated in [52].

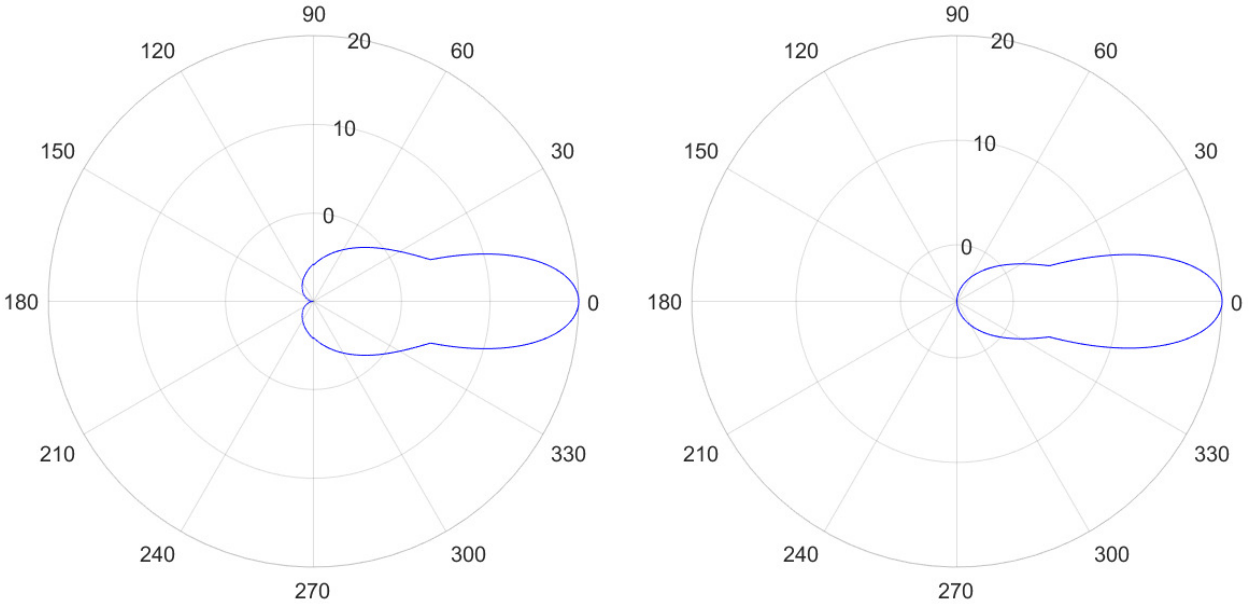

Figure 5.2: Azimuth and elevation radiation patterns for MH13-20 MS antenna

5.2.2.2 RLAN parameters

The RLAN paramters used in the simulations are indicated in Table 5.2. The number of 13-GHz capable APs is projected for 2028 and the method is the same as the one described in chapter 3. To be consistent with the FCC rules for the 6 GHz band, the simulations assume that only LPI APs will be authorized to allow coexistence with incumbent MS links in the entire 13 GHz band. In these simulations, we increase the power spectral density (PSD) from 5 dBm/MHz, as proposed for 6 GHz [39], to 8 dBm/MHz to take advantage of the increased path loss, which is expected to cause less interference. The maximum EIRP is 30 dBm for a maximum Wi-Fi channel bandwidth of 320 MHz, according to the FCC rules in the 6 GHz band [39]. The EIRP distribution is based on the ECC report 302 [21], as detailed in Table 4.3.

The RLAN airtime utilization distribution is based on the 5-GHz Wi-Fi measurements using software-defined radio described in section 4.2.2.2. The simulations use the airtime utilization

Table 5.2: RLAN simulation parameters in the 13 GHz band

Parameter	**Value**
Year simulated	2028
Market penetration rate	68%
Population per household	2.46
Internet usage ratio	91.28%
Maximum PSD	8 dBm/MHz
EIRP	Distribution based on Table 4.3 [21]
RLAN airtime utilization	Distribution based on measurements (Figure 4.7)
Channel bandwidth	Distribution based on Table 3.2
Outdoor APs	0
Propagation model	WINNER II
Building entry loss (dB)	Distribution based on ITU-R P.2109
Antenna polarization mismatch (dB)	3
AP height (m)	Distribution based on Lidar data

measured in a home environment, which has a weighted average of 1.38%. The Wi-Fi channel bandwidth is based on Table 3.2, as in the previous simulations.

5.2.2.3 Channel parameters

The propagation model used to calculate the interference from LPI APs to terrestrial links is WINNER II [59]. Although it is based on measurements up to 6 GHz, this model has been used in coexistence studies in the 6 GHz band [21][77] and it has been selected in this study due to its advantage of considering both the transmitter and receiver heights, as well as different environments that represent urban, suburban, rural and large indoor scenarios simulated here. The distribution of building entry loss is considered based on ITU-R P.2109 [57]. New York City is simulated with 30% of thermally efficient buildings and 70% of traditional buildings, while in the other scenarios these percentages are assumed to be 50%. In addition, we use a polarization mismatch of 3 dB due to the polarization in the incumbent antenna.

Table 5.3: Scenarios

Parameter		NYC	LA	Boulder	Louisville	Leon
Population		8398748	3990456	107353	21163	701
Area simulated (km^2)		784	1214	100	100	1.9
FS RX height (m)	90th percentile	313	84	45	30	30
	Median	270	57	30	22	22
	10th percentile	148	43	15	15	15

5.2.2.4 Scenarios

Five representative scenarios are simulated: New York City (New York), Los Angeles (California), Boulder (Colorado), Louisville (Colorado), and Leon (Kansas), as detailed in Table 5.3. The first three correspond to urban environments, while Louisville and Leon are suburban and rural, respectively. The table indicates the population, area simulated and the 90th, 50th and 10th percentile of the incumbent FS heights in each scenario, according to the ULS database for 13 GHz links [28]. To be conservative and avoid underpredicting the interference, the simulations use the 10th percentile of FS heights. The elevation angle of the incumbent antenna is 1° for FS and 0° for MS. The APs are distributed according to the building heights extracted from 3D elevation maps using LiDAR data [96], at 1.5 m above each floor and assuming 3-m storey heights.

In the case of MS links, the receiver can be located outdoors, in a central receive site or on a ENG truck, or indoors. Since the central receive site corresponds to a fixed high location, the results will be similar to the FS analysis. Therefore, the simulations will only consider two other MS scenarios: indoor camera to indoor receiver and outdoor camera to ENG truck. The camera is mounted on a shoulder, at 1.8 m height and it has an ENG transmitter and an antenna attached. The indoor receiver is simulated at 4.9 m height [6] and the receive antenna on the ENG truck is assumed to be located between 1.5 m and 15 m, hence both heights are analyzed. Considering that Wi-Fi implements a contention-based protocol based on CSMA/CA, it will be unlikely to have more than one AP operating in a certain channel in the same room and, therefore, the indoor scenario only simulates one AP that could potentially overlap in frequency with the incumbent MS receiver.

5.2.3 Results

The aggregate interference to terrestrial incumbents is calculated through Monte Carlo simulations, used to generate independent sets of parameters for 100000 iterations and quantitatively estimate the risk of interference. These computationally intensive simulations are run on Summit Supercomputers with Intel Xeon E5-2680 CPUs.

5.2.3.1 Interference to FS

Figure 5.3 plots the probability of aggregate I/N to an incumbent FS link considering the two most representative antennas in the 13 GHz band, P6-122 and P4-122, in five scenarios. The aggregate I/N is always lower than the -6 dB threshold due to the use of LPI APs only and the higher path loss and building penetration loss in this band, as compared to 6 GHz, which makes coexistence with terrestrial FS possible. I/N is higher in more densely populated areas, except for the rural case, where it is impacted by lower path loss. P6-122, the antenna with the highest gain, will cause higher I/N than P4-122 in more densely populated scenarios due to the increased number of APs, which are more likely to be located within the HPBW of the FS receiver antenna and, therefore, cause higher interference. In the rural case, only 12 APs in the simulated area will have frequency overlap with the incumbent FS and it will be more likely that they will be located outside the HPBW of the FS antenna, which reduces the probability of interference using a more directive antenna.

5.2.3.2 Interference to MS

Figure 5.4 shows the aggregate I/N to an ENG truck antenna located at 15 m or 1.5 m height in different scenarios and to an indoor receiver at 4.9 m height. In the rural case, I/N is higher for an ENG truck antenna height of 1.5 m because all the APs are simulated at the same height. In urban and suburban scenarios, the aggregate I/N is higher for ENG truck antenna heights of 15 m because of the higher AP locations. The aggregate I/N will be higher than the threshold of -6 dB when the ENG truck antenna height is 15 m in NYC, 1.5 m in Leon and in the indoor case.

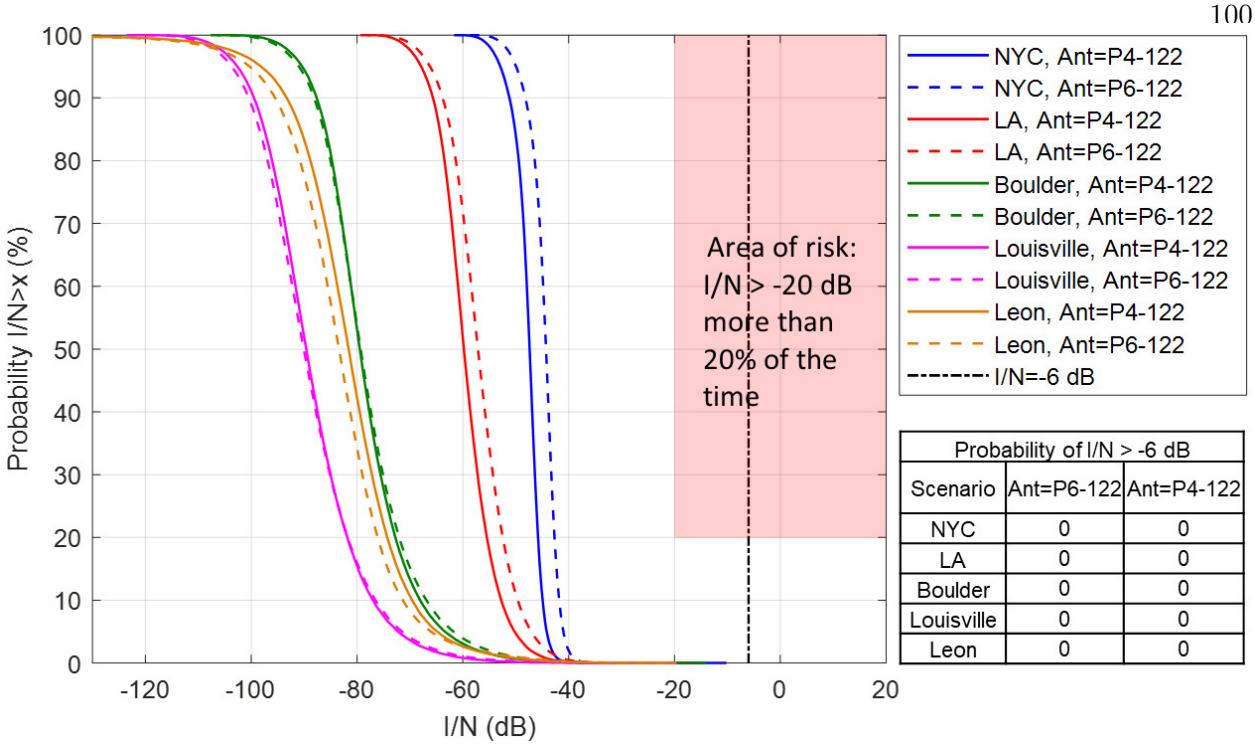

Probability of I/N > -6 dB		
Scenario	Ant=P6-122	Ant=P4-122
NYC	0	0
LA	0	0
Boulder	0	0
Louisville	0	0
Leon	0	0

Figure 5.3: Probability of aggregate I/N on a FS incumbent exceeding values on the X-axis using P4-122 and P6-122 antennas. APs are LPI operating at a maximum PSD of 8 dBm/MHz.

In these scenarios, the SINR is calculated, as shown in Table 5.4. Due to the lack of information about ENG camera back transmitters in the 13 GHz band, previous measurements at 6 GHz are used to determine the SINR threshold for harmful interference [12]. According to them, the MS link will be robust at a SINR of 10 dB considering a BER of 10^{-8} and a high Wi-Fi airtime utilization of 93%. The SINR is significantly higher than this threshold in outdoor-to-outdoor cases. In the indoor-to-indoor scenario, the SINR is higher than 10 dB only up to distances of 20 m. However, this represents the worst case scenario, as it is not very likely that the AP will be transmitting in the same band as an indoor MS receiver, considering the Wi-Fi LBT mechanism.

5.2.3.3 Risk-Informed Interference Assessment approach

The Risk-Informed Interference Assessment approach has been applied to quantitatively analyze the likelihood and consequence of the interference to FS and MS links in the 13 GHz band. The interference protection criterion is the same as the one used in the simulations in the 6 GHz

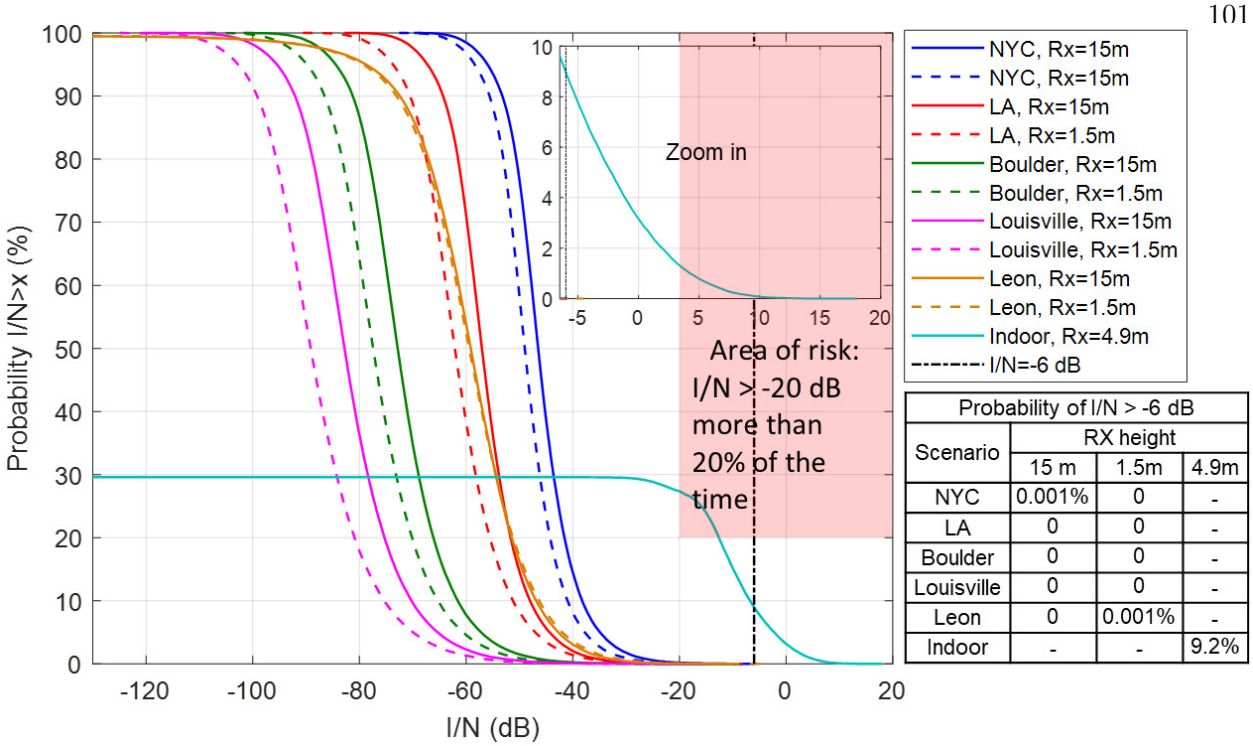

Probability of I/N > -6 dB			
Scenario	RX height		
	15 m	1.5m	4.9m
NYC	0.001%	0	-
LA	0	0	-
Boulder	0	0	-
Louisville	0	0	-
Leon	0	0.001%	-
Indoor	-	-	9.2%

Figure 5.4: Probability of aggregate I/N on a MS incumbent at 1.5 m and 15 m height exceeding values on the X-axis. APs are LPI operating at a maximum PSD of 8 dBm/MHz.

Table 5.4: Minimum SINR (dB) if I/N>-6 dB for MS incumbent

Configuration		**Scenario**	**Distance MS TX - RX**			
TX	RX		20 m	50 m	70 m	100 m
Indoor (1.8 m)	Indoor (4.9 m)	All	14.3	9.3	7.4	5.2
Outdoor (1.8 m)	Outdoor (15 m)	NYC	37	38.5	38.6	36.9
Outdoor (1.8 m)	Outdoor (1.5 m)	Leon	57.8	49.3	61.3	55.2

band, which consists of establishing an unacceptable area of risk determined by an aggregate I/N higher than -20 dB during more than 20% of the time. As shown in the red-colored area in Figure 5.3, there is no risk of harmful interference to a FS incumbent. In the case of a MS incumbent, only the indoor-to-indoor configuration could cause harmful interference, as indicated in Figure 5.4. However, this event corresponds to not only a worst case scenario, but also a very unlikely one, as a Wi-Fi AP would avoid transmitting on the same channel as the MS incumbent, due to the LBT

mechanism.

5.3 Coexistence with satellite incumbents

The coexistence with FSS incumbents is based on the model presented in section 4.3. The aggregate interference to FSS links is also based on a space, time and frequency domain approach. In the spatial domain, the model estimates the impact of all the potential APs in the Contiguous United States (CONUS) territory operating in the 13 GHz band located in the footprint of the satellite antenna. In the time domain, it simulates different airtime utilization values and, in the frequency domain, it calculates the average channel overlap between the APs and the incumbent satellite. The model is used to estimate the interference to representative geostationary satellite orbits (GSO) and non-GSO (NGSO) satellites.

5.3.1 Interference to FSS GSO

5.3.1.1 Aggregate interference model

For aggregate interference simulations to a GSO incumbent, the number of APs simulated is based on the population density in each census tract. As in the simulations in the 6 GHz band, the aggregate interference is calculated considering different longitude locations on the Equator, at a resolution of 0.5°.

5.3.1.2 Simulation parameters

The parameters used for FSS GSO and NGSO links are obtained from the International Bureau Filling System dabatase [25]. A representative FSS GSO satellite with spot beam partially covering the CONUS is Intelsat 37e, which has an antenna gain-to-noise-temperature (G/T) of 13.4 dB in the 13-13.25 GHz band [47]. Assuming an average satellite receiver temperature of 450 K [49], the satellite receive antenna gain is 40.2 dBi. The transponder bandwidth is 36 MHz and the noise floor considered in the simulations is -98.48 dBm, which corresponds to the Intelsat 35e

satellite suggested by incumbents in the 6 GHz coexistence studies [48]. The GSO parameters are summarized in Table 5.5.

The RLAN parameters are indicated in Table 5.6. The simulations are projected for 2028, assuming that the 13 GHz band will open in 2023 for unlicensed use. The procedure to calculate the total number of 13-GHz capable APs in the CONUS is the same as the one followed in the 6 GHz simulations. Considering these parameters, the number of 13-GHz APs in the CONUS will be 83.3 million in 2028.

The interference to satellite incumbents has been calculated using the same path loss model, clutter loss, building entry loss, atmospheric attenuation as in the 6 GHz simulations in section 4.3. The only difference is that the 13 GHz simulations consider low-power indoor APs only transmitting at a maximum PSD EIRP of 8 dBm/MHz, considering the higher path loss, which would cause less interference. Therefore, the weighted average EIRP calculated numerically is 17.68 dBm, which is slightly higher than in the 6 GHz simulations, where the maximum PSD EIRP is 5 dBm/MHz. The three RLAN airtime utilization values simulated in the sensitivity analysis are 0.4%, 1.38% and 4%.

Table 5.5: Parameters of FSS incumbents in the 6 GHz band

Parameter	**Incumbent service**
	FSS GSO
Transponder bandwidth (MHz)	36
Satellite simulated	Intelsat 37e
Antenna gain (dBi)	40.2
Peak G/T on spot beam (dB/K)	13.4
Satellite antenna noise temperature (K)	450 (*)
Noise floor (dBm)	-98.48 (**)

*Based on ITU-R S.1328-2

**Based on Intelsat 35e satellite

5.3.1.3 Results

The maximum I/N allowed for coexistence with FSS links varies from a conservative value of -20 dB, considering interference from any source, to -5.7 dB, considering the total interfering

Table 5.6: RLAN simulation parameters

Parameter	**Incumbent FSS**	
	GSO	NGSO
Band	13 GHz	
Year simulated	2028	
Market penetration rate	68%	
Population per household	2.46	
Internet usage ratio	91.28%	
Power restriction	Maximum PSD=8 dBm/MHz	
Weighted average EIRP (dBm)	17.68	
RLAN airtime utilization	0.4%, 1.38% and 4%	4%
Weighted average channel bandwidth (MHz)	142	
Outdoor APs	0	
Propagation model	Free space path loss	
Clutter loss (dB)	Median value based on ITU-R P.2108 for urban and suburban and on ITU-R P.452 for rural environments	
Building entry loss (dB)	Median value based on ITU-R P.2109	
Antenna polarization mismatch (dB)	3	
AP height (m)	20, 7.5 and 1.5 in urban, suburban and rural scenarios, respectively	
Atmospheric loss (dB)	0.1 dB for high elevation angles, < 1 dB for elevation angles $< 5°$	

signal power, both of which are set according to Table 4.13 [70]. Figure 5.5 plots the aggregate I/N from all the APs in the CONUS to a GSO satellite at different longitudes along the Equator. We simulate the impact on Intelsat 37e satellite, although only a significantly smaller percentage of APs will impact on the satellite due to its partial CONUS coverage. A sensitivity analysis using average RLAN airtime utilization values of 0.4%, 1.38% and 4% indicates that RLANs will not cause harmful interference on FSS GSO receivers considering I/N thresholds of -5.7, -7, -12 and -20 dB. The maximum aggregate I/N is -41.1 dB for a RLAN airtime utilization of 4% and it occurs at longitude -139° E. Intelsat 37e is located at -18° E and the maximum I/N it will receive is -43.1 dB considering an airtime utilization of 4%. The results indicate that RLANs will not cause harmful interference on FSS GSO satellites and coexistence should be possible.

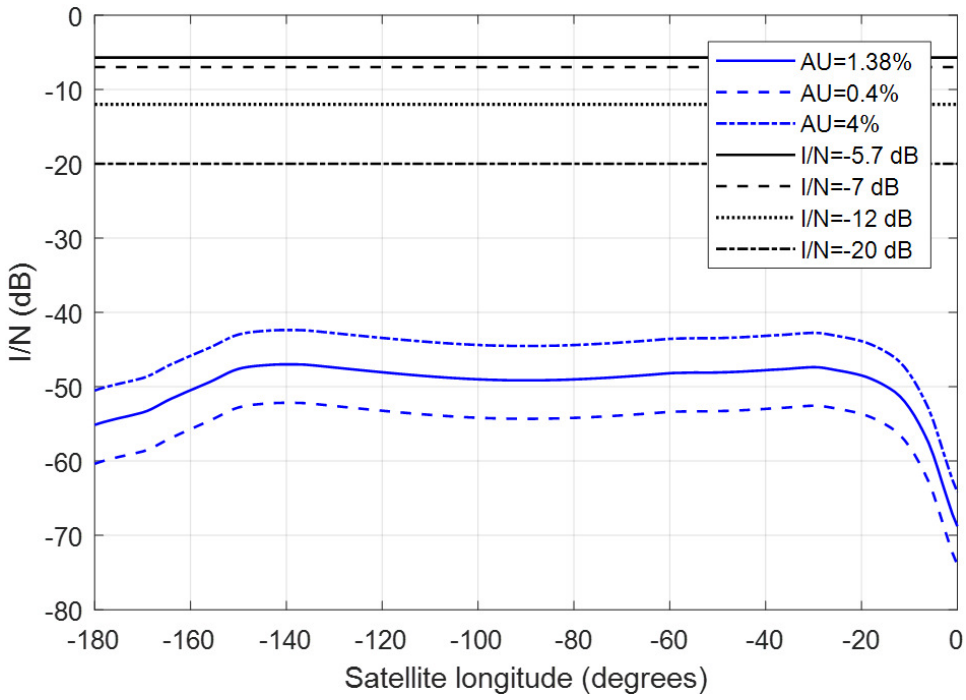

Figure 5.5: Aggregate I/N on FSS GSO incumbent

5.3.2 Interference to FSS NGSO

5.3.2.1 Aggregate interference model

Similar to the simulations of interference to a FSS GSO incumbent, the study considers the distribution of APs in the CONUS. However, instead of calculating the interference from each census tract, in the case of a NGSO incumbent we use the population density at a higher resolution of 1 km^2 [14] due to the smaller footprint of the satellite.

The interference is calculated considering satellite locations above the CONUS at a resolution of 0.5°. I/N is used as an interference protection criteria and the most conservative threshold is -20 dB, as in the other simulations of interference to a FSS incumbent. Similarly, these simulations do not include terrain shadowing, which would increase the path loss and reduce the interference to FSS.

5.3.2.2 Simulation parameters

Two NGSO constellations in 12.75-13.25 GHz band will orbit above the United States [38]. The first one is SpaceX Starlink constellation, which will include 4425 low-Earth orbit (LEO) NGSO satellites on a circular orbit at an average altitude of 1150 km. The operational satellites have started to be launched in 2019. Considering a user beam uplink in the 12.75-13.25 GHz band, the maximum G/T is 9.8 dB/K [35] and the maximum antenna gain is 37.1 dBi [33]. The satellite bandwidth is 125 MHz [35]. The maximum HPBW of the antenna is 2.54° [35] and, according to [43], the radius of the coverage area is 13 km. Assuming a noise figure of 1 dB and a satellite receiver noise temperature of 290 K, the noise floor is -92 dBm.

The other satellite constellation that will partially cover the CONUS is Theia, which will consist of 112 NGSO satellites on an elliptical orbit at an average altitude of 800 km (LEO) [37]. Since the number of Starlink satellites will be significantly higher, we simulate them in different locations in the CONUS and calculate the aggregate interference caused by all the APs within this area in the 13 GHz band. The simulation parameters of an NGSO incumbent based on the Starlink constellation are summarized in Table 5.7.

Table 5.7: Parameters of FSS NGSO incumbent in the 13 GHz band

Parameter	**Incumbent service**
	FSS NGSO
Transponder bandwidth (MHz)	125
Satellite simulated	SpaceX Starlink
Number of satellites in the constellation	4425
Type of orbit and altitude	LEO, 1150 km altitude
Antenna gain (dBi)	37.1
Maximum G/T (dB/K)	9.8
Maximum HPBW	2.42°
Receiver noise temperature (K)	290
Noise floor (dBm)	-92

The RLAN simulation parameters applied are indicated in Table 5.6. The only difference with the GSO case is that here we only simulate the maximum RLAN airtime utilization of 4%,

which is proposed by incumbents and is the most conservative of the three values considered in the GSO simulations.

5.3.2.3 Results

Figure 5.6 shows the aggregate I/N to a SpaceX Starlink NGSO satellite, which can be located anywhere in the CONUS at a height of 1150 km. The simulations consider a conservative RLAN airtime utilization of 4%. I/N is higher for satellite locations above more densely populated areas. The maximum I/N is -42.2 dB, which is below the most conservative I/N threshold of -20 dB for an FSS incumbent. This indicates that RLAN devices can coexist with NGSO satellites in the 13 GHz band.

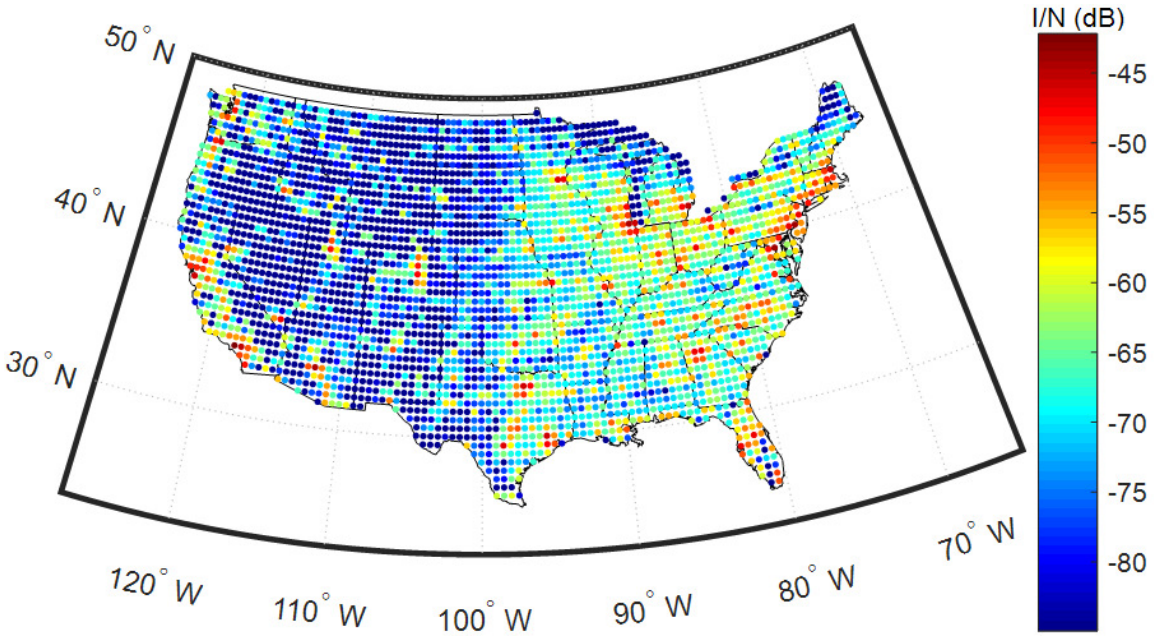

Figure 5.6: Aggregate I/N on FSS NGSO incumbent

5.3.3 Discussion

We have conducted simulations of aggregate interference from potential RLANs in the 13 GHz band to current incumbents. The simulations are built upon novel simulation models developed in sections 4.2.1 and 4.3.1 for terrestrial (FS and MS) and satellite FSS (GSO and NGSO) incumbent

links, respectively. The RLAN rules assumed are consistent with the ones recently proposed by the FCC in the 6 GHz band and the parameters are based on real data and realistic projections. Considering the interference protection criterion of I/N<-6 dB, the results show that LPI APs can coexist with current FS and MS links without the need of mitigation techniques. In the case of a MS incumbent, coexistence is possible for indoor-to-indoor and outdoor-to-outdoor configurations considering both I/N and SINR. For indoor-to-outdoor links, independently of the interference levels, the MS link will not be feasible if the received MS signal is lower than the receiver sensitivity. For GSO and NGSO satellite incumbents, the aggregate I/N is significantly below the most conservative threshold -20 dB, which indicates that RLANs can coexist with them.

Chapter 6

Conclusions and future work

The simulations and measurements conducted in this dissertation enabled us to analyze the feasibility of spectrum coexistence in the 6 GHz and 13 GHz bands. This chapter presents the main conclusions and future work on this topic.

6.1 Conclusions

Spectrum sharing between Radio Local Area Networks (RLANs) and current terrestrial and satellite incumbents in the 6 GHz and 13 GHz bands is feasible based on the simulations and measurements conducted in this work. The 6 GHz band has just been opened for unlicensed use and the 13 GHz band is a good future candidate due to the same types of incumbents.

First, we have conducted path loss measurements at 7 and 13 GHz in four different scenarios in mixed LOS/NLOS urban environments. We generated a dual-slope path loss model for each of these frequencies and quantitatively compared them with empirical path loss models, such as WINNER II, Close-In free space reference distance (CI), ABG and 3GPP. Based on the measurements, CI is the model that provides the closest prediction, but the other models can also be used in our coexistence studies, including WINNER II in the 13 GHz band. We have compared the 7 GHz measurements with the Anderson 2D model, which is a deterministic model that includes terrain and clutter data, and evaluated its level of accuracy using different resolutions. As expected, this site-specific model is more accurate than the deterministic models, especially when using higher resolution data, but it requires increased computational resources and high-resolution terrain and clutter databases.

The aggregate interference from Wi-Fi APs to fixed service (FS) and mobile service (MS) terrestrial incumbent links has been estimated using two approaches. The first one is based on a case study in the Denver metro area for FS incumbents in the 6 GHz U-NII-8 band and the 13 GHz band, which includes a site-specific propagation model with terrain and clutter information, and real data of the incumbent links in the area. The second approach is applied to FS and MS incumbents and it corresponds to an aggregate interference model based on space, time and frequency-domain considerations. Monte Carlo simulations are conducted in five urban, suburban and rural scenarios in the United States and they incorporate RLAN parameters randomly generated using a probabilistic approach based on real data and ITU recommendations.

To verify the case study-based simulations, emissions from Broadcast Auxiliary Service (BAS) links in the Denver metro area have been measured in a few locations. The measurements also permitted to analyze the real utilization of these bands by the incumbents. Most of the measurements show that the broadcasters were using less bandwidth than allowed in their license and, in some cases, they were transmitting only a continuous wave (CW) signal. Additionally, the measurements were always lower than the predicted interference from incumbent links, which indicates that the simulations are conservative.

For FS and MS terrestrial incumbents, the interference protection criterion used is the aggregate interference-to-noise ratio (I/N) of -6 dB. The I/N is always below this threshold considering low-power indoor (LPI) APs in the 6 GHz U-NII-6 and U-NII-8 bands transmitting at a maximum power spectral density (PSD) of 5 dBm/MHz. The same applies to the 13 GHz band using LPI APs with a maximum PSD of 8 dBm/MHz. Without using an automated frequency coordination (AFC) system, there is a small probability that I/N is above -6 dB in the 6 GHz U-NII-5 and U-NII-7 bands, due to standard-power indoor and outdoor APs transmitting at a maximum EIRP of 36 dBm. In these cases, the signal-to-interference-plus-noise ratio (SINR) is calculated as a second metric to assess the impact of the interference compared with the received signal level. The results show that the SINR is always higher than the minimum level needed to avoid significant signal degradation in terms of BER or modulation scheme in the 6 GHz and the 13 GHz bands. The risk

of interference can be further reduced by using AFC.

In the simulations of interference to FS and MS incumbents, the Risk-Informed Interference Assessment has also been used as an alternative to quantify the likelihood and impact of the interference instead of just relying on the worst-case scenario. The interference protection criterion used in this approach defines an area of unacceptable risk if I/N>-20 dB during more than 20% of the time. The results show that there is no risk of harmful interference to incumbent FS links and outdoor-to-outdoor MS configurations. There is a risk of harmful interference to indoor-to-indoor MS configurations, but, due to Wi-Fi's Listen-Before-Talk method, it will not be very likely that the AP will transmit in a busy channel, so this case represents a very conservative scenario.

The simulations of aggregate interference to a Fixed-Satellite Service (FSS) uplink are calculated considering APs distributed in the entire contiguous United States (CONUS). FSS satellites are GSO (geosynchronous orbit) in the 6 GHz band and GSO or NGSO in the 13 GHz band. The simulations use the aggregate I/N as an interference protection criterion, which is always below the most conservative threshold of -20 dB in both bands. This indicates that no harmful interference is expected on the satellites.

We have also conducted simulations of interference from FS incumbents to indoor Wi-Fi APs based on a case study in the Denver metro area in the 6 GHz and 13 GHz bands. The results show that current incumbents can cause a small impact on the APs and the probability would be very small. However, in reality, Wi-Fi's CSMA/CA protocol should be able to sense the channel as busy and transmit in another idle channel. In the worst case, Wi-Fi can adapt its modulation scheme or allow a BER increase to coexist with the incumbents.

The simulation approach used in the case study of interference to a FS link and to a satellite incumbent is based on weighted average values for each RLAN parameter, which are numerically calculated and applied to smaller regions within the total simulated area, instead of to individual APs. On the other hand, the aggregate interference model simulates every AP in the area of interest and the parameters are randomly selected from distributions based on real data, projections and ITU recommendations. This generates a complementary CDF with higher maximum aggregate I/N

values, which are based on a combination of worst-case RLAN parameters and AP locations with respect to the incumbent.

In the further notice of proposed rulemaking of April of 2020, the FCC seeks comments about increasing the maximum power spectral density from 5 dBm/MHz to 8 dBm/MHz for low-power indoor APs in the 6 GHz band. Our simulations show that this would only increase the I/N by up to 1 dB, considering that the AP transmit power is based on an EIRP distribution instead of maximum PSD values. Hence, coexistence is also possible without causing harmful interference to incumbents.

Additionally, the RLAN airtime utilization has been measured in home, classroom and office environments using a software-defined radio in the Wi-Fi 5 GHz band. The measurements in the home environment produce the highest weighted average airtime utilization of 1.38%, considering that they are mainly based on video streaming during the peak hour. The weighted average in the classroom and office environments is only 0.3% and both are primarily based on web browsing. To be conservative and avoid underestimating the interference, the RLAN airtime utilization distribution based on the home scenario has been used in the simulations of interference to terrestrial incumbents. In the case of satellite incumbents, a sensitivity analysis has been conducted, additionally considering two airtime utilization values of 0.4% and 4% proposed by Wi-Fi advocates and incumbents, respectively. In all these cases, there is no risk of harmful interference to satellite FSS uplinks.

Finally, these conclusions indicate that RLANs can coexist with current terrestrial and satellite incumbents in the 6 GHz and 13 GHz bands using the rules recently proposed by the FCC.

6.2 Future work

Based on the results presented in this dissertation, additional work can be proposed to extend the scope of these coexistence studies. The simulations presented here estimate the interference only based on Wi-Fi APs and do not consider client devices, which, although transmitting at significantly lower power, could cause a non trivial additional impact considering their increasing amount due to

the development of new technologies and applications. The simulations could also be extended to analyze coexistence with 5G NR-U in the 6 GHz band, which will enable 5G networks to operate in unlicensed bands.

In addition to the interference power level, it will be useful to quantify the degradation of incumbent links in terms of performance metrics according to the technology used by each incumbent. I/N is the interference protection criterion widely used in the 6 GHz coexistence studies and the SINR can indicate the impact on the incumbent's performance, which can be further complemented by quantifying the impact on throughput, latency and probability of packet collision.

The FCC proposed to implement a contention-based protocol for low-power indoor APs across the 6 GHz band to protect licensed incumbents. The detection threshold to determine if the channel is sensed as idle or busy still needs to be determined. Wi-Fi devices use CSMA/CA as a contention-based protocol, but there might be other protocols more suitable to protect licensed microwave links, especially considering other types of unlicensed users, such as 5G NR-U, wideband and ultra-wideband devices. As the FCC points out, it should be determined if the contention-based protocol can also allow coexistence between these various unlicensed technologies. For example, to facilitate coexistence between Wi-Fi and 5G NR-U, it will be necessary to choose between energy detection (ED) and preamble detection (PD) as the best mechanism to determine if the channel is busy or idle based on a threshold level. ED is simple to implement and only measures the energy, while PD requires the transmission of a known preamble, which will be detected by the sensing device. The advantage of PD is that it permits to know the duration of the transmission after decoding the preamble, so the sensing device can save power by entering into sleep mode during this time. It will also be useful to perform additional measurements of spectrum occupation in the 6 GHz and the 13 GHz bands to analyze the real utilization by incumbents in different environments and determine the best thresholds to consider in the contention-based protocol.

As part of the contention-based protocol, machine learning can be implemented for spectrum sensing. This will enable unlicensed devices to learn about the environment conditions over time and adjust their parameters to avoid collisions. It will also be useful to measure and predict path loss to

estimate the propagation characteristics to adapt its transmit power to avoid or reduce interference to licensed incumbents and facilitate coexistence with other unlicensed devices in the same band.

The FCC is seeking for comments through the further notice of proposed rulemaking. In this dissertation, we conclude that the impact of increasing the PSD from 5 dBm/MHz to 8 dBm/MHz in low-power indoor APs is minimal and does not cause harmful interference to incumbents. It is still to be determined if very-low power APs in the entire 6 GHz band for indoor and outdoor operations should be authorized, which will depend on the identification of the use cases and the maximum power level considering different parameters, such as the antenna pattern, activity factor and use of a contention-based protocol. Another future work consists of calculating the impact of authorizing mobile standard-power APs with AFC and standard-power APs with AFC operating at higher power levels in fixed point-to-point configurations and, if so, determine the maximum power levels permitted to protect the incumbents.

Finally, it would be useful to use Lidar data to discriminate between line-of-sight (LOS) and non line-of-sight (NLOS) conditions in the path loss measurements and generate separate path loss models for each of them at 7 and 13 GHz. The models presented in this work represent mixed LOS/NLOS conditions, which is appropriate for coexistence studies. However, it would be more precise to distinguish between LOS and NLOS scenarios, so the formulas can be better compared with empirical models that consider each of them separately.

Bibliography

[1] 3rd Generation Partnership Project (3GPP). 3GPP TR 38.901. Study on channel model for frequencies from 0.5 to 100 GHz (Release 15), 2018.

[2] 5GCM. 5G Channel Model for bands up to 100 GHz. Technical report, 2016.

[3] A. H. Systems. SAS-571 Double Ridge Guide Horn Antenna.

[4] ABI Research. 5 GHz Wi-Fi is Now Mainstream. Technical report, 2015.

[5] Alcatel-Lucent. 9500 Microwave Packet Radio, 2010.

[6] Alion Science and Technology. Ex Parte: Analysis of Interference to Electronic News Gathering Receivers from Proposed 6 GHz RLAN Transmitters, 2019.

[7] Analog Devices. ADALM-PLUTO Software-Defined Radio Active Learning Module.

[8] Harry R. Anderson. Fixed Broadband Wireless System Design. John Wiley & Sons, 2003.

[9] Antenna Research Associates (ARA). Technical manual for conical monopole antenna CMA-118-A, 1 GHz - 18 GHz, 2007.

[10] Apple et al. Comments of Apple Inc. et al. in the matter of Unlicensed Use of the 6 GHz Band and Expanding Flexible Use in Mid-Band Spectrum between 3.7 and 24 GHz.

[11] AT&T. Ex Parte: Radio Local Area Network (RLAN) to Fixed Service (FS) Microwave Interference in the 6 GHz Band Analysis of Select Real World Scenarios. Technical report, 2019.

[12] Broadcom. Broadcom March 10, 2020 Ex Parte, 2020.

[13] CableLabs. Ex Parte: 6 GHz Low Power Indoor (LPI) Wi-Fi / Fixed Service Coexistence Study, 2019.

[14] Center for International Earth Science Information Network - CIESIN - Columbia University. Gridded Population of the World, Version 4 (GPWv4): Population Density Adjusted to Match 2015 Revision UN WPP Country Totals, Revision 11, 2018.

[15] Comsearch. Ex Parte Presentation WT Docket No. 10-153, 09-106 and 07-121: Categorization of Transmit Antenna Size and Performance for the 5,925-6,425 MHz Band, 2011.

[16] CTIA. Ex Parte: 6 GHz Interference Analysis. Technical report, 2020.

[17] Jean Pierre De Vries. Risk-Informed Interference Assessment: A Quantitative Basis for Spectrum Allocation Decisions. In TPRC 43: The 43rd Research Conference on Communication, Information and Internet Policy Paper, 2015.

[18] Jean Pierre De Vries. Risk-Informed Interference Assessment: A Quantitative Basis for Spectrum Allocation Decisions. Forthcoming in Telecommunications Policy, 2017.

[19] Jean Pierre De Vries, Uri Livnat, and Susan Tonkin. A Risk-Informed Interference Assessment of MetSat/LTE Coexistence. IEEE Access, 2017.

[20] Greg Durgin, Theodore S. Rappaport, and Hao Xu. Partition-based path loss analysis for in-home and residential areas at 5.85 GHz. In IEEE Globecom, 1998.

[21] ECC. ECC Report 302: Sharing and compatibility studies related to Wireless Access Systems including Radio Local Area Networks (WAS/RLAN) in the frequency band 5925-6425 MHz, 2019.

[22] EDX Wireless. EDX Software Reference Manual. Technical report, 2012.

[23] EDX Wireless. Clutter Database use in EDX SignalPro. Technical report, 2016.

[24] EGS Technologies Corporation. Geodata.

[25] FCC. International Bureau Filing System.

[26] FCC. Site / Market / Frequency Query.

[27] FCC. Title 47 CFR, Part 78 - Cable Television Relay Service.

[28] FCC. Universal Licensing System.

[29] FCC. Part 74 - Experimental Radio, Auxiliary, Special Broadcast and Other Program Distributional Services, 2009.

[30] FCC. Title 47 CFR 2.1: Terms and definitions, 2011.

[31] FCC. Title 47 CFR, Part 74 - Experimental Radio, Auxiliary, Special Broadcast and Other Program Distributional Services. 2014.

[32] FCC. Part 101 - Fixed Microwave Services, 2015.

[33] FCC. Schedule S, SpaceX NGSO Constellation, 2016.

[34] FCC. Notice of Inquiry: Exploring Flexible Use in Mid-Band Spectrum Between 3.7 GHz and 24 GHz, 2017.

[35] FCC. Technical Information to Supplement Schedule S, SpaceX NGSO, 2017.

[36] FCC. Notice of Proposed Rulemaking, in the matter of Unlicensed Use of the 6 GHz Band, 2018.

[37] FCC. FCC Fact Sheet: Theia Authorization, 2019.

[38] FCC. Promoting a Competitive and Innovative Satellite Telecommunications Marketplace, 2019.

[39] FCC. FCC 20-51: Report and Order and Further Notice of Proposed Rulemaking in the Matter of Unlicensed Use of the 6 GHz Band, 4 2020.

[40] FCC Technological Advisory Council. A case study of risk-informed interference assessment : MetSat / LTE coexistence in 1695 - 1710 MHz, 2015.

[41] FCC Technological Advisory Council. A Risk Assessment Framework for NGSO-NGSO Interference, 2017.

[42] Fixed Wireless Communications Coalition. Studies Regarding RKF's Frequency Sharing for Radio Local Area Networks in the 6 GHz Band Proposal, 2018.

[43] Gary Gordon and Walter Morgan. Principles of communication satellites. 1993.

[44] Dirk Grunwald, Rob Alderfer, and Ken Baker. Sophisticated Wireless Interference Analysis : A Case Study for Spectrum Sharing Policy. In TPRC Conference Paper, 2014.

[45] Katsuyuki Haneda, Jianhua Zhang, Lei Tan, Guangyi Liu, Yi Zheng, Henrik Asplund, Jian Li, Yi Wang, David Steer, Clara Li, Tommaso Balercia, Sunguk Lee, Youngsuk Kim, Amitava Ghosh, Timothy Thomas, Takehiro Nakamura, Yuichi Kakishima, Tetsuro Imai, Haralabos Papadopoulos, Theodore S. Rappaport, George R. Maccartney, Mathew K. Samimi, Shu Sun, Ozge Koymen, Sooyoung Hur, Jeongho Park, Charlie Zhang, Evangelos Mellios, Andreas F. Molisch, Saeed S. Ghassamzadeh, and Arun Ghosh. 5G 3GPP-like channel models for outdoor urban microcellular and macrocellular environments. In IEEE 83rd VTC Spring, 2016.

[46] Jacek Ilow, Dimitrios Hatzinakos, and Anastasios Venetsanopoulos. Performance of FH SS Radio Networks with Interference Modeled as a Mixture of Gaussian and Alpha-Stable Noise. IEEE Transactions on Communications, 46:509–520, 1998.

[47] Intelsat. Intelsat 37e: Engineering Statement, 2016.

[48] Intelsat License LLC and SES Americom Inc. Comments of Intelsat License LLC and SES Americom, Inc. in the matter of Unlicensed Use of the 6 GHz Band and Expanding Flexible Use in Mid-Band Spectrum between 3.7 and 24 GHz, 2019.

[49] ITU-R. Recommendation S.1328-2: Satellite System Characteristics to be Considered in Frequency Sharing Analyses Between Geostationary-Satellite Orbit (GSO) and Non-GSO Satellite Systems in the Fixed-Satellite Service (FSS) Including Feeder Links for the Mobile-S, 2000.

[50] ITU-R. Recommendation F.1094-2: Maximum allowable error performance and availability degradations to digital fixed wireless systems arising from radio interference from emissions and radiations from other sources, 2007.

[51] ITU-R. Recommendation SM.337-6: Frequency and distance separations, 2008.

[52] ITU-R. Recommendation M.1824-1: System characteristic of television outside broadcast, electronic news gathering and electronic field production in the mobile service for use in sharing studies, 2015.

[53] ITU-R. Recommendation P.452-16: Prediction procedure for the evaluation of interference between stations on the surface of the Earth at frequencies above about 0.1 GHz, 2015.

[54] ITU-R. Recommendation P.2108-0: Prediction of clutter loss, 2017.

[55] ITU-R. Recommendation F.1336-5: Reference radiation patterns of omnidirectional, sectoral and other antennas for the fixed and mobile services for use in sharing studies in the frequency range from 400 MHz to about 70 GHz, 2019.

[56] ITU-R. Recommendation F.758-7: System parameters and considerations in the development of criteria for sharing or compatibility between digital fixed wireless systems in the fixed service and systems in other services and other sources of interference, 2019.

[57] ITU-R. Recommendation P.2109-1: Prediction of building entry loss, 2019.

[58] ITU-R. Sharing and compatibility studies of WAS/RLAN in the 5150-5250 MHz frequency range, Annex 11, 2019.

[59] P. Kyösti, T. Meinilä, L. Hentilä, and Et Al. WINNER II Channel Models. Technical Report IST-4-027756 WINNER II D1.1.2 V1.2, 2007.

[60] W.C.Y. Lee. Estimate of local average power of a mobile radio signal. IEEE Transactions on Vehicular Technology, 34(1):22–27, 1985.

[61] Lyngsat. Satellite database.

[62] Microsoft Corporation. Comments of Microsoft Corporation in the matter of Unlicensed Use of the 6 GHz Band and Expanding Flexible Use in Mid-Band Spectrum between 3.7 and 24 GHz, 2019.

[63] Microwave Radio Communications. Digital Analog Heterodyne Microwave Radio System.

[64] Multi Resolution Land Characteristics Consortium (MRLC). National Land Cover Database 2011.

[65] Tanbir Bakth Nabil. Analysis for frequencies for future 5G system by positioning receiver at different altitudes, 2020.

[66] NASA/METI/AIST/Japan Spacesystems and U.S./Japan ASTER Science Team. ASTGTM: ASTER Global Digital Elevation Model v002, 2009.

[67] National Association of Broadcasters. Comments of the National Association of Broadcasters in the matter of Unlicensed Use of the 6 GHz Band and Expanding Flexible Use in Mid-Band Spectrum between 3.7 and 24 GHz, 2019.

[68] National Spectrum Management Association. GN Docket No. 17-183, Expanding Flexible Use in Mid-Band Spectrum Between 3.7 and 24 GHz, Ex Parte Communication, 2018.

[69] NTIA. Report 90-267: An Extended Database of Microwave Common Carrier Antenna Gain Patterns. 1990.

[70] NTIA. Interference Protection Criteria: Phase 1 - Compilation from Existing Sources, 2005.

[71] NTIA. Description of a model to compute the aggregate interference from Radio Local Area Networks employing dynamic frequency selection to radars operating in the 5 GHz frequency range. Technical report, 2009.

[72] NTIA. Digital Nation Data Explorer, 2020.

[73] Nucomm. CamPac2: COFDM Camera-Back Transmitter, 2010.

[74] Yimin Pang, Joey Padden, and Rob Alderfer. Sophisticated Spectrum Sharing Analysis: The Case of the 5.9 GHz Band. TPRC 46: The 46th Research Conference on Communication, Information and Internet Policy Paper, 2018.

[75] Qualcomm Incorporated. Comments of Qualcomm Incorporated in the matter of Unlicensed Use of the 6 GHz Band and Expanding Flexible Use in Mid-Band Spectrum between 3.7 and 24 GHz, 2019.

[76] Theodore S. Rappaport, George R. MacCartney, Mathew K. Samimi, and Shu Sun. Wideband millimeter-wave propagation measurements and channel models for future wireless communication system design. IEEE Transactions on Communications, 63(9):3029–3056, 2015.

[77] RKF Engineering Solutions. Frequency Sharing for Radio Local Area Networks in the 6 GHz Band, 2018.

[78] Roberson and Associates LLC. Impact of Proposed Wi-Fi operations on Microwave Links at 6 GHz, 2020.

[79] Ruckus Networks. Ruckus antenna guide, 2014.

[80] S. Salous, J. Lee, M. D. Kim, M. Sasaki, W. Yamada, X. Raimundo, and A. A. Cheema. Radio propagation measurements and modeling for standardization of the site general path loss model in International Telecommunications Union recommendations for 5G wireless networks. AGU Radio Science, 2020.

[81] Satbeams. Satellite Coverage Maps and Charts.

[82] Thomas Schwengler and Mike Gilbert. Propagation models at 5.8 GHz-path loss and building penetration. In IEEE Radio and Wireless Symposium, 2000.

[83] SES Americom. Application of SES Americom, Inc. For Authority to Launch and Operate a Replacement Satellite at 87° W.L., 2011.

[84] Elvino Sousa. Performance of a spread spectrum packet radio network link in a Poisson field of interferers. IEEE Transactions on Information Theory, 38:1743–1754, 1992.

[85] William Stallings. Wireless Communications and Networks. 2nd edition, 2005.

[86] Shu Sun, Theodore S. Rappaport, Sundeep Rangan, Timothy A. Thomas, Amitava Ghosh, Istvan Z. Kovacs, Ignacio Rodriguez, Ozge Koymen, Andrzej Partyka, and Jan Jarvelainen. Propagation path loss models for 5G urban micro- and macro-cellular scenarios. In IEEE 83rd VTC Spring, 2016.

[87] Christopher Szymanski, Vinko Erceg, and Thomas Derham. Comments of Broadcom in the matter of Unlicensed Use of the 6 GHz Band and Expanding Flexible Use in Mid-Band Spectrum between 3.7 and 24 GHz, 2019.

[88] Telecom Advisory Services. Assessing the Economic Value of Unlicensed Use in the 5.9 GHz & 6 GHz Bands. Technical report, 2020.

[89] The Internet and Television Association and CableLabs. Ex Parte filing ET Docket No. 13-49: Tests Confirm That 5.9 GHz Rechannelization Protects Adjacent-Channel DSRC Safety Operations, 2017.

[90] The Spectrum and Receiver Performance Working Group of the Federal Communications Commission's Technological Advisory Council. A Quick Introduction to Risk-Informed Interference Assessment, 2015.

[91] Susan Tonkin and Jean Pierre De Vries. NewSpace Spectrum Sharing: Assessing Interference Risk and Mitigations for New Satellite Constellations. In SSRN Electronic Journal, 2018.

[92] U.S. Census Bureau. Census tract database 2010, 2010.

[93] U.S. Census Bureau. Projections of the Size and Composition of the U.S. Population: 2014 to 2060, 2015.

[94] U.S. Census Bureau. Defining Rural at the U.S. Census Bureau. Technical report, 2016.

[95] U.S. Census Bureau. Average Population Per Household and Family, 2019.

[96] USGS. The National Map: 3D Elevation Source Data (3DEP) - LiDAR, lfSAR, 2015.

[97] Utilities Technology Council and Edison Electric Institute. Comments of the Utilities Technology Council and the Edison Electric Institute in the matter of Unlicensed Use of the 6 GHz Band and Expanding Flexible Use in Mid-Band Spectrum between 3.7 and 24 GHz, 2017.

[98] J. Ward-Bailey. Risk Assessment in Spectrum Policy, 2015.

[99] Wanchun Yang, Yanxia Hu, Xieping Gao, Kai Hu, Fen Xiao, and Chunhong Cao. The Duty Cycle Analysis for Electromagnetic Field Exposure from WLAN in a Busy Period. IEEE Transactions on Electromagnetic Compatibility, 58(6):1772–1775, 2016.

[100] Xueshi Yang and Athina Petropulu. Co-Channel Interference Modeling and Analysis in a Poisson Field of Interferers in Wireless Communications. IEEE Transactions on Signal Processing, 51:64–76, 2003.

[101] Nadia Yoza-Mitsuishi, Ruoyu Sun, and Peter Mathys. Spectrum Sharing Between WLANs and Fixed Microwave Links in 6 and 13 GHz Bands: a Case Study. In IEEE International Symposium on Dynamic Spectrum Access Networks, 2019.

Appendix A

Calibration for field measurements

We have conducted a power level calibration of the measurement system and determined the loss through cable and connectors that were considered to calculate the path loss in Chapter 1.

Additionally, we performed a frequency calibration in the lab, with the purpose of determining the frequency shift between the signal generator and the spectrum analyzer for both 7 and 13 GHz transmit frequencies during more than 40 minutes.

A GPS calibration was conducted at the transmitter site. We powered on the RTK GPS base station, configure the output message protocol as RTCM 3 (Radio Technical Commission for Maritime Services) and the baud rate as 19200. Then, we configured the GPS to perform a survey of all the satellites available for at least 5 minutes to obtain a position accuracy of at least 2 meters. The longer the survey time, the higher the position accuracy.

In the receiver site, we configured the input message protocol as RTCM 3 and the baud rate also as 19200. We then started recording the GPS data as NMEA 0183 messages. NMEA 0183 is a data specification that is used by GPS and other instruments. The NMEA fix quality parameter indicates the accuracy of the GPS measurements, which also depends on the quality of the wireless link between the GPS base station and GPS rover station.

Appendix B

Code to simulate the aggregate interference from Wi-Fi APs to an FSS incumbent in the 6 GHz and 13 GHz bands

The code (in Matlab) is available in the following link:

https://github.com/nadiayoza/CoexistenceFSS